

Myelin pruning by microglia during development

Dissertation

for the award of the degree
"Doctor rerum naturalium" (Dr.rer.nat)

of the Georg-August-University Göttingen,
Faculty of Biology

within the doctoral program
"Molecular Physiology of the Brain"
of the Georg-August University School of Science
(GAUSS)

submitted by

Ulrich Maximilian Weikert

from
Reutlingen, Germany

Göttingen,

28th February 2019

Thesis Committee

Prof. Dr. Mikael Simons

Research Group of Cellular Neuroscience/Molecular Neurobiology
Max-Planck Institute for Experimental Medicine/German Research Center for Neurodegenerative Diseases

Prof. Dr. Thomas Bayer

Division of Molecular Psychiatry
University Medical Center

Prof. Dr. André Fischer

Department for Psychiatry and Psychotherapy
University Medical Center/German Research Center for Neurodegenerative Diseases

Members of the Examination Board

Referee: Prof. Dr. Mikael Simons

Research Group of Cellular Neuroscience/Molecular Neurobiology
Max-Planck Institute for Experimental Medicine/German Research Center for Neurodegenerative Diseases

2nd Referee: Prof. Dr. Thomas Bayer

Division of Molecular Psychiatry
University Medical Center

Further members of the Examination board

Prof. Dr. André Fischer

Department for Psychiatry and Psychotherapy
University Medical Center/German Research Center for Neurodegenerative Diseases

Prof. Dr. Dr. Hannelore Ehrenreich

Clinical Neuroscience
Max-Planck Institute for Experimental Medicine

Prof. Dr. Christine Stadelmann-Nessler

Clinic for Neurology
University Medical Center

Prof. Dr. Ralf Heinrich

Department of Cellular Neurobiology
Schwann-Schleiden Research Centre

Date of oral examination: 24.04.2019

Affidavit

I hereby declare that the PhD thesis entitled "Myelin pruning by microglia during development" has been written independently by myself, with no other contributory sources and aids than quoted.

Göttingen, 28. Februar 2019

.....

Ulrich Maximilian Weikert

Für

MAPA

Acknowledgement

First of all, I would like to thank my supervisor Prof. Dr. Mikael Simons for allowing me to conduct my research in his laboratory. His scientific way of thinking was an inspiration and provided important guidance for the project. I would also like to thank him for the scientific discussions during my PhD project and teaching me a lot about science apart from experiments.

I want to thank my thesis committee members Prof. Dr. André Fischer and Prof. Dr. Thomas Bayer for their interest in my project and their contribution during my progress reports. Furthermore, I would like to acknowledge Prof. Dr. Thomas Bayer for agreeing to act as a second reviewer. I also thank Prof. Dr. Dr. Hannelore Ehrenreich, Prof. Christine Stadelmann-Nessler and Prof. Ralf Heinrich for being part of my extended examination board.

I thank my collaborators, Dr. Stefan Bonn, Dr. Magali Hennion, Dr. Ramon Vidal, M.Sc. Michele Binder, Angelika Mönnich, Prof. Dr. David Liebetanz, Dr. Christoph Wrede, Dr. Jan Hegermann, Prof. Dr. Moritz Rossner, M. Sc. Nirmal Raman Kannaiyan, Dr. Gesine Saher, M.Sc. Tim Düking, M.Sc. Stefan Berghoff, M. Sc. Simon Besson-Girard for their supportive contribution towards my project.

I would like to highlight how much I appreciate the invaluable help of the EM facility with Wiebke, Torben, Boguscha, Anna and Christos that I will always remember as my happy place in the MPI. A special thanks to Wiebke and Torben not only for the awesome scientific support, but also for the emotional support.

Many thanks to my lab colleagues Ludo, Dirk, Sebastian, Maryam, Paula, Tina, Caro, Shima and Minhui for the nice working atmosphere.

Also I wanted to thank David, Marcel, Beate, Jan, Tim, Martin, Stefan, Iva and Ramona for being my adopted lab and friends.

Thresel, I am thankful for your support and patients with me. It has not been easy sometimes, but you were always there for me and managed to not give up on me. You have not been so bad for me!

Finally, I want to thank my parents Wolfgang and Elisabeth and my siblings Georg, Edith and Bernhard for their support and believe in me. Thank you for always encouraging me to follow my goals.

Table of content

1	<i>Introduction</i>	1
1.1	Central nervous system and its main functions	1
1.2	Functions of oligodendrocytes	3
1.3	Myelin composition	5
1.3.1	Myelin lipids	5
1.3.1.1	Cholesterol	5
1.3.1.2	Galactolipids	7
1.3.1.3	Phosphatidyl-inositols	8
1.3.2	Myelin proteins	8
1.3.2.1	Myelin basic protein (MBP)	8
1.3.2.2	Proteolipid protein (PLP)	9
1.3.2.3	Other myelin proteins	9
1.4	Origins of oligodendrocytes and formation of myelin	9
1.5	Epigenetic control of the myelin sheath	12
1.6	Plasticity of the myelin sheath	13
1.7	Origins of microglia and their function during development	16
1.8	Main microglia receptors	18
1.9	Microglia function in diseases	20
1.10	Project aim	22
2	<i>Materials and Methods</i>	23
2.1	Material	23
2.1.1	Chemicals and consumables	23
2.1.2	Antibodies	23
2.1.3	General buffers and solutions	24
2.1.3.1	PBS	24
2.1.3.2	PFA	24
2.1.3.3	Blocking solution	24
2.1.3.4	Mowiol	25
2.1.3.5	Anesthetic	25
2.1.3.6	Phosphate buffer (PB)	25
2.1.3.7	Formvar	25

2.1.3.8	Richardson's Methylene Blue / Azur II blue	25
2.1.3.9	Low sucrose buffer (nuclei isolation)	26
2.1.3.10	High sucrose buffer	26
2.1.3.11	Lysis buffer for meDIP	26
2.1.4	Software	27
2.2	Methods	27
2.2.1	Animal handling	27
2.2.2	Complex running wheel	28
2.2.3	Tissue preparation for Immunohistochemistry	28
2.2.4	Immunocytochemistry of optic nerve	29
2.2.5	Cell counting	29
2.2.6	Tissue preparation for Electron microscopy	29
2.2.7	Cutting of ultrathin sections for TEM analysis	31
2.2.8	Sample preparation for 3View imaging	31
2.2.9	EM quantification	31
2.2.10	Nuclei isolation	31
2.2.11	Staining of isolated nuclei for FACS	32
2.2.12	Fluorescence associated cell sorting (FACS)	32
2.2.13	Methylated DNA immunoprecipitation (meDIP)-seq protocol	33
2.2.14	Magnetic activated cell sorting (MACS) of microglia cells	33
2.2.15	RNAseq library preparation	34
2.2.16	Transcriptome Data analysis	35
2.2.17	Pathway analysis	35
2.2.18	Statistics	35
3	Results	36
3.1	Changes in DNA-Methylation after running wheel exercise	36
3.2	Changing populations of glia cells in the optic nerve after birth	46
3.3	Ultrastructure of optic nerve myelination	50
3.4	MERTK is not a receptor responsible for myelin pruning	57
3.5	TREM2 deficient microglia show less activation	58
3.6	RNA profile of microglia in the corpus callosum and cortex	61
4	Discussion	65
4.1	Effects of DNA-methylation on complex motor skill learning	65

4.2	Optic nerve development	68
4.3	Ultrastructural changes during optic nerve development	69
4.4	MerTK/TREM2 involvement in pruning	72
4.5	DAM-response during development	75
5	<i>Summary</i>	77
6	<i>Appendix</i>	79
7	<i>Bibliography</i>	88
8	<i>CV</i>	102

List of figures

<i>Figure 1: Central nervous system composition</i>	2
<i>Figure 2: Myelin membrane composition</i>	6
<i>Figure 3: Wrapping of oligodendrocyte membrane around the axon</i>	11
<i>Figure 4: Speculated timeline of adaptive myelination</i>	15
<i>Figure 5: Different types of microglia receptors and relation to inflammation</i>	19
<i>Figure 6: Running wheel paradigm scheme</i>	37
<i>Figure 7: Comparison of running performance between normal and complex wheel</i>	39
<i>Figure 8: Fluorescence-activated cell sorting of corpus callosum nuclei</i>	40
<i>Figure 9: DNA-methylation profile of the complex runners compared to the control group</i>	42
<i>Figure 10: Oligodendrocyte and OPC maturation in the optic nerve during development</i>	47
<i>Figure 11: Astrocytes and microglia distribution in the optic nerve during development</i>	49
<i>Figure 12: Myelin outfoldings occur during normal development</i>	51
<i>Figure 13: Myelin debris are attached to the axon during normal optic nerve development</i>	52
<i>Figure 14: Microglia phagocytose myelin debris during normal development in the optic nerve</i>	53
<i>Figure 15: Microglia actively pull myelin off of internodes</i>	54
<i>Figure 16: Increase of myelinated axons and decrease of myelin degeneration during development</i>	55
<i>Figure 17: Myelin is phagocytosed by microglia cells during development</i>	56
<i>Figure 18: MerTK KO mice show no apparent difference in amount of degeneration</i>	58
<i>Figure 19: Trem2 KO mice show more degenerated myelin during development</i>	59
<i>Figure 20: Trem2 KO show less microglia activation in the optic nerve during development</i>	60
<i>Figure 21: Microglia show differentially expressed genes in grey and white matter upon maturation</i>	62
<i>Figure 22: Top 10 regulated KEGG - Pathways</i>	63
<i>Figure 23: DAM response genes are not activated during myelinogenesis</i>	64
<i>Figure 24: 3D-electron microscopy stack of 14 day old optic nerve of a wild type mouse</i>	70
<i>Figure 25: Developmental processes in the CNS</i>	72
<i>Figure 26: FACS control stainings of mouse corpus callosum</i>	79
<i>Figure 27: Principal Component Analysis of the samples tested for MeDIP sequencing</i>	80
<i>Figure 28: Sample reads</i>	82
<i>Figure 29: Alignment to genome</i>	83
<i>Figure 30: Principle component analysis of different microglia conditions</i>	84
<i>Figure 31: Sample to Sample Distance</i>	85
<i>Figure 32: Most differentially expressed genes from wt mice at P14 and P60</i>	86

List of tables

<i>Table 1: Antibodies used for immunohistochemistry</i>	23
<i>Table 2: Software used to analyze produced data</i>	27
<i>Table 3: Enriched genes during motor skill learning from trained and untrained mice</i>	44
<i>Table 4: Sample barcode</i>	81

List of abbreviations

°C	Degree Celsius
µm	micrometer
µM	micromole
5mC	5-methylcytosine
BSA	Bovine serum albumin
BS	Blocking solution (histology)
CAP	Compound action potential
cc	Corpus callosum
CG	Control group
CGT	UDP-galactose:cerebroside galactosyl transferase
CNP	2',3'-Cyclic-nucleotide 3'-phosphodiesterase
CNS	Central nervous system
d	Day
DAPI	4',6-Diamidin-2-phenylindol
ddH ₂ O	Double distilled water
DMG	Differentially methylated gene
DMR	Differentially methylated region
DNA	Deoxyribonucleic acid
DTT	Dithiothreitol
EDTA	Ethylenediaminetetraacetic acid
EM	Electron microscopy
FACS	Fluorescence-activated cell sorting
FC	Fold change
G	Wire Gauge
g	Gram
G	Standard gravity
h	Hour
HEPES	4-(2-hydroxyethyl)-1-piperazineethanesulfonic acid
ip	intraperitoneal
KO	Knock out, constitutive mutant
l	Liter
MACS	Magnetic-activated cell sorting
MBP	Myelin basic protein
meDIP	Methylated DNA immunoprecipitation
min	minute
ml	milliliter
MLG	Motor learning group
mM	millimolar
mol	molarity
MOSS	Motor skill sequence
MS	Multiple sclerosis
MYRF	Myelin regulatory factor
n	Number of biological replicates
Nm	nanomole
OL	Oligodendrocyte

OPC	Oligodendrocyte precursor cell
p	P-value
P	Postnatal day
PB	Phosphate buffer
PBS	Phosphate buffered saline
PBS-T	Phosphate buffered saline with Tween-20
PCD	Programmed cell death
PFA	paraformaldehyde
pH	Potential of hydrogen
RIPA	Radioimmunoprecipitation assay buffer, lysis buffer
RNA	Ribonucleic acid
RNAseq	RNA sequencing
RT	Room temperature
s	Second
Sd	Standard deviation
SDS	Sodium dodecyl sulfate
SEM	Scanning electron microscope
SBF-SEM	Serial block face imaging Scanning electron microscope
TEM	Transmission electron microscopy
UMG	University medical center Göttingen
Wt	Wild type
DNMT	DNA-methyl-transferase
PAD	Peptidyl arginine deiminase
PDGFR α	Platelet-derived growth factor receptor α
PMD	Pelizaeus-Merzbacher disease
APC	Adenomatous polyposis coli protein
GFAP	Glial fibrillary acidic protein
IBA1	Ionized calcium-binding adaptor molecule 1
MERTK	MER proto-oncogene tyrosine kinase
Trem2	Triggering receptor expressed on myeloid cells 2

Abstract

Myelin is a lipid rich membrane produced by oligodendrocytes in the central nervous system. During development, oligodendrocyte precursor cells find their target axons and start to wrap their processes around axons, thereby creating a multilayered insulating sheath. Those sheaths are regularly distributed along the axon with small, intersecting gaps called Nodes of Ranvier. This insulation results in increase in signaling conduction velocity. Furthermore, recent publications suggest that myelin is a dynamic structure that can adapt to environmental changes.

I investigated the epigenetic control of oligodendrocytes during motor skill learning, since it was suggested in literature, that myelin is necessary for complex learning. Mice were subjected to a complex running wheel and the corpus callosum, a region with high myelin density, were collected for batch isolation of tissue specific methylated DNA immunoprecipitation (Bits-meDIP), before and several days after complex learning. Thereby i could not identify changes of differentially methylated regions or genes.

Myelin plasticity is also visible during development, where the formation of the myelin sheath is accompanied by myelin outfoldings, which are normally linked to disease pathology. Here, I investigated the ultrastructural changes of myelin by 2D and 3D electron microscopy during optic nerve development. Thus, I could see degenerated myelin debris additional to outfoldings in wild type optic nerves. Interestingly, degenerated myelin was not only seen in the extracellular space, but also still attached to otherwise normal looking myelin sheath. Additionally, microglia were found to be associated with myelin outfoldings and phagocytose degenerated myelin. This phenomenon has already been described for demyelinating disease models, however not yet for normal myelin development. Activation of microglia during that time seemed to be dependent on triggering receptor on myeloid cells 2 (TREM2) signaling, since TREM2 deficient animals showed less expression of the activation markers. Despite that RNA sequencing of white and grey matter microglia at 14 and 60 days after birth did not show an increase in genes usually expressed in disease-associated microglia (DAM) – a microglial subtype which arises in a Trem2-dependent manner. Pathway analysis showed that P14 microglia in cortex and corpus callosum expressed genes related to extracellular matrix interaction, cytokine signaling, focal adhesion and protein digestion, when compared to P60 microglia. Hence, redundant myelin during development is unlikely to be sufficient to trigger severe disease related gene expression.

1 Introduction

1.1 Central nervous system and its main functions

The central nervous system (CNS) that is directly or indirectly controlling our body's functions through neuronal networks, consists of the brain and the spinal cord. Every neuronal cell outside of this system that connects the brain to organs and limbs belongs to the peripheral nervous system (PNS). Together these systems are in charge of controlling voluntary actions (e.g. movement, thinking) and involuntary actions (e.g. reflexes, blood pressure, breathing) of the body. The brain is the most complex organ in the human body and it is crucial for the coordination of complex motor functions, thinking and memory formation, but also exerts control over the rest of the body through e.g. hormones.

The cortex of the brain allows for cognition and abstract thoughts. Inside the central nervous system, there are several different cell types, such as the neurons and glia cells that support and maintain the neuronal integrity. Glia cells can be split into three groups: namely astrocytes, oligodendrocytes and microglia. The neurons, astrocytes and oligodendrocytes originate from the ectoderm, while microglia are derived from the yolk sac.

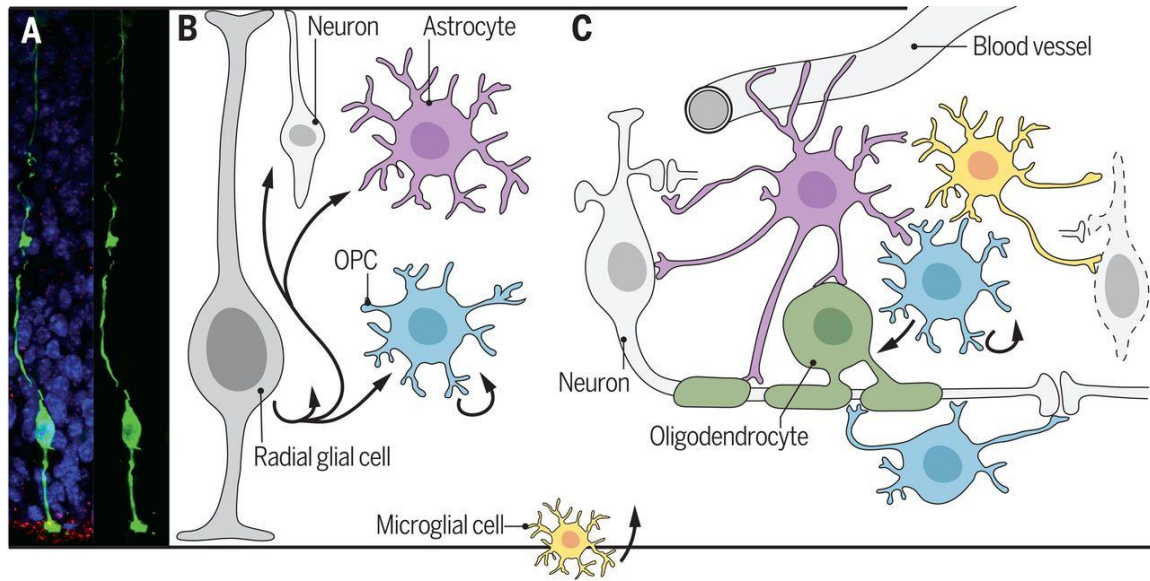


Figure 1: Central nervous system composition

In the central nervous system (CNS), most of the cells originate from the radial glia cells. Neurons, as well as OPCs and astrocytes are differentiating during development. Microglia on the other hand, the CNS resident immune cells, invade the brain from the yolk sac during embryonic development. Together, they form functional connections, which leads to a complex circuit known as the central nervous system. The CNS is responsible for coordinating all biological functions of the organism. OPC = oligodendrocyte precursor cell, CNS = central nervous system. Modified from (Allen & Lyons, 2018)

Astrocytes fulfill several functions in the nervous system. The two most important ones, are metabolic support of neurons and controlling extracellular ion levels at the synapses. It has been shown by many studies, that astrocytes are able to alter local blood flow upon neuronal activation (Gordon, Choi, Ellis-Davies, & MacVicar, 2012; Takano et al., 2006; Zonta et al., 2003). This is an important function, since it enables adaption of the system to the local need for additional nutrients. The second important function is the ability of astrocytes to buffer extracellular ion concentrations at the synapse to decrease harm to the neurons. It has been shown that an increased potassium ion concentration can lead to epileptic seizure-like events in hippocampal slice cultures (Gabriel et al., 2004) and even cell-death after prolonged ischemic insults (Leis, Bekar, & Walz, 2005). Therefore, clearance of excess potassium ions is extremely crucial to assure normal neuronal function and has been shown to be regulated by astrocytes (Bellot-Saez, Kékesi, Morley, & Buskila, 2017; Ma et al., 2016; Wallraff et al., 2006).

Microglia also have several distinct functions in the central nervous system. They are considered as tissue-resident immune cells, as they scavenge the tissue in search of pathogens and apoptotic debris. Additionally, microglia are able to phagocytose debris and further trigger immune response e.g. through cytokine-mediated signaling. During CNS development, they are also responsible for synaptic pruning (Paolicelli et al., 2011), which is a process by which microglia remove non-functional synapses between axons and dendrites to help form mature neuronal circuits. In disease related context, microglia also play an important role by phagocytosing e.g. myelin debris in demyelinating diseases, such as Multiple Sclerosis (MS) or Charcot-Marie Tooth disease as well as Alzheimer's disease and Parkinson's disease.

The third major cell type in the CNS are oligodendrocytes which generate myelin – a complex lipid membrane structure that spirally wraps around axons to enable saltatory nerve conduction and metabolic support (Nave, 2010).

1.2 Functions of oligodendrocytes

Mature oligodendrocytes fulfill several functions: they are mainly known to accelerate the conduction velocity of neuronal signal transmission by insulating the axonal membrane. The ion channels and pumps at the axonal membrane are clustered to regions between two neighboring myelin sheaths, which are called nodes of Ranvier. When a depolarization wave progresses along the axon, only at the nodes of Ranvier they can be extended and further transmitted. In between, the ions cannot exchange with the extracellular space due to the myelin shielding around the axon. Therefore, the depolarization jumps from node to node, accelerating the conduction velocity. This was evolutionary developed in different taxa, since the only other way to increase conduction velocity would otherwise be to increase axon diameter (Hartline & Colman, 2007; Huxley & Stampfli, 1949; Sato, Sato, & Suzuki, 1985).

In recent years, other functions of oligodendrocytes have emerged. Different research groups have shown that oligodendrocytes, together with astrocytes, are able to metabolically support the axons. It was shown that oligodendrocytes are able to shuttle lactate through monocarboxylate transporter 1 (MCT1) into the periaxonal space. From there, lactate can be taken up by the axon through MCT2 transporters and used for energy metabolism

(Bélanger, Allaman, & Magistretti, 2011; Funfschilling et al., 2012; Y. Lee et al., 2012; Tekkök, Brown, Westenbroek, Pellerin, & Ransom, 2005). Another study also pointed out that glucose might be the main metabolite of choice to deliver energy to axons in the corpus callosum (Meyer et al., 2018). Loading of cells with glucose, not lactate or pyruvate, prevented the reduction of compound action potential (CAP), which is the sum of action potentials of a group of axons. Additionally, studies with mice deficient in connexin 47, a protein which couples oligodendrocytes through gap junctions, validated that only functional oligodendrocyte networks could rescue CAP loss (Maglione et al., 2010).

Oligodendrocytes are expressing glutamate receptors during development, thereby being able to react to axon activity and glutamate signaling. This triggers proliferation and myelination, which will support the axonal needs (Gautier et al., 2015; Gudz, 2006; Wake, Lee, & Fields, 2011; Ziskin, Nishiyama, Rubio, Fukaya, & Bergles, 2007). It has further been proposed that neuregulin is important to switch between an activity-dependent and independent mechanism by regulating expression of N-methyl-D-aspartate receptors (NMDAR). During remyelination, glutamate signaling has been shown to be dependent, suggesting an important role for receptor mediated myelination (Lundgaard et al., 2013).

1.3 Myelin composition

1.3.1 Myelin lipids

Due to its high lipid content (70% of dry weight) myelin represents a unique type of membrane (Morell & Quarles, 1999). There are three types of major myelin lipids, namely cholesterol, galactolipids and inositols, which are crucial for the specialized function of this membrane.

1.3.1.1 Cholesterol

Cholesterol is an important lipid as it can regulate membrane fluidity, permeability and protein function (Espenshade & Hughes, 2007). Neurological phenotypes, like ataxia and tremor can be observed in mice that lack oligodendroglial squalene synthase, which is an enzyme necessary for the committing step in cholesterol synthesis. Oligodendrocytes lacking this enzyme are functionally impaired which results in delayed myelination and downregulated mRNAs for myelin proteins (Mathews et al., 2014; Saher et al., 2005). This highlights the importance of cholesterol in proper myelin formation and function. In a demyelinating disease models, it has been shown that increased myelin uptake by aged phagocytes can lead to the formation of cholesterol crystals that actually pierce the membrane and harm the cells itself. Moreover, this delays the clearance of debris and remyelination (Cantuti-Castelvetri et al., 2018). However, external cholesterol fed with chow can also be helpful for remyelination after cuprizone induced demyelination (Berghoff et al., 2017).

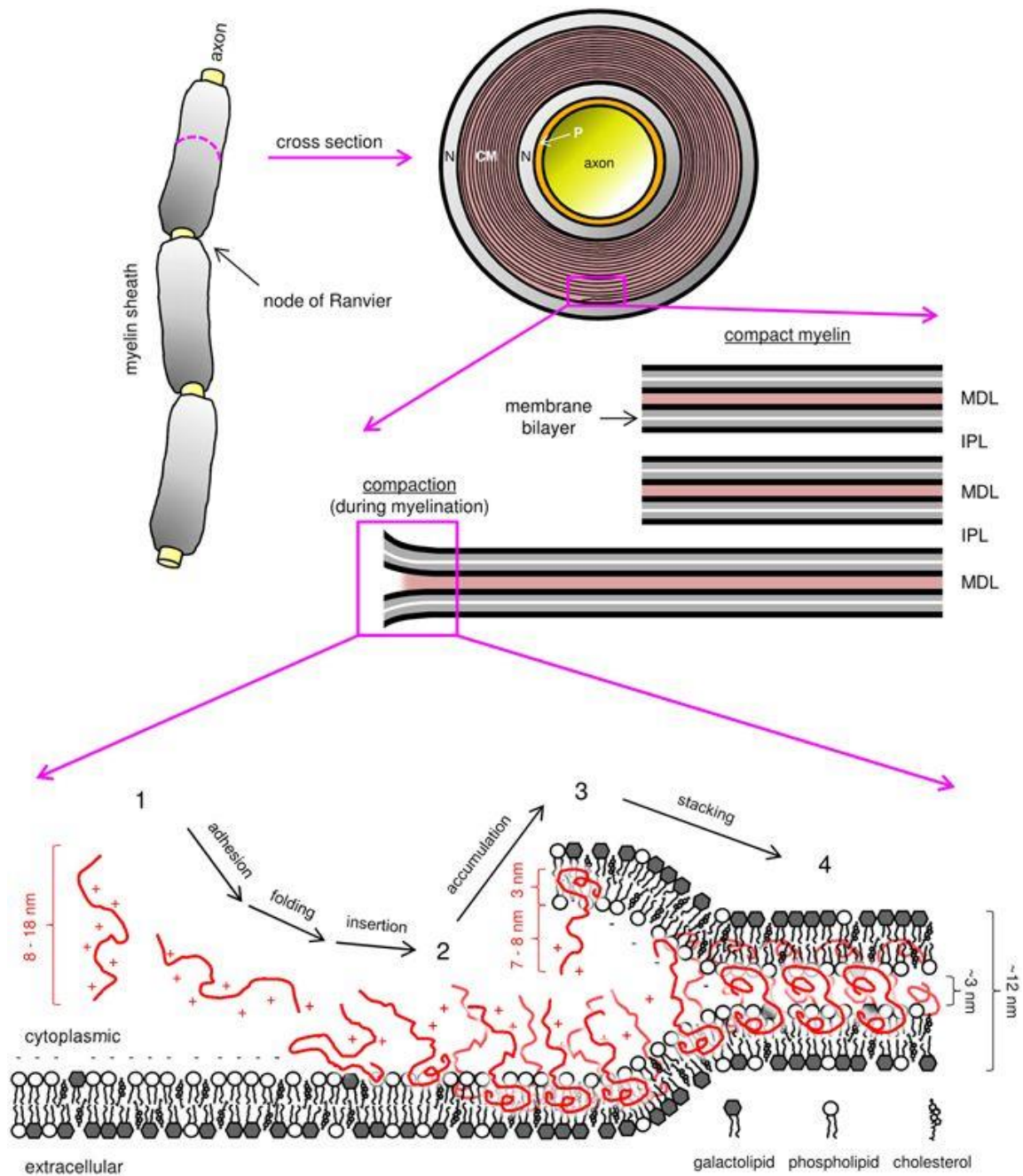


Figure 2: Myelin membrane composition

Myelin basic protein (MBP, red) is attracted to a negatively charged membrane (1). After the positive charge of MBP is neutralized, the protein is inserted into the membrane (2) and its accumulation favors the stacking (3) of another membrane layer. Conformational change of MBP leads to even further compaction of the two membranes, thereby forming the major dense line (MDL) (4). MBP = myelin basic protein, CM = compact myelin, N = non-compact myelin, P = periaxonal space; MDL = major dense line, IPL = intraperiod line. Modified from (Raasakka et al., 2017)

1.3.1.2 Galactolipids

The galactosphingolipid galactocerebroside has been shown to also affect normal myelin function. In a mouse mutant, that is deficient for UDP-galactose ceramide galactosyltransferase (CGT), oligodendrocytes were not able to synthesize galactocerebroside out of ceramide. This led to a decrease in conduction velocity and an early death of the mouse. Another study found, that galactocerebroside, in a CGT mutant mouse, could be replaced by a lesser efficient ceramide derivate glucocerebroside. Despite that, additional ataxia and tremor, as well as hind-limb paralysis in aged mice were visible (Bosio, Binczek, & Stoffel, 1996; Coetzee et al., 1996). Moreover these UDP-galactose ceramide galactosyltransferase deficient mice revealed changes in paranode formation but proper myelin function. Ultrastructural abnormalities like altered nodal length and absence of transverse bands were observed. Interestingly, these changes were only seen in the central, not in the peripheral nervous system (JL Dupree, Coetzee, Blight, Suzuki, & Popko, 1998; Jeffrey L. Dupree, Girault, & Popko, 1999)

Furthermore, deficiency in galactocerebroside enzyme function that is the enzyme responsible for removing galactose from ceramides, was found to be causative of Krabbe disease, also known as galactosylceramide lipidoses, an autosomal leukodystrophy. It is known to have a demyelinating outcome in the central and peripheral nervous system. In a genome-wide association study, the authors found six different mutations of the enzyme in patients with Krabbe disease, linking galactocerebroside processing with white matter integrity (Xu, Sakai, Taniike, Inui, & Ozono, 2006).

Galactocerebroside already seems to be important for proper myelin function. Another derivate of this molecule is sulfatide, which is also important for structural regulation. By genetically blocking the synthesis of sulfatides, which are synthesized from galactocerebroside by cerebroside sulfotransferase, mice displayed hind-limb ataxia and tremor and abnormalities in paranodal junctions (Honke et al., 2002). One of these studies additionally showed, that sulfatide deficient mice had a decreased sodium and potassium channel clustering on myelinated axons. Formation of the clusters and myelination itself was normal except the nodal length was altered again (Ishibashi et al., 2002).

1.3.1.3 Phosphatidyl-inositols

Phosphatidyl-inositols are another class of lipids that have been shown to be involved in myelin structure. Phosphatidylinositol 4, 5-bisphosphate (PIP₂) binds myelin basic protein (MBP), which is an important protein for compaction of membranes, to the membrane. When hydrolyzed by phospholipase C, upon increased Ca²⁺ concentration in the cytosol, MBP dissociated from the membrane. Additionally, vesiculation and de-compaction was observed (Nawaz et al., 2009; Weil et al., 2016). Another study also showed the connection between PIP₂ and MBP (Musse, Gao, Homchaudhuri, Boggs, & Harauz, 2008). Therefore, PIP₂ is crucial for binding MBP to the inner leaflet and leading to the compaction of the myelin sheaths.

Phosphatidylinositol-3, 4, 5-triphosphate (PIP₃) is produced by the phosphorylation of PIP₂ by phosphoinositide 3-kinase (PI3K). This lipid was found at the leading edge during myelination emphasizing its importance for myelin biogenesis. Besides, when PIP₃ levels drop again after myelination also the cytoplasmic channels close down. When PIP₃ is reintroduced by knocking out phosphatase and tensin homolog (PTEN), which inhibits myelination, myelination seems to re-start and the channels open up again (Snaidero et al., 2014). Other studies showed that the disruption of the PTEN together with mammalian disks large homolog 1 (DLG1) (Cotter et al., 2010) lead to redundant myelin formation in form of outfoldings and tomaculae (S. Goebbels et al., 2010; Sandra Goebbels et al., 2012). Therefore, PIP₃ is of great importance regarding the regulation of myelination in development and during adulthood.

1.3.2 Myelin proteins

1.3.2.1 Myelin basic protein (MBP)

Proteins are the second major component of the myelin sheath making up to 30% of dry weight. As aforementioned MBP is important for compaction of the myelin sheaths (Snaidero et al., 2017). Its function is also important for CNS integrity, since MBP defects have severe consequences for myelin ultrastructure due to the formation of membrane tubules as shown with a natural occurring mouse mutant called shiverer (Chernoff, 1981). As the name suggests, these mice are shivering due to impaired axonal insulation. More precisely, initial formation of the myelin sheath is not affected, but its compaction is absent leading to the formation of membrane tubules. Thus, these mice die prematurely and

develop severe tremor two weeks after birth. (Shen, Billings-Gagliardi, Sidman, & Wolf, 1985). This highlights the importance of MBP in formation of the compacted myelin sheath. It has further been shown in animal models, mimicking MS, like experimental autoimmune encephalomyelitis (EAE) or neuromyelitis optica (NMO), that loss of MBP leads to vesiculation at the inner tongue. This might be triggered by Ca^{2+} influx leading to ultrastructural changes within the myelin sheath ultimately resulting in the loss of compaction (Weil et al., 2016).

1.3.2.2 Proteolipid protein (PLP)

Proteolipid protein (PLP) is together with MBP the most abundant protein in the myelin sheath, which mainly interacts with cholesterol and galactosylceramide lipids (Simons, Krämer, Thiele, Stoffel, & Trotter, 2000). Therefore, it is able to stabilize the intraperiodal line, which is formed by compaction of adjacent membranes (Klugmann et al., 1997). Defects in this protein are linked to Pelizaeus-Merzbacher disease (PMD), highlighting its importance in normal myelin function (Lyahtai et al., 2018; Yool, Edgar, Montague, & Malcolm, 2000). PMD has clinical hallmarks like tremor, loss of movement of the limbs and horizontal movement of the eyes (Osório & Goldman, 2018). Another study showed that progression of PMD was prevented by external cholesterol treatment due to a cholesterol-rich diet. Notably, there is evidence that cholesterol is important for PLP trafficking and incorporation in the myelin sheath (Saher et al., 2012; Simons et al., 2000).

1.3.2.3 Other myelin proteins

Other abundant proteins within the myelin membrane include 2', 3'-cyclic nucleotide 3'-phosphodiesterase (CNP), myelin oligodendrocyte glycoprotein (MOG), myelin-associated glycoprotein (MAG), which all fulfill important roles like axon-glia adhesion (MAG), process outgrowth (CNP) and speculated adhesive function (MOG) (Johns & Bernard, 1999; J. Lee, Gravel, Zhang, Thibault, & Braun, 2005; Schnaar et al., 1998). Together, the balance of lipids and proteins in the myelin sheath are important for its assembly, maintenance and proper function.

1.4 Origins of oligodendrocytes and formation of myelin

Myelin was firstly described by Rudolf Virchow (1854), who tested and compared different tissues on their chemical properties. Later on Louise-Antoine Ranvier (Ranvier, 1878)

described in more detail how myelin is wrapped around the nerve fibers and that the nodes of Ranvier are regularly appearing along the axon. In 1962 (Bunge, Bunge, & Pappas, 1962), it was shown for the first time that the myelin sheath was connected to oligodendrocytes on ultrastructural level using electron microscopy.

Oligodendrocytes derive from oligodendrocyte precursor cells (OPC), which are descendants of neural stem cells (Naruse et al., 2016). The OPCs colonize the brain in different waves and from different areas. The forebrain is getting colonized with a first wave at embryonic day 12.5 from the medial ganglionic eminence. Under physiological conditions OPCs from this wave are later on not found anymore. In case of malfunctioning of the other waves, however, these cells can compensate (Kessaris et al., 2006). The second wave arises from a more dorsal point, namely from the caudal ganglionic eminences at embryonic day 15.5. Finally, the third wave, which later migrates into the cortex, derives from the dorsal subventricular zone. Cerebellar and spinal cord OPCs are generated in other regions and time points as reviewed by (Naruse, Ishizaki, Ikenaka, Tanaka, & Hitoshi, 2017; van Tilborg et al., 2018).

Migration of the newly produced OPCs to their site of destination have been described broadly: this can be mediated by either growth factors, extracellular matrix components, axon guidance factors and NMDA receptor mediated signaling (Bribián, Barallobre, Soussi-Yanicostas, & de Castro, 2006; Milner, Edwards, Streuli, & French-Constant, 1996; Okada, Tominaga, Horiuchi, & Tomooka, 2007; C. Wang et al., 1996; H. Zhang, Vutskits, Calaora, Durbec, & Kiss, 2004). Moreover, blood vessels have been recently shown to act as a guidance for migration for OPCs (Tsai et al., 2016).

Once the OPCs have reached their destination, they start to extend their processes to find axons that can be myelinated. Not all axons are myelinated, which can depend on size and activity (Klingseisen & Lyons, 2018). Once contact is established, oligodendrocytes start to wrap their processes around the axon with the growing myelin membrane, the so called leading edge moving around the axolemma, thereby extending underneath the previously formed layers. The layers start to extend laterally until neighboring sheaths are close by, ultimately forming small unmyelinated gaps called Node of Ranvier. The finally regularly spaced myelin segments are called internodes. At the nodes ion channels on the axonal membrane are clustered allowing for interaction with the extracellular space.

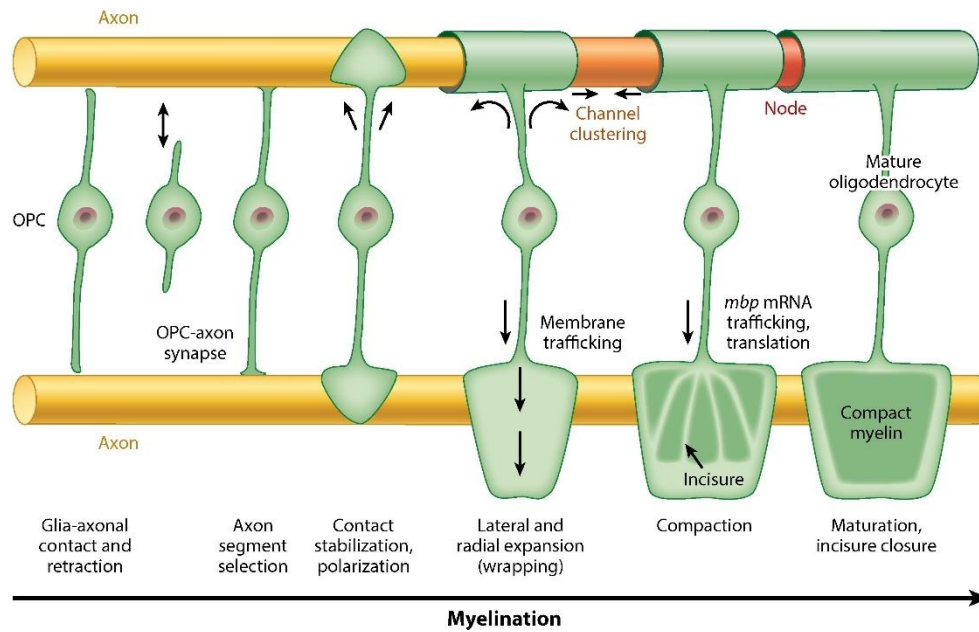


Figure 3: Wrapping of oligodendrocyte membrane around the axon

Oligodendrocyte precursor cells (OPC) extend their processes until they reach an appropriate axon. After contact is established, the sheath rolls around the axon by inserting the leading edge underneath the previous wrap in order to form a multilayered sheath. Lateral and radial expansion occurs during growth of the myelin sheath. Membrane trafficking is achieved through transport along non-compacted incisures in already compacted layers. The mature sheath loses its channels and compact myelin establishes insulation of the axon. OPC = oligodendrocytes precursor cell, node = Node of Ranvier, MBP= myelin basic protein, mRNA = messenger RNA. Modified from (Nave & Werner, 2014)

During the growth of the myelin sheath, cytoplasmic channels, which are regulated by an interplay between the two major myelin protein CNP and MBP are necessary in order to transport the newly synthesized membrane to the leading edge (Snaidero et al., 2017). When MBP expression is increased upon maturation of the sheaths, the non-compact myelin that is rich in cytosol starts to compact, thereby slowly closing the cytoplasmic channels. In this process, MBP acts as a molecular sieve and extrudes protein with a certain size in order to bring the opposing membranes together.

The lateral growth of the myelin sheath is accompanied by the occurrence of myelin outfoldings, which starts to decrease again in the first 8 postnatal weeks (Snaidero et al., 2014). Their presence at later stages is usually associated with pathological myelin in disease states (Bolino et al., 2004)

1.5 Epigenetic control of the myelin sheath

DNA methylation was shown to drive oligodendrocytes lineage differentiation: a study has suggested that DNA methylation transferase 1 (DNMT1), which is responsible for maintenance of methylation, is important for differentiation of OPCs. Due to a DNMT1-deficiency in a mouse mutant, OPC growth was arrested accompanied by severe endoplasmic reticulum stress. Furthermore, Moyon *et al.* showed a correlation between methylation status and gene expression: hypomethylated promotor regions correlated with an upregulation of genes related to lipid metabolism, phospholipid biosynthesis and cholesterol biosynthesis. In contrast, hypermethylated promoter regions correlated with downregulation of genes important for cell cycle, morphogenesis and cell migration. Hence, less oligodendrocytes and less myelination was seen compared to the wild type control (Moyon et al., 2016). Furthermore, a second study suggested that although DNMT1 was reported to be important for developmental OPC regulation, DNMT3 was essential to be more important for a proper remyelination after lysolecithin-induced demyelination, as DNMT1 mutants did not show reduced remyelination compared to DNMT1/3 and DNMT3 mutant mice (Moyon et al., 2017).

Furthermore, another study has led to the assumption that there is a relationship of MBP to DNA methylation in context of MS. Here, the authors observed a decrease in the methylation of the promotor region of peptidyl arginine deiminase 2 (PAD2) in DNA from MS patients. This enzyme is responsible for citrullination of MBP, which is known to be linked to loss of compacted membrane due a less stable interaction of MBP to the negatively charged membrane. The concentration of citrullinated and less positively charged MBP is increased in myelin from MS patients. Therefore, changes in DNA methylation status may play a critical role in MS pathology (Fabrizio G. Mastronardi, Abdul Noor, D. Denise Wood, Tara Paton, 2007; Moscarello, Mastronardi, & Wood, 2007)

Other epigenetic regulators include histone modifications and micro RNAs, that have been shown to influence OPC differentiation as reviewed by (J. Liu, Moyon, Hernandez, & Casaccia, 2016). Micro-RNA miR-23 was described to be inhibiting PTEN, which is responsible for repression of myelination, through the long intergenic noncoding RNA (lincRNA) 2700046G09Rik (Lin, Heng, Ptáček, & Fu, 2014). This led to increased oligodendrocyte differentiation.

Histone deacetylase 3 (HDAC3) was shown to be important for the commitment of the neural precursor cell to either the oligodendrocyte or astrocyte lineage. If HDAC3 binds to p300, NF1A and Stat3 mediated astroglialogenesis is blocked and oligodendrogenesis is favored (L. Zhang et al., 2016). Another study showed that HDAC1 and HDAC2 can stimulate the differentiation of oligodendrocytes by acting on transcriptional repressors HES5 and ID2/4 that are induced by Notch and Wnt signaling. When HDAC1 and 2 are present they compete with NICD and β -catenin, which would normally lead to repression (Ye et al., 2009).

1.6 Plasticity of the myelin sheath

Myelination is not just a normal developmental process, but it is also necessary in order to adapt and learn from experience. For a long time glia were only seen as supporting cells. But over the last two decades it has been acknowledged that these cells have a more important role in network adaptation.

McKenzie and colleagues (2014) showed that mice that are devoid of the transcription factor myelin regulatory factor (MyRF) in newly formed oligodendrocytes are not capable of acquiring the skill to run on a complex running wheel. This study showed a form of plasticity related to adaptive myelination, since the mice were already in an adult stage where most of myelin biogenesis is thought to be completed. Furthermore, their lab could show, that this increase in oligodendrocyte production and myelination occurs already as early as a few hours after the environment changed (L. Xiao et al., 2016). This means myelination can be seen as a tool to adapt the circuit to the needs of environmental changes.

Similar events were seen in another study, where the stimulation of neurons was achieved by a new technique called optogenetic stimulation. Here, channelrhodopsin 2 was genetically coupled to Thy1 neurons in the premotor cortex. This channel allows for induction of neuronal spiking with a pulse of blue light at 470 nm wavelength. This leads to a region and cell type specific activation similar to voluntary movement. Consequently, an increase in oligodendrocyte precursor cell proliferation and a change in myelin thickness at the corpus callosum underneath the premotor cortex could be shown by the authors (Gibson et al., 2014).

On an ultrastructural level, Tomassy *et al.* (2014) showed new patterns of myelination in the adult brain. They detected different patterns of myelination in the visual and somatosensory cortex. Axons from pyramidal neurons showed prolonged gaps between myelin internodes of up to 55 μm length, that have never been described before. Noteworthy, normal nodes of Ranvier have a length of 1 μm . Hence, these prolonged gaps could be another form of neuronal network regulation as synapses were also detected at those gaps. This could imply signaling capabilities, rather than random occurrence during normal development. These new pattern raise the question of its function, because such an arrangement is not compatible with saltatory nerve conduction. It is known from an earlier study, that only 30% of axons are myelinated in the corpus callosum of 240 day old mice (Sturrock, 1980). Taken together, this could mean that the other 70% of unmyelinated axons could be used to fine tune myelination and therefore, nerve conduction as reaction to environmental changes in early adulthood. This is supported by the work of Hughes *et al.* which show through in vivo imaging the dynamic myelination after environmental enrichment (Hughes, Orthmann-Murphy, Langseth, & Bergles, 2018). Although, another study suggested that the gaps close as the mice are maturing (Hill, Li, & Grutzendler, 2018). Therefore, this might just be a temporary way of adapting to the environment, such as running on a complex wheel, during development.

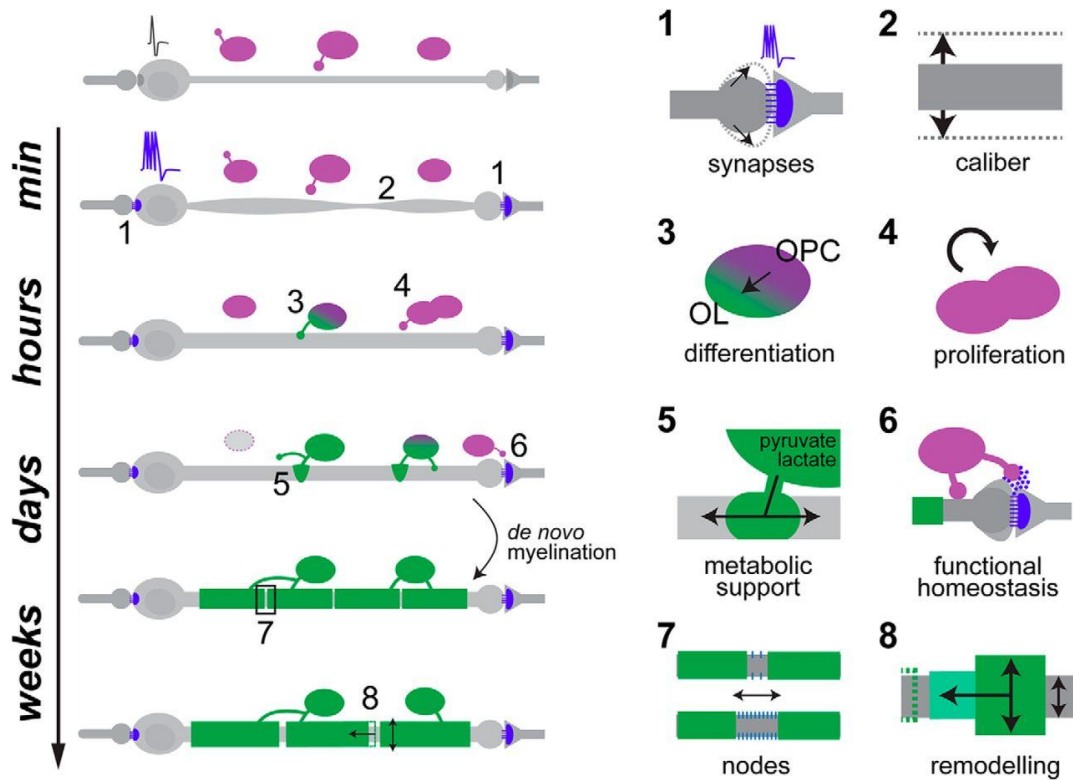


Figure 4: Speculated timeline of adaptive myelination

Myelin can be adjusted in different ways in order to change conduction velocity. Synaptic (1) or axonal caliber (2) changes can occur within minutes. This can trigger oligodendrocyte precursor cell (OPC) differentiation (3) and proliferation (4). Newly formed oligodendrocytes (OL) are able to metabolically support (5) the axon or regulate homeostasis at the synapse (6). This can be observed within hours and days after stimulation. Internodes can be remodeled either in length (7) at the nodes of Ranvier or in thickness (8) to change circuit timing. This happens during days and weeks after stimulation. OPC = oligodendrocyte precursor cell, OL = oligodendrocyte, nodes= Node of Ranvier, Modified from (Almeida & Lyons, 2017)

Studies with human subjects were also conducted looking at the effects of physical training like juggling (Scholz, Klein, Behrens, & Johansen-Berg, 2009) or musical training (Schmithorst & Wilke, 2002) on white matter plasticity. Here, changes in the genu of the corpus callosum or the white matter under the intraparietal sulcus could be observed. Other examples of human behavioral changes after meditation or reasoning are described in a review by Wang & Young (2014). However, those studies were not done on cellular basis, but done using magnetic resonance imaging (MRI), and do not have the necessary resolution to elucidate functional mechanisms after stimulation.

Other forms of plasticity were shown during early development, by three different groups within the zebrafish model system. The first one described a novel form of myelin pruning by the oligodendrocyte itself during the first 7 days after fertilization of the egg. Here, 28% of myelin segments of the developing spinal cord actually were retracted again. One potential mechanism for this could be through NRG-ErbB signaling as pruning was reduced upon NRG knockdown (P. Liu, Du, & He, 2013).

Following this study, two other groups both described Ca^{2+} dependent retraction of myelin sheaths. Live imaging revealed that axonal activity induced calcium transients can regulate myelin sheath retraction or elongation. Elongation is favored by high frequency Ca^{2+} transients, while retraction is preceded by low frequency Ca^{2+} transients (Baraban, Koudelka, & Lyons, 2018; Krasnow, Ford, Valdivia, Wilson, & Attwell, 2018). This also links neuronal activity to developmental myelin modulation.

Opposite effects are seen, when mice are not challenged, but socially isolated: here, a reduced myelin thickness in the prefrontal cortex could be shown. Mice were socially isolated for two weeks after weaning. Those mice showed a significant reduction in social exploration compared to mice that were housed in regular or enriched environments. Furthermore, the myelin thickness seemed to be reduced in the medial prefrontal cortex. Interestingly, this happened only when mice were isolated at an early developmental time point. When the same experiments were performed with older mice, these effects were not seen (Makinodan, Rosen, Ito, & Corfas, 2012). This suggests a short time span during development, where plasticity is possible.

Along those lines, another paper showed the effects of sensual deprivation by cutting of whiskers of mice on myelination. Here, they could show that sensual deprivation leads to a decrease in myelinated axons at p60 in the barrel cortex, as well as a delayed and reduced onset of local field potentials after stimulation (Barrera et al., 2013).

1.7 Origins of microglia and their function during development

The tissue-resident immune cells of the CNS, the so called microglia arise from yolk-sac myeloid progenitor cells. They enter the brain in two different waves around embryonic day 9 and 14 (Ginhoux et al., 2010; Rigato, Buckinx, Le-Corronc, Rigo, & Legendre, 2011; Swinnen et al., 2013). During early development, they are actively scavenging the tissue for

cellular debris from apoptotic cells fulfilling their role as resident immune cells. Therefore, they take on a ramified morphology, which allows them to quickly screen their environment (Davalos et al., 2005; Nimmerjahn, Kirchhoff, & Helmchen, 2005). Throughout life microglia are able to maintain their population by self-renewal in contrast to other cells of the myeloid lineage (Ajami, Bennett, Krieger, Tetzlaff, & Rossi, 2007; Lawson, Perry, & Gordon, 1992).

During normal development, microglia are important for pruning of synapses. For instance it was shown that they are actively engulfing and phagocytosing PSD95 positive synapses. Furthermore, the amount of dendritic spines at day 15 on pyramidal neurons of the CA1 region of the hippocampus was significantly increased in microglia knock out mice (Paolicelli et al., 2011). Others also show a remodeling function of microglia through complement receptor 3 (CR3)/C3-mediated pruning of presynaptic inputs (Schafer et al., 2012).

Microglia also play an important role in neuronal circuit formation by regulating the neuronal cell number, e.g. as they are actively involved in inducing programmed cell death (PCD) in Purkinje cells via superoxide ions (Marín-Teva et al., 2004). Another study showed, that CD11b and DNAX-activation protein 12 (DAP12) deficient mice are not able to induce hippocampal neuronal PCD (Wakselman et al., 2008). A recent study even presented a microglia population that is associated to white matter proliferative regions during development. This population seems to display an amoeboid morphology and expresses genes that are normally seen in disease-associated microglia (DAM) which are found amongst others in neurodegenerative diseases. Those DAM associated genes are mainly responsible for lipid sensing and metabolism, as well as for phagocytosis of debris. Lately it was shown that those microglia associated to proliferative zones are phagocytosing newly myelinating oligodendrocytes (Keren-Shaul et al., 2017; Li et al., 2019).

Further roles include trophic support of subcerebral and callosal projection neurons through insulin-like-growth factor 1 (IGF-1) signaling (Ueno et al., 2013) and arranging embryonic neural precursor proliferation (Antony, Paquin, Nutt, Kaplan, & Miller, 2011).

1.8 Main microglia receptors

There are two kinds of receptors used by microglia for different ligands and to trigger different responses. Toll like receptors (TLRs) or Fc-receptors (FcRs) are triggered by viral or microbial intruders. As a reaction they promote inflammation by secreting molecules like tumor necrosis factor α (TNF α), interleukin-1 β (IL-1 β) and nitric oxide (NO) (Stridh et al., 2013; Yao et al., 2013). This triggers an immune response in order to clear the intruding microbes (Olson & Miller, 2004).

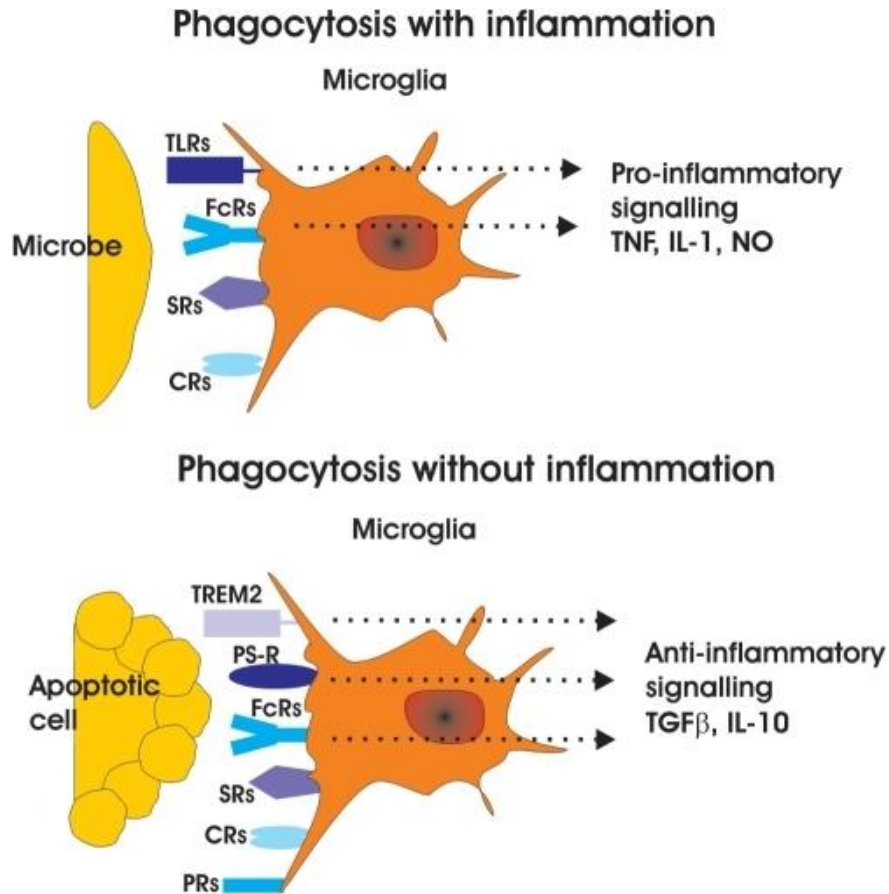


Figure 5: Different types of microglia receptors and relation to inflammation

Microglia receptors can lead to a pro-inflammatory response through TNF, IL-1 and NO signaling by sensing microbes through receptors such as TLRs, FcRs and SRs. In contrast to that, other receptors like TREM2, PS-Rs and PRs sense apoptotic cells and then trigger an anti-inflammatory response through TGF β and IL-10 signaling. TLRs = toll like receptors, FcRs = Fc-receptors, SRs = scavenger receptors, CRs = complement receptors, TNF = tumor necrosis factor- α , IL-1 = interleukin-1 β , NO = nitric oxide, TREM2 = triggering receptor expressed on myeloid cells-2, PS-R = phosphatidylserine receptors, PRs = purine receptors, TGF β = transforming growth factor- β , IL-10 = interleukin-10, Modified from (Neumann, Kotter, & Franklin, 2009)

The second kind of receptor recognizes apoptotic cellular debris from neurons or other cells, but does not trigger inflammation. Receptors like triggering receptor expressed on myeloid cells-2 (TREM2) or phosphatidylserine receptors (PSRs) fall into this category. Through activation of these receptors, anti-inflammatory response can be mediated through transforming growth factor beta (TGF- β) and interleukin-10 (IL-10) (Bohlen et al., 2017; Butovsky et al., 2014; Krasemann et al., 2017; Lively, Lam, Wong, & Schlichter, 2018; Y. Q. Xiao et al., 2008). It was shown, that TREM2 mediated clearance of apoptotic debris, at

the peak of demyelination in an EAE model, was increased and an anti-inflammatory environment was observed marked by boosted IL-10 levels (Takahashi, Prinz, Stagi, Chechneva, & Neumann, 2007). By TREM2 ablation microglia did indeed tend towards a pro-inflammatory direction and were not able to phagocytose apoptotic neurons. Furthermore, the interaction with DAP12, also known as TYRO protein tyrosine kinase-binding protein (TYROBP), leads to a reorganization of the cytoskeleton and phagocytosis of the debris (Takahashi, Rochford, & Neumann, 2005). Mutations in TREM2-DAP12 have also been linked to Nasu-Hakola disease, which is characterized by early progressive dementia and bone cysts (Paloneva et al., 2000, 2002). The secondary role of DAP12 is crucial for osteoclast development (Humphrey et al., 2004).

1.9 Microglia function in diseases

During the progression of Alzheimer's disease (AD), microglia fulfill multiple functions as they are able to sense, surround and phagocytose extracellular protein accumulations, namely β -amyloid plaques, amongst others through TREM2 signaling (Y. Wang et al., 2015; Yuan et al., 2016). Certain lipids that bind to β -amyloid plaques that might be responsible for neurotoxic spreading, can be retained by microglia clustering through TREM2 sensing (Y. Wang et al., 2016; Yuan et al., 2016). Furthermore, TREM2 is able to take up A β -peptides, mediated through binding to apolipoprotein E and J (APOE/APOJ) (Parhizkar et al., 2019; Yeh, Wang, Tom, Gonzalez, & Sheng, 2016).

The TREM2 signaling is not only necessary for uptake, but also for proliferation and survival of the microglia cells themselves (Keren-Shaul et al., 2017; Y. Wang et al., 2015). This might be a mechanism regulated through mammalian target of rapamycin (mTOR)-signaling, since TREM2 deficiency in an Alzheimer's mouse model lead to changed metabolism and increased cell death of microglia (Carlyle et al., 2015). Interestingly, TREM2 mutations correlate with a high risk of developing late onset Alzheimer's disease (Guerreiro et al., 2013; Jonsson et al., 2013).

In models of MS, microglia can fulfill multiple functions like releasing pro-inflammatory cytokines or clearing myelin debris as reviewed by Luo *et al.* (2017). Additionally, microglia and macrophages have been shown to promote oligodendrocyte precursor proliferation in mouse model for MS in demyelinated lesions (Miron et al., 2013). Another

study showed that during an EAE induced demyelination, macrophages that are recruited from monocytes from the peripheral system, move towards nodes and initiate demyelination and a pro-inflammatory response, while tissue-resident microglia are actually phagocytosing debris without an pro-inflammatory answer (Yamasaki et al., 2014). Furthermore, patient samples from MS patients have been shown, to have an increased concentration of soluble TREM2 (sTREM2) in their cerebrospinal fluid (CSF). This is actually decreased after patients have been treated with natalizumab or mitoxantrone, highlighting sTREM2 as a possible marker for microglia activation (Öhrfelt et al., 2016). Another study also suggested a regulatory function of sTREM2 in disease progression, but the exact function can only be speculated (Piccio et al., 2008). High levels of Tau, which correlates better with AD progression than A β pathology, where accompanied by increased amounts of sTrem2 in the CSF. Notably, in the presence A β pathology, sTrem2 levels were decreased (Schwarz et al., 2016; Suárez-Calvet et al., 2019). STREM2 might also be a feed-forward signal induced by interleukin-13 (IL-13) signaling, to stimulate macrophage proliferation and a pro-inflammatory response that leads to chronic inflammation. But this has only been shown in macrophages, not in CNS microglia (Wu et al., 2015).

1.10 Project aim

This study was conducted to further investigate the plasticity of myelin during developmental and environmental changes. Recent technology like batch isolation of tissue specific methylated DNA for immunoprecipitation (Bits-meDIP) was used to investigate the gene expression control, during complex motor skill learning of mice on a running wheel. Furthermore, serial block-face scanning electron microscopy (SBF-SEM) and transmission electron microscopy (TEM) and RNA sequencing were used to elucidate the ultrastructural changes of myelin during optic nerve development. Moreover, I aimed to identify changes in gene expression in microglia during pruning of myelin.

2 Materials and Methods

2.1 Material

2.1.1 Chemicals and consumables

All chemicals used were from SIGMA Aldrich, Thermo-Fischer or Roche, EMS, Science Services, Merck unless stated otherwise.

2.1.2 Antibodies

Following antibodies were used:

Table 1: Antibodies used for immunohistochemistry

Epitope	Reactivity	Dilution	Producer	Cat. No.
GFAP	guinea pig	1:400	Synaptic System	173004
Iba1	rabbit	1:400	Wako	019-19741
APC (CC1)	mouse	1:100	Calbiochem	OP80
PDGFRα	rat	1:500	Affymetrix eBioscience	14-1401
CD68	rat	1:100	Bio-Rad	MCA1957GA
Mac2/ Galectin-3	rat	1:200	Biolegend	125402
LAMP1	rat	1:100	Santa Cruz	SC-19992
MBP	rabbit	1:300	Dako	A0623
MBP	sheep	1:4000	Chemicon	AB9046
MHC II	rat	1:200	Affymetrix eBioscience	14-5321

NeuN	ms	1:500	Millipore	MAB377
Olig2	rb	1:500	IBL	18953
Mac-3	rat	1:50	BD Bioscience	553322

2.1.3 General buffers and solutions

2.1.3.1 PBS

A stock solution of 10X was prepared like the following:

80 g	NaCl
2 g	KCl
14.4 g	Na ₂ HPO ₄
2.4 g	KH ₂ PO ₄
H ₂ O (VE) ad 1l	

Adjust pH to 7.4

2.1.3.2 PFA

A stock solution of 500 ml 16% pFA in 1X PBS was prepared like the following:

400 ml of ddH₂O were heated in the microwave to 60 °C. Then 80 g of pFA powder, 50 ml of 10X PBS and one pellet of NaOH were added and stirred under the hood until the pellet was dissolved. Then the pH was adjusted to 7.4 with 37% HCl. DdH₂O was added until 500 ml were reached. 50 ml aliquots were stored at -20 °C.

2.1.3.3 Blocking solution

A stock solution of 500 ml in 1X PBS was prepared like the following:

50 ml of fetal calf serum, 50 ml of bovine serum albumin and 50 ml of fish gelatin were dissolved in 350 ml of PBS. This mixture was then aliquoted in 50 ml conical tubes and stored at -20 °C.

2.1.3.4 Mowiol

The mowiol solution was prepared by mixing 2.4 g mowiol with 6 ml of ddH₂O and 6 g glycerol for a few hours at room temperature (RT). Then, 12 ml of 0.2 M Tris-HCl (pH 8.5) were added and stirred at 60 °C for 10 min until it was centrifuged at 4000 g for 15 min. This solution was then aliquoted in 2 ml tubes and stored at -20°C.

2.1.3.5 Anesthetic

The mouse was anesthetized according to the body weight. 6 µg of Ketamine (10% Ketamine, WDT, Garbsen, Germany) and 900 µg of Xylazine (2% Rompun, Bayer Vita, Leverkusen, Germany) per 10 g of body weight were injected intraperitoneally (ip).

2.1.3.6 Phosphate buffer (PB)

A stock solution of 5X PB 0.1 M 200 ml was prepared like the following:

0.36 g NaH₂PO₄*H₂O

3.1 g Na₂HPO₄*2H₂O

ddH₂O ad 200 ml

The working solution was prepared by diluting 5X with ddH₂O.

2.1.3.7 Formvar

This solution was prepared by mixing 50 ml chloroform with 625 mg Formvar (Plano, Wetzlar, Germany) for 30 mins. It was stored at room temperature (RT) for up to 2 months, while protected from light by aluminum foil.

2.1.3.8 Richardson's Methylene Blue / Azur II blue

This solution was used for staining of lipid rich areas in semithin sections. Here, two solutions consisting off 1% [w/v] Azur II in ddH₂O and 1% [w/v] Methylene Blue in ddH₂O containing 1% sodium borate were mixed 1:1. This was produced freshly and filtered through a 0.22 µm millipore filter before use.

2.1.3.9 Low sucrose buffer (nuclei isolation)

0.32 M	sucrose
5 mM	CaCl ₂
5 mM	Mg(Ac) ₂
0.1 mM	HEPES pH 8
1 mM	DTT
0.1%	Triton-X-100

→add protease inhibitors (Complete, Roche) by dissolving 1 tablet in 10 ml (10x) and dilute it to 1x for use

2.1.3.10 High sucrose buffer

1 M	sucrose
3 mM	Mg(Ac) ₂
10 mM	HEPES pH8
1 mM	DTT

2.1.3.11 Lysis buffer for meDIP

140 mM	NaCl
1 mM	EDTA
1%	Triton-X-100
0.1%	sodium deoxycholate
10 mM	Tris-Cl, pH 8
1%	SDS

2.1.4 Software

Following software was used:

Table 2: Software used to analyze produced data

Name	Use	Developer
ImageJ	Image processing	Wayne Rasband (NIH)
MIB	Image reconstruction	Ilya Belevich, Merja Joensuu, Darshan Kumar, Helena Vihinen. Eija Jokitalo, University of Helsinki
Imaris	Image reconstruction	Bitplane
LSM software	Image acquisition	Leica
ImageSP	Image acquisition	SYS-PROG & TrS
Mendeley	Reference Manager	Mendeley Ltd.
GraphPadPrism	Statistics	GraphPad Software, Inc.
Adobe Illustrator	Image Illustration	Adobe Systems
R	Statistics	Lucent Technologies

2.2 Methods

2.2.1 Animal handling

All the wild type animals in this study were bred in the animal facility of the Max-Planck Institute of Experimental Medicine and kept in a 12 h light/dark cycle with food and water *ad libitum*. The experiments in this thesis were performed according to the German animal welfare law and the regulations of the state of Lower Saxony for animal experiments.

MerTK Transgenic mice were generated in the laboratories of Trevor Kilpatrick and Michele Binder at the Florey Institute of Neuroscience and Mental Health in collaboration

of Dr. Renate Lewis of the Transgenic Vectors Core at the Hope Center for Neurological Disorders (St Louis, MO, USA). In brief, exon 2 of the *Mertk* gene was flanked with loxP sites to allow for cre-mediated deletion, thereby introducing early stop codons. Cx3Cr1Cre mice (Goldmann et al., 2013) were purchased from the centre national de la recherche scientifique (CNRS, Paris, France).

B6.129P2-*TREM2*^{tm1cln} (*TREM2*) transgenic mice (Exon 3 and 4 were replaced by a floxed neomycin cassette, which was excised in the germline and backcrossed to C57Bl/6) were kindly provided by Christian Haas (Turnbull et al., 2006).

2.2.2 Complex running wheel

This behavior experiment was done in collaboration with Prof. Dr. Liebetanz from the University Medical Center Göttingen (UMG). The motor skills sequence (MOSS) paradigm was performed also at the UMG.

Animals were single housed with a 12/12 hour light/dark cycle. Water and food was available *ad libitum*. One group ran for three weeks on the training wheel with all rungs intact. The other group ran for two weeks on the training wheel and for the last week on the complex wheel where different rungs were missing according to an irregular pattern (Liebetanz et al., 2007). Running activity, speed and distance was measured automatically with a sensor connected to the wheel. On day 0, day 3 and day 7 after the complex wheel was inserted into the cage, tissue was collected and flash frozen in liquid nitrogen and stored at -80°C.

2.2.3 Tissue preparation for Immunohistochemistry

The mouse was weighed and the respective amount of a Ketamin/Xylazin solution was injected ip into the animal. After the absence of eye and foot reflexes was ensured the animals abdominal cavity was cut open to expose the heart. Then, a 29 G butterfly needle (B. Braun, Melsungen) was inserted into the left ventricle and the right atrium was cut open. First, the blood was flushed out by perfusion with ice cold PBS through a peristaltic pump (0.2-0.5 ml/sec). After the liver turned pale yellow and the arteries lost the red color, the solution was switched to ice-cold 4% pFA (in PBS) until the mouse turned stiff (~10 min). The respective tissue of interest was dissected and fixed further over night at 4 °C in the fixation solution. Water within the sample was removed by incubation in 30% sucrose (in

PBS) solution at 4 °C until the sample sank to reduce morphological damage upon freezing. In the next step, the tissue was frozen embedded in Tissue-TekCryo OCT (Thermo Scientific, Epsom, UK) and stored at -80 °C until they were cut. Tissue sections (~15 µm) were produced using a Leica cryostat (Leica CM1950, Leica Biosystems, Nussloch, Germany) and either directly mounted on a glass slide or stored in cryoprotective solution (25% glycerol, 25% ethylene glycol in PBS) at -20 °C.

Optic nerves were removed without perfusion after cervical dislocation of the animal and then, immediately immersion-fixed overnight in 4% pFA (in PBS) solution at 4°C. Afterwards the sample was processed as described above.

2.2.4 Immunocytochemistry of optic nerve

The 15 µm sections were first rehydrated with 1X PBS for 5 minutes at room temperature. Afterwards, the sections were blocked for 1 h with 100% BS and 0.1% Triton-X-100 at room temperature. Then, they were incubated with primary antibodies diluted in 2.5% BS at 4 °C overnight. The next day, the sections were washed three times for 10 minutes with PBS and incubated with the secondary antibodies diluted 1:1000 in PBS for 1 h at room temperature or overnight at 4 °C. Finally, they were washed three times with PBS and one time with ddH₂O before being mounted on a coverslip with Mowiol at room temperature. The same stainings were usually imaged with the same laser intensities. The percent area fraction covered was calculated with the same threshold for the development time series using the FIJI measurement tool.

2.2.5 Cell counting

For the quantification of immunohistochemical stainings a tilescan of one 15 µm thick longitudinal section from at least 3 animals was taken whole. Then a region of interest (ROI) was defined by manually drawing along the optic nerve making sure to exclude the epineural area. Here, the ROI was measured and the cells were counted with the CellCounter plugin in ImageJ. Then the number of cells per area was calculated and plotted in Excel.

2.2.6 Tissue preparation for Electron microscopy

The animals were sacrificed by cervical dislocation and the optic nerves were cut away from the eyeballs and the chiasm. They were immersion fixed for 24 h in Karlsson Schultz

solution (4% pFA, 2.5% glutaraldehyde in 0.1M PB (pH 7.3)) (Schultz & Karlsson, 1965) at 4 °C. Afterwards, they were processed with a modified reduced osmium-thiocarbohydrazide-osmium (rOTO) protocol (Mikula, Binding, & Denk, 2012; Yokota & Okada, 1996) to increase the contrast. At first they were washed 3 times with 0.1M PB buffer followed by 3 h of 2% OsO₄ and 0.25% K₄[Fe(CN)₆] incubation at 4°C to reduce OsO₄ to OsO₂. Then the samples were washed in ddH₂O and incubated with 0.1% thiocarbohydrazide (in ddH₂O) for 1 hour at room temperature. Contrast was achieved by incubation with 2% OsO₄ for 90 minutes followed by (after washing with ddH₂O) 2.5% uranyl acetate incubation over night at 4°C. The samples were washed again in ddH₂O and dehydrated using increasing concentrations of acetone (always 15 minutes at 30%, 50%, 75%, 90%, 3x 100%). Lastly, the samples were embedded using an increasing concentration of Durcupan resin (without component D) in acetone (1.5 hours at 25%, 50%, 75%, and overnight at 100% Durcupan). The next day, samples were incubated for 5 hours in 100% Durcupan with component D followed by embedding in silicone molds with fresh resin from the same composition. They were polymerized for 48 hours at 60 °C until the blocks hardened.

Durcupan solution was mixed with the following components (Electron Microscopy Sciences (EMS) Catalog #14040):

11.4 g	component A (epoxy resin)
10 g	component B (964 hardener)
0.3 g	component C (964 accelerator)
0.1 g	component D (Dibutyl phthalate)

2.2.7 Cutting of ultrathin sections for TEM analysis

The blocks were trimmed to a pyramidal shape (Reichert Jung, Ultratrimm) and cut into semi-thin (500 nm) sections on an ultramicrotome (UC7 Leica Microsystems, Vienna) with a diamond knife (3.5 mm, 35° Diatome, Biel, Switzerland). Afterwards, the sections were stained with Richardson blue to verify tissue integrity and assess localization of region of interest. After further trimming ultrathin sections were cut at 50 nm thickness from the resin blocks. They were caught in a small water reservoir before being placed on a 100 hexagonal mesh copper grid (Gilder, UK), which were coated beforehand with a thin layer of Formvar. Finally images were obtained using a Zeiss Leo 912 Omega transmission electron microscope equipped with the ImageSP software at 6300 x magnification.

2.2.8 Sample preparation for 3View imaging

The sample in the resin was exposed over a block length of ~400 μm on four sides by trimming away the excess resin using a trimming diamond knife (Ultratrimm 90°, Diatome, Biel, Switzerland). The trimmed block was mounted on an aluminum Gatan pin with CW2400 conductive epoxy resin and baked for additional 3 days at 60 °C. Finally, the block was sputter coated with 20 nm of platinum (ACE600 Leica Microsystems, Vienna) before imaging at the Zeiss Merlin VP Compact SEM equipped with a Gatan3view2XP system. The SEM images were taken by an alternating procedure of cutting 80 nm and imaging with a pixel time of 0.5 μs and an image size of 80 x 80 μm . The pixel size was 10 nm at 1147 x magnification.

2.2.9 EM quantification

For the TEM quantifications 15 images covering an area of 2693 μm^2 at 6300 magnification were randomly taken across the optic nerve, per animal and at least three animals per condition and age were quantified. Counting was performed using the CellCounter plugin for ImageJ.

2.2.10 Nuclei isolation

The animals were killed by cervical dislocation and the corpus callosum was dissected and snap frozen in liquid nitrogen as fast as possible. To prepare and isolate the nuclei for staining the tissue of 4 animals was pooled and the corpus colossi transferred to a 1.5 mL tube. They were mixed immediately with 250 μl of ice cold low sucrose buffer and

homogenized on ice using a small micro-pestle. Then the volume was adjusted by using the same buffer to 500 μ l and 13 μ l of 37% formaldehyde (final concentration 1%) were added to fix the nuclei for 5 min at room temperature on a rotating wheel. To block remaining aldehyde groups, 52 μ l of 1.25 M glycine (final concentration 125 mM) was added to the mixture and incubated for 5 min at room temperature. Then the sample was centrifuged at 2000 g for 3 min at 4 °C. The supernatant was removed and the nuclei resuspended in 1 mL ice-cold low sucrose buffer (containing protease inhibitors). For mechanical homogenization the volume was adjusted to 6 mL and the ultraturax (IKA Labortechnik, Staufen in Breisgau) was used for less than a minute on ice. The homogenate was divided onto 4 cushions of 6 mL high sucrose buffer. At 3200 g for 10 minutes at 4 °C, the nuclei were separated from the cell debris using a swing bucket table top centrifuge (Eppendorf Centrifuge 5810 R). The supernatant was discarded and the nuclei pellet was carefully resuspended in 0.2 mL of ice cold PBS. To get rid of aggregates the nuclei were filtered through a 70 μ m filter. From this solution 50 μ l were taken for negative controls later on. The rest of the nuclei were pelleted in 2 mL tubes for staining.

2.2.11 Staining of isolated nuclei for FACS

Nuclei were resuspended in 1 mL of PBS-T (PBS with 0.1% Tween) + 5% BSA. Then 30 μ L of goat serum and 2 μ L of NeuN (Millipore, Cat.No.: mab377) and Olig2 (IBL, Cat.No.: 18953) antibody was added to the solution. This was incubated for 30 min at 4 °C on a rotating wheel. The samples were centrifuged at 2000 g for 3 min and the supernatant was removed. After that the samples were washed with 1.5 mL of PBS-T for 4 times for 5 min. Next, the nuclei were stained in 1 mL PBST + 5% BSA + 30 μ L goat serum and 1 μ L of anti-mouse Alexa 488 secondary antibody for 15 min at 4 °C on a rotating wheel. Then they were washed again in PBS-T for 2 min before they were resuspended in 1.5 mL of PBS-T + 5% BSA. This solution was pressed through a 26 G needle to make sure there are no aggregates right before cell sorting.

2.2.12 Fluorescence associated cell sorting (FACS)

The FACS was performed by Dr. Magali Hennion from the Stefan Bonn lab at the European Neuroscience Institute (ENI Göttingen).

The stained nuclei were sorted with a FACSAria II (BD Bioscience) into ice-cold conical tubes that were incubated with 1mL of 5% BSA in PBS solution. The NeuN⁺ and Olig2⁺

stained nuclei were gated according to cell size and cell density. Unstained fractions were also collected, which contain other glia cells (Astrocytes, Microglia). The purity of the sorted nuclei was above 95%. Tubes with the sorted cells were centrifuged at 3200g for 15 min at 4°C in a swing bucket table top centrifuge. Supernatant was removed by pouring and the pellet was further processed.

2.2.13 Methylated DNA immunoprecipitation (meDIP)-seq protocol

The MeDIP-seq protocol was performed in collaboration with Dr. Magali Hennion from the Stefan Bonn lab at the European Neuroscience Institute (ENI) in Göttingen and Ramon Vidal from the German Center for Neurodegenerative Diseases (DZNE) in Göttingen.

Pellet obtained after FACS was resuspended in lysis buffer (10 mM Tris-Cl pH 7.5, 10 mM NaCl, 2 mM EDTA, 0.5% SDS, 100 µg Proteinase K) and incubated 16 h at 65 °C. The genomic DNA was extracted using phenol-chloroform and precipitated with 0.3 M sodium acetate pH 5.2 and 100% ethanol. A pellet was obtained after centrifugation at 20.000 rcf for 20 min at RT. This was resuspended in TE buffer (10 mM Tris-Cl pH 7.5 and 1 mM EDTA) with addition of 20 µg/ml RNase A and incubated half an hour at 37 °C and 1 additional hour at 65 °C. The DNA was sheared with a Bioruptor NGS (Diagenode) for 10 cycles (30 s ON, 30s OFF) to a fragment size of ~300 bp. Around 700 ng of the fragments was used for library preparation. Afterwards NEBNext Chip-Seq Library Prep Master Mix (NEB, E6240 kit) was used for end-repair and adaptor ligation according to the kit's manual. Illumina paired-end sequencing adaptors (Sigma-Aldrich) were ligated as stated in the kit's protocol. From this 100 ng of adaptor ligated DNA was used for immunoprecipitation with an anti-5-methylcytosine (5mC) antibody (Eurogentec BI-MECY-100). The resulting enriched DNA was amplified according to the kit's guidelines and further purified using AgencourtAMPure XP beads (Beckman Coulter, A63880). The MeDIP libraries were then sequenced with a HiSeq 2000 (Illumina) system, according to manufacturer's manual. Modified from (Halder et al., 2015).

2.2.14 Magnetic activated cell sorting (MACS) of microglia cells

The MACS protocol was performed in collaboration with M.Sc. Tim Düking and M. Sc. Stefan Berghoff from the Saher group in the Department of Neurogenetics at the Max-Planck Institute for Experimental Medicine in Göttingen.

Mice were killed by cervical dislocation and the brain was removed from the skull. After the meninges were removed the brain was cut with a brain slicer into 1-2 mm sections by using two to three razor blades. Then, the whole corpus callosum and the whole cortex were removed with a fine scalpel. All steps were performed on ice. First, the cells were dissociated using the Adult Brain Dissociation Kit mouse/rat from MACS MiltenyBiotec (Cat.No.: 130-107-677). The protocol was performed according to the manufacturer's guidelines. Tissue was washed with ice-cold PBS and then dissociated with two enzyme mixes in the gentleMACS Octo-Dissociator with heaters. Then the suspension was strained using a MACS SmartStrainer (70 μ m). The debris and red blood cells were removed using the debris removal and red blood cell removal solution provided by the kit. Cell solutions were then sorted by using the CD11b MicroBeads mouse/human from MACS MiltenyBiotec (130-049-601). The cell suspensions were resuspended in 90 μ l of buffer followed by adding 10 μ l of CD11b MicroBeads. This solution incubated for 15 min at 4°C. Cells were sorted in the next step by using a MS column for the MACS Separator. After washing with buffer, the cells were eluted from the magnet. The pellet obtained after centrifugation was then frozen at -80 °C until further processing for RNA sequencing.

2.2.15 RNAseq library preparation

The RNAseq was performed in collaboration with Nirmal Raman Kannaiyan from the Moritz Rossner group in the Department of Molecular and Behavioral Neurobiology at the Ludwig-Maximilians-University clinic in Munich.

Sequencing was performed with 2 biological replicates for each condition. The cells from 2 mice were pooled for one biological replicate to maximize the transcriptome diversity. RNA was extracted using Qiagen Micro-RNAeasy Kit (Qiagen, Cat. No. 74004) according to the kit protocol provided by the manufacturer. 1 μ l of ERCC RNA Spike-In Mix (ThermoFisher, Cat No. 4456740) diluted at 1:5000 fold was added to the isolated RNA as external control. cDNA was synthesised using Ovation RNA-Seq system v2 (NuGEN, Cat. No.7102).100 ng of cDNA was used as input for library preparation using the IonXpress plus gDNA and Amplicon library preparation kit (ThermoFisher, Cat no: 4471269). The library was size selected using 2% E-Gel and the samples were barcoded and then amplified. Each sample library was further quantified using Kapa Library Quantification Kit (Kapa, Cat. No. KK4827). Equal quantities of each sample were then pooled and sequenced on an Ion Torrent Sequencer.

2.2.16 Transcriptome Data analysis

The raw reads (Fastq) were split into sample specific reads based on the barcodes. The reads were then checked for sequence quality and sequence repeats. Low quality bases and short reads were trimmed or removed from further analysis. The reads were then mapped to *Mus musculus* genome (mm10) using TMAP Aligner and quantified using Ensembl annotation 86 using Partek Flow software. Genes with at least 5 reads in at least 80% of the samples were considered for further analysis. Differentially expressed genes (DEGs) were determined in R with the DESeq2 package (Love, Huber, & Anders, 2014). Genes with at least one-fold change and adjusted p-Value of less than or equal to 0.05 were considered as differentially expressed.

2.2.17 Pathway analysis

Overrepresentation analysis was performed with KEGG Pathways using WebGestalt implementation (J. Wang, Vasaikar, Shi, Greer, & Zhang, 2017).

2.2.18 Statistics

Statistics were calculated in GraphPad Prism. The comparison of two groups with normal distribution and one independent variable was performed with a one way ANOVA. When two groups with two or more independent variables were compared two way ANOVA was used. A Bonferroni correction and Wilcoxon correction were used to correct for multiple testing as indicated in the figures. P-values above 0.5 were considered non-significant (n.s.); values below as significant with * (<0.5), ** (<0.1) and *** (<0.01).

3 Results

3.1 Changes in DNA-Methylation after running wheel exercise

Learning a new motor skill is associated with an increase in the proliferation of oligodendrocyte precursor cells (OPCs) and even more with an increase in newly formed oligodendrocytes (OLs). When the differentiation from precursor to mature, myelin-producing OL was blocked, mice were not able to learn to run on a complex wheel compared to control groups (Mckenzie et al., 2014). This occurs rather fast as changes in subcortical white matter could already be seen 2.5 hours after the complex wheel was introduced (L. Xiao et al., 2016). Similarly, when mice are fed with the copper chelator cuprizone, demyelination - especially in the corpus callosum - is observed. This also leads to a reduced ability to run on a complex running wheel (Liebetanz & Merkler, 2006). Along the same line, mice that lack the corpus callosum completely, either from birth, or surgically altered after birth show a significantly decreased running speed on the complex running wheel (Schalomon & Wahlsten, 2002). Other bimanual coordination test were also harder for mice that lack the corpus callosum (Mueller, Marion, Paul, & Brown, 2009). These studies describe the decrease in performance, but the involved molecular pathway is still not described. Our aim was to investigate the changes that occur during the learning phase by studying the methylation profile in order to identify the genes responsible for the changes. Therefore, I used a learning paradigm developed by Liebetanz and Merkler (Liebetanz & Merkler, 2006) that is able to detect even small changes in learning ability. The mice were trained to run on a running wheel setup with all the rungs for two weeks. This has multiple effects on the mice: first, after two weeks of training one can neglect the cardiopulmonary and musculoskeletal effect that the mice gain from running daily on a wheel. Second, the motivation for the mice to run is increased as it is a voluntary activity and, compared to the complex wheel, it is not too challenging for the mice. When the animals are finally introduced to the complex running wheel lacking certain rungs, bi-hemispherical motor coordination needs to be trained in order to achieve maximum running speed. Hence, they need to form a running strategy to be able to run without slipping or falling in the gaps.

Motor learning group 1 (MLG1) was introduced to the complex wheel setup in the third week (Figure 6 A), whereas motor learning group 2 (MLG2) continued on the training wheel for another week (Figure 6 B). Samples for investigating the genome-wide DNA

methylation patterns were obtained on day 0, 3 and 7 after introducing the complex wheel. There was also a control group (CG) of mice that did not run at all for three weeks, but was also single housed, under the same conditions as the runners.

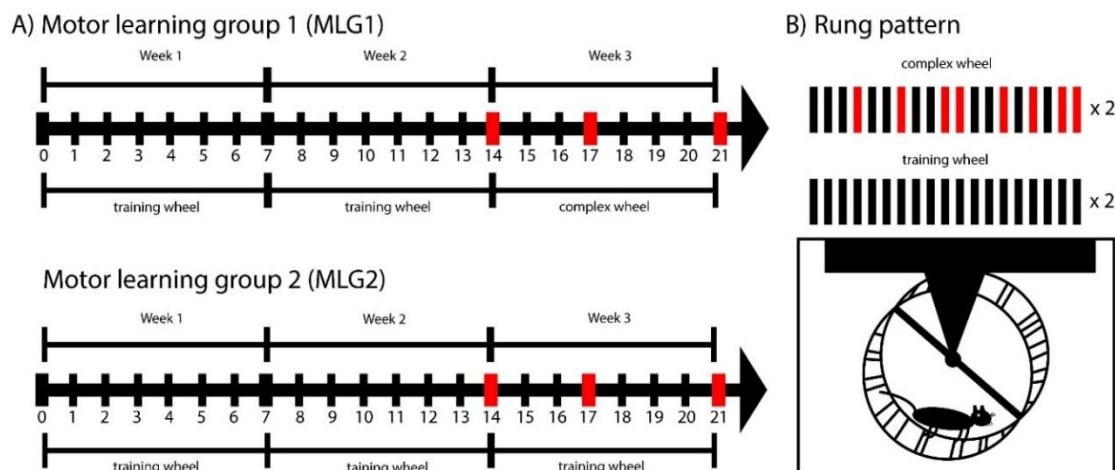


Figure 6: Running wheel paradigm scheme

A) Motor learning group 1 (MLG1) trained two weeks on the training wheel before the complex wheel was set up for one additional week. Motor learning group 2 (MLG2) ran on the training wheel for three weeks. The control group (CG) did not have access to a running wheel. At day 0, 3 and 7 after the complex wheel was put in place (marked by red bars) mice were sacrificed and the corpus callosum was prepared for isolation of nuclei. B) Illustration of different rung patterns. Missing rungs are marked in red.

To investigate underlying changes at gene level, I decided to investigate the DNA-methylation genome-wide to get a better understanding of changing gene clusters. I therefore went for the DNA-methylome of the corpus callosum at three different days of motor skill learning, to investigate whether changes in genes related to myelination are detectable. The first sample was taken after two weeks of training before the complex wheel was introduced to get the effects of two weeks exercise (day 0). To assess early changes in DNA methylation, another cohort was sacrificed after 3 days. To monitor later changes, the final cohort was analyzed at 7 days after the complex wheel was introduced. In all three cohorts, I always pooled 4 mice for one biological replicate (total n=2) in order to get sufficient amount of nuclei for immunoprecipitation.

At first the running distance and maximum running speed were assessed to see the effects of training and learning on the complex wheel. Figure 7 shows the comparison of MLG1 to MLG2 to investigate the impact of the complex running wheel to training only. On the

training wheel, over the course of 14 days, it could be observed that all mice are running longer distances over the two weeks of training and that the velocity also increased, but not significantly. The distance traveled rose from 3 km to almost 8 km during 24 h. The running speed barely increased from around 15 cm/s to 20 cm/s. This showed that both groups had the same conditions and were not affected differently by the running itself. Then, the complex wheel was introduced and the effects were visible immediately after the first day. The running distance in MLG1 decreased significantly from almost 7 km to 4 km per 24 h and the running speed slowed down from 22 cm/s to 14 cm/s. The maximum running speed in the MLG1 increased again after 7 days on the complex wheel, while the MLG2 stayed on a plateau. The distance traveled also plateaued at about 6 km per day, whereas for the MLG1 it was about 4 km per day over a course of 1 week. Even after training on the complex wheel for 7 days, the running distance did not increase whereas the velocity in MLG1 did. This might be due to the mice not being prone to not run too long distances at this complexity.

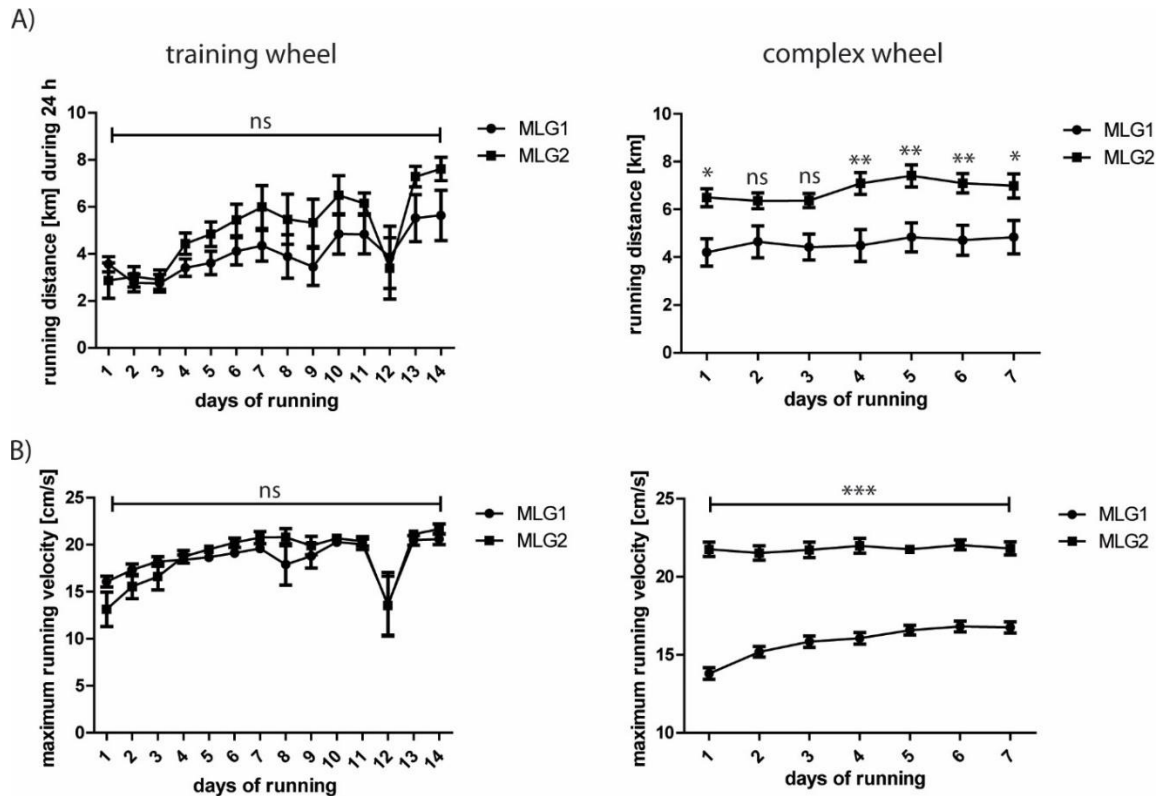


Figure 7: Comparison of running performance between normal and complex wheel

Mice were subjected to the MOSS paradigm for three weeks. Left panels in A and B show performance on the training wheel and right panels show the performance on the complex wheel over the individual days after inserting the complex wheel. A) Distance run over the course of 24 h was always measured at 9 am in the morning. B) Average maximum speed achieved was calculated to cm/s. $n = 8$; Two-way repeated measure ANOVA with a Bon Ferroni Post-Hoc test. ($p < 0.05 = *$, $p < 0.01 = **$, $p < 0.001 = ***$) ns = not significant. Shown are the mean values +/- standard deviation (SD).

The animals on day 0, 3 and 7 after introducing the complex wheel were sacrificed and the corpus callosum was dissected fresh and immediately flash frozen in liquid nitrogen. The sample of four animals were pooled and the NeuN⁺ and Olig2⁺ stained nuclei were further sorted according to fluorescence.

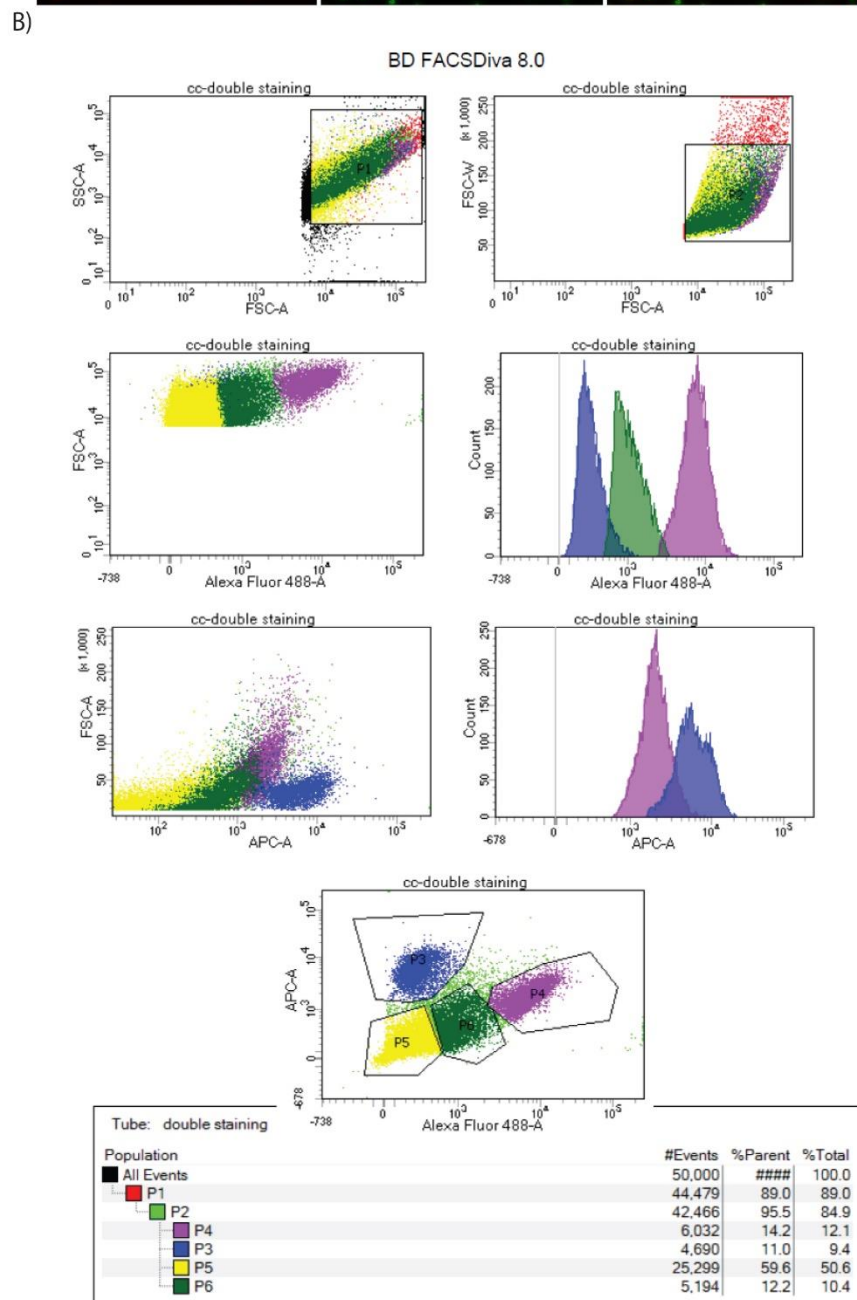
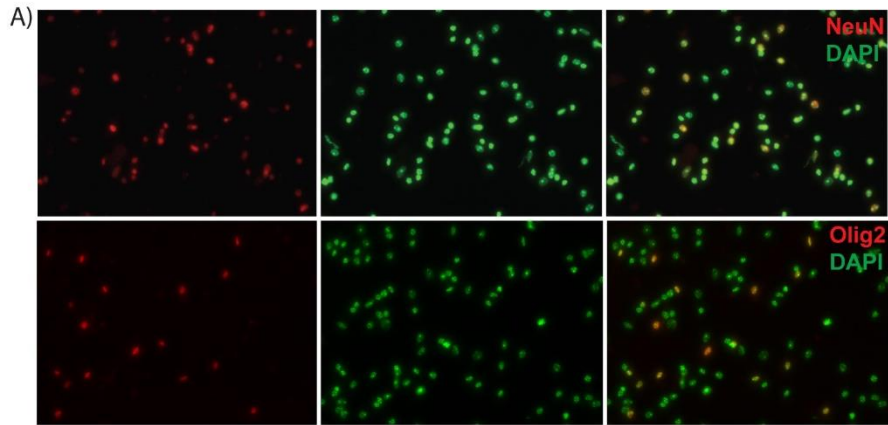


Figure 8: Fluorescence-activated cell sorting of corpus callosum nuclei

A) Purified nuclei from mice were stained for Olig2 and NeuN. B) Nuclei were sorted with gate P3 and P4 to exclude doublets, other cell types and debris. Oligodendroglial nuclei marker Olig2 was stained with Alexa 647 (red) and neuronal nuclei marker NeuN was stained with Alexa 488 (green). Gate P6 were other cells and debris was collected in gate P5.

Figure 8 shows the gating strategy to exclude debris (gate P1) and doublets of nuclei (gate P2). The Olig2⁺ oligodendrocyte nuclei were then sorted with gate P3 according to their high fluorescence signal for Alexa 647 (APC). NeuN⁺ neuronal nuclei were sorted with gate P4 according to their high fluorescence signal for Alexa 488. Gate P5 and P6 were set to catch the remaining cell types and everything else remaining.

The sorted nuclei were then further processed for methylated-DNA immune precipitation followed by Illumina sequencing. The data obtained were processed by the Stefan Bonn laboratory at the European Neuroscience Institute (ENI) in Göttingen. Here, we sequenced the MLG1 and the non-runner CG. I chose those two groups as they were expected to show the highest differences in DNA-methylation. As shown in Figure 9 (A-B) almost no changes between the two groups were visible. Not surprisingly, no significant differences were obtained, when comparing MLG1 at different days of running or comparing to the CG.

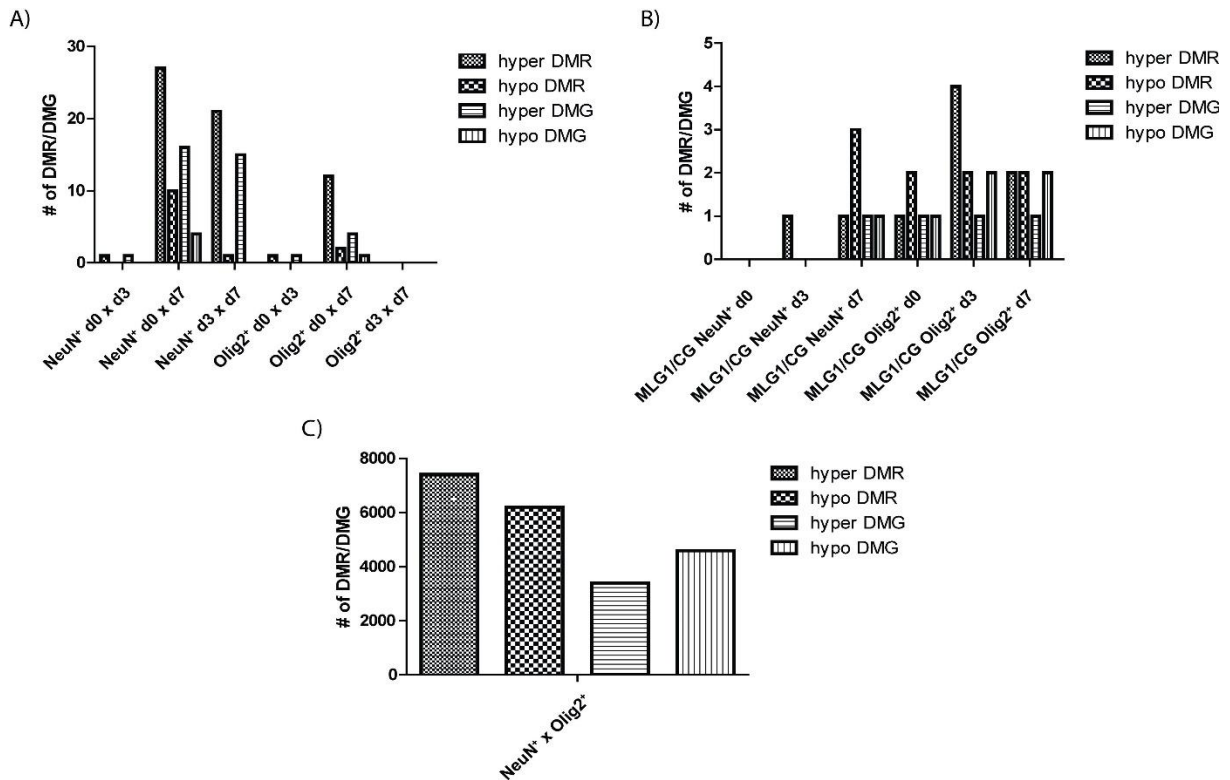


Figure 9: DNA-methylation profile of the complex runners compared to the control group

A) MLG1 was compared with itself on different days, in respect to NeuN⁺ and Olig2⁺ sorted cells (e.g. NeuN⁺ from day 0 to NeuN⁺ from day 3). Shown are the number of differentially methylated regions (DMR) / genes (DMG) in respect to neuronal and oligodendrocyte cells. B) MLG1 was compared with the CG that did not run at all. Shown are the number of DMR/DMGs in respect to neuronal and oligodendrocyte cells. C) The comparison of DMGs and DMRs between neurons (NeuN⁺) and oligodendrocytes (Olig2⁺) of MLG1 as means of control.

The technical control consisted of two internal NeuN⁺ and Olig2⁺ samples from the Bonn lab (data not shown) that were compared to our samples. The control samples showed similar DNA-methylation patterns for each cell type. Therefore, I concluded that there were no technical problems of sample preparation for this analysis.

NeuN⁺ nuclei were compared to Olig2⁺ nuclei directly to test for cell type specificity. Figure 9 C shows between 6000 to 7500 differentially methylated regions (DMR) and between 3500 to 4500 differentially methylated genes (DMG). This displays substantial differences which would be expected from two different cell types. However this diversity was not detected in regards to motor learning on NeuN⁺ or Olig2⁺ cells alone.

The differentially methylated genes from Figure 9 A did not show a functional connection to either myelin-related genes or neuronal signaling molecules. Table 3 shows the genes that were differentially methylated when comparing NeuN⁺ nuclei and Olig2⁺ nuclei on different days with each other.

Table 3: Enriched genes during motor skill learning from trained and untrained mice

Table shows genes that were differentially regulated with logFoldchange (logFC) and the adjusted p-values, as well as the gene names and the transcript IDs. In the first column, the different conditions that were compared are listed. NeuN⁺ nuclei from day 0, 3 and 7 and Olig2⁺ nuclei from day 0, 3 and 7. Color code ranges from $\leq -1,5$ (blue) to $\geq +1,5$ (red).

Comparison	Gene name	TranscriptId	logFC	p-adjust	Comparison	Gene name	TranscriptId	logFC	p-adjust
NeuN+ d0 x d3	C230014012Rik	ENSMUST00000134921	1,48	0,0276	Olig2+ d0 x d3	Gm9013	ENSMUST00000132939	1,32	0,0438
NeuN+ d0 x d7	Slc13a3	ENSMUST00000029208	1,55	0,0106	Olig2+ d0 x d7	AC116720.1	ENSMUST00000181093	2,27	0,0006
	Gm853	ENSMUST00000124528	1,28	0,0915		Gm15405	ENSMUST00000120530	1,58	0,0355
	Gm6270	ENSMUST00000132731	1,23	0,0906		Tnfrsf8	ENSMUST00000123027	1,46	0,0839
	Haus4	ENSMUST00000022784	1,19	0,0570		201011101Rik	ENSMUST00000091560	1,44	0,0114
	Trim14	ENSMUST00000136978	1,17	0,0124		Tfeb	ENSMUST00000086932	1,43	0,0355
	5830454E08Rik	ENSMUST00000064646	1,14	0,0157		Gm12380	ENSMUST00000119012	1,40	0,0547
	2010315B03Rik	ENSMUST00000071300	1,02	0,0000		Pappa	ENSMUST00000084501	1,30	0,0839
	Spata19	ENSMUST00000034473	1,02	0,0555		Atfb	ENSMUST00000015605	1,25	0,0481
	Gm10801	ENSMUST00000099684	1,02	0,0000		Ms4a4b	ENSMUST00000136366	1,23	0,0506
	Gm26282	ENSMUST00000178138	1,00	0,0153		Gm12380	ENSMUST00000119012	1,09	0,0547
	Gm5614	ENSMUST00000091097	0,99	0,0000		Slc2a10	ENSMUST00000029196	1,07	0,0220
	Gm10800	ENSMUST00000099683	0,98	0,0001		Tinagl1	ENSMUST00000030560	0,78	0,0839
	Tmem125	ENSMUST00000128098	0,97	0,0042		Anks1	ENSMUST00000114842	-1,36	0,0355
	Creg1	ENSMUST00000111432	0,97	0,0797		Gm10705	ENSMUST00000098980	-1,80	0,0091
	Gm21738	ENSMUST00000177817	0,96	0,0000	Olig2+ d3 x d7	/			
	Gm10722	ENSMUST00000151376	0,96	0,0428					
	Gm10720	ENSMUST00000099050	0,95	0,0172					
	Gm17535	ENSMUST00000178641	0,94	0,0185					
	Gm7120	ENSMUST00000099147	0,92	0,0006					
	Cdk5rap2	ENSMUST00000144099	0,89	0,0006					
	Chl1	ENSMUST00000066905	0,88	0,0127					
	2210408121Rik	ENSMUST00000168779	0,88	0,0347					
	Kcnh5	ENSMUST00000042299	0,85	0,0378					
	Gm6020	ENSMUST00000092094	0,84	0,0491					
	Sspn	ENSMUST00000111702	0,79	0,0153					
	Gm7120	ENSMUST00000099147	0,76	0,0003					
	Mdga2	ENSMUST00000037181	0,72	0,0062					
	Gm25577	ENSMUST00000083414	-1,42	0,0948					
	Gm23176	ENSMUST00000104365	-1,45	0,0170					
	Cgnl1	ENSMUST00000121322	-1,49	0,0192					
	BC043934	ENSMUST00000070500	-1,52	0,0188					
	Gm15218	ENSMUST00000131006	-1,59	0,0959					
	Cyp26b1	ENSMUST00000168003	-1,69	0,0625					
	Klk10	ENSMUST0000014058	-1,69	0,0572					
	Gm13659	ENSMUST00000145460	-1,71	0,0106					
	Rb1	ENSMUST00000164624	-1,85	0,0862					
	Agri	ENSMUST00000075787	-1,85	0,0430					
NeuN+ d3 x d7	Gli2	ENSMUST00000062483	1,48	0,0740					
	5830454E08Rik	ENSMUST00000064646	1,06	0,0287					
	Tmem125	ENSMUST00000128098	0,78	0,0071					
	2010315B03Rik	ENSMUST00000071300	0,76	0,0037					
	Gm5614	ENSMUST00000091097	0,74	0,0000					
	AC131780.1	ENSMUST00000181572	0,72	0,0834					
	Gm10801	ENSMUST00000099684	0,71	0,0022					
	Gm10800	ENSMUST00000099683	0,71	0,0707					
	Cdk5rap2	ENSMUST00000144099	0,70	0,0365					
	Gm10722	ENSMUST00000151376	0,68	0,0048					
	Gm10720	ENSMUST00000099050	0,68	0,0095					
	Gm10718	ENSMUST00000099046	0,68	0,0001					
	Gm10717	ENSMUST00000177875	0,67	0,0008					
	Gm10717	ENSMUST00000179839	0,66	0,0000					
	Gm21738	ENSMUST00000177817	0,65	0,0000					
	Gm17535	ENSMUST00000178641	0,62	0,0226					
	Gm7120	ENSMUST00000099147	0,61	0,0888					
	Ly6c2	ENSMUST00000100542	0,58	0,0706					
	Mdga2	ENSMUST00000037181	0,56	0,0128					
	Gm7120	ENSMUST00000099147	0,54	0,0174					
	RP23-81C12.3	ENSMUST00000182010	0,29	0,0106					
	Gm23024	ENSMUST00000158770	-1,96	0,0740					

Even though I could not detect significant differences within the methylation pattern, several genes that were changed could potentially be involved in network modulation.

Cell adhesion molecule L1 like (CHL1) was slightly upregulated when comparing the first and last day neuronal cells. This gene encodes for a protein that promotes neurite outgrowth of cerebellar and hippocampal neurons. Furthermore, genes that regulate the response to neurotransmitters, such as Potassium voltage-gated channel subfamily H member 5 was moderately upregulated.

Additionally, neurons also seem to regulate their synthesis of cholesterol, steroids and other lipids – due to hyper/hypomethylation of Cyp26b1.

In comparison to that, transcription factor EB (TFEB) showed an increase in methylation in oligodendrocytes when comparing day 0 and day 7. This transcription factor is involved in activating expression of lysosomal genes. Additionally, it has been shown that TFEB signaling is actually an inhibitor of myelination as it leads to apoptosis of oligodendrocytes in unmyelinated brain regions (Sun et al., 2018).

Genes that regulate the glucose homeostasis, such as solute Carrier Family 2 member 10 (Slc2a10) were slightly upregulated in oligodendrocytes.

Taken together the mice seemed to learn over the period of 7 days on the complex wheel, although speed was not drastically increased and did not match the level of mice on the training wheel. This might be reflected in the methylated DNA analysis since no genes which are responsible for plasticity or related to myelin were affected. Therefore, I decided not to further investigate in this direction.

3.2 Changing populations of glia cells in the optic nerve after birth

After the exercise did not show the expected plasticity in gene regulation in our experimental paradigm, I wanted to look at the already naturally occurring plasticity during development. Our laboratory has shown that myelin during development in the optic nerve displays outfoldings that are disappearing in later stages of development (Snaidero et al., 2014). Therefore, I wanted to assess what physiological changes at cellular level during normal development are. Since the optic nerve is relatively early myelinated, I wanted to get a baseline for different cell types and start of myelination.

As starting point, I investigated the number of PDGFR α positive oligodendrocyte precursor cells and APC positive mature oligodendrocytes in young mice from the age of 4 days to 3 weeks. Furthermore, I quantified the MBP positive area in the optic nerve to determine the time point when myelination begins.

I could detect that myelination roughly starts at around 7-8 days after birth as first patches of single isolated MBP producing oligodendrocytes are detectable (Figure 10). Myelination progresses which is indicated by increased amounts of MBP shown by immunohistochemical staining (B). Furthermore, the amount of PDGFR α positive oligodendrocyte precursor cells decreases (A) and the amount of APC positive oligodendrocytes increases (C) from day 8 to day 14 after birth onward.

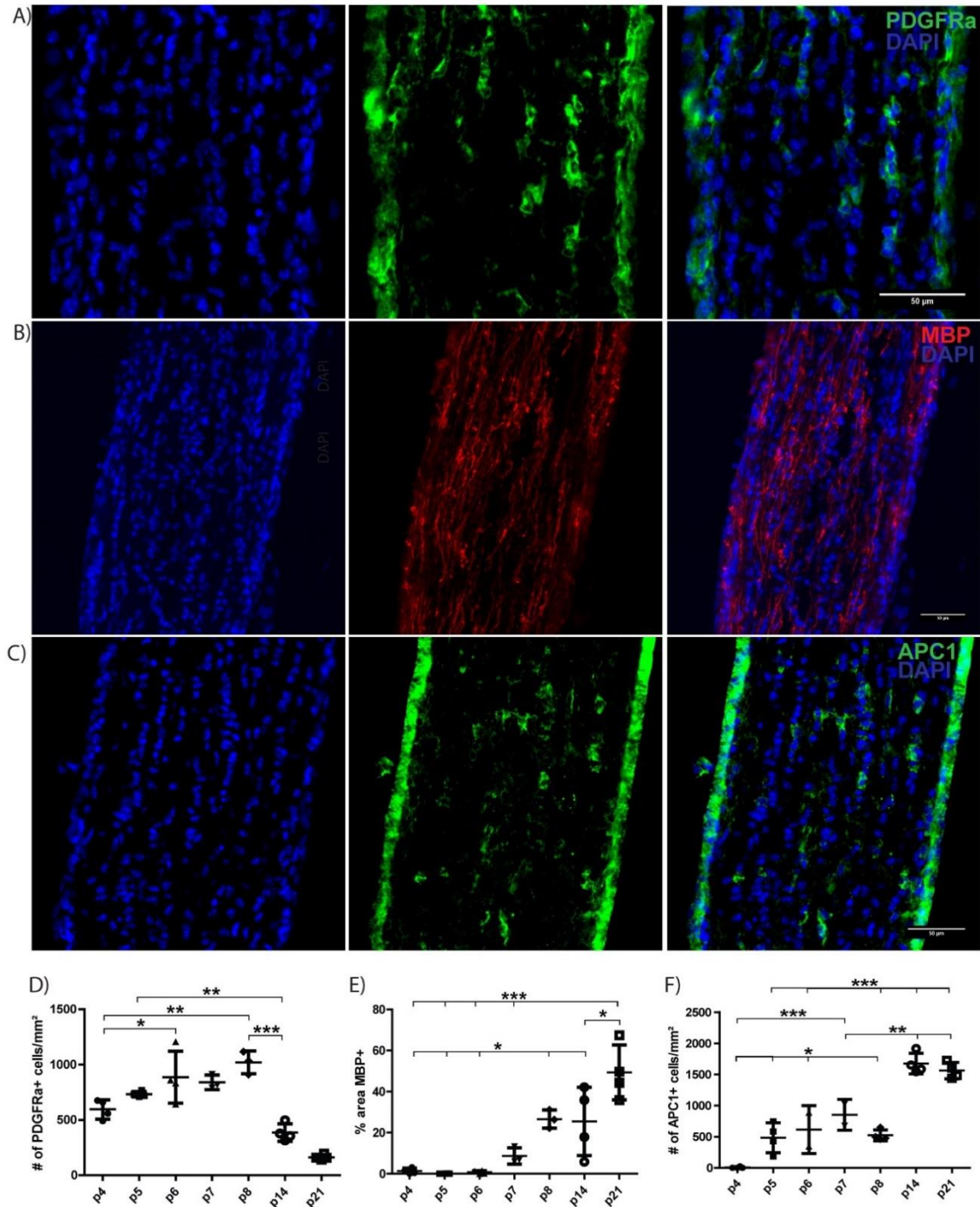


Figure 10: Oligodendrocyte and OPC maturation in the optic nerve during development

Representative epifluorescent pictures A-C of 8 day old optic nerves from C57Bl/6 wildtype mice. Followed by the quantification of 3-4 animals D-F. A) Representative image of a staining of the optic nerve for the oligodendrocyte precursor receptor PDGFR α (green). B) Representative image of a MBP (red) staining for mature oligodendrocytes. C) Representative image of an APC staining (green) for mature oligodendrocytes. D) Number of PDGFR α + cells counterstained with DAPI (blue) for the nucleus. E) Percentage of area fraction covered by MBP+ pixels. F) Number of APC+ cells, counterstained with DAPI (blue) for the nucleus. Shown are the mean with the standard deviation. One-way ANOVA with a Bon

Ferroni Post-Hoc test was performed for statistical analysis. ($p < 0.05 = *$, $p < 0.01 = **$, $p < 0.001 = ***$) scale bar = 50 μm .

To better understand the physiological interplay between different cell types, I wanted to see how the migration and proliferation of other glial cell types, namely astrocytes (positive for glial fibrillary acidic protein (GFAP⁺) and microglia (IBA1⁺) is related to the myelination process. Figure 11 A displays the presence and distribution of IBA1 and GFAP at P8. When I quantified the number of Iba1⁺ microglia cells, I could reveal an increase from day 4 to day 7 and then a small decrease from day 8 until day 21. Interestingly, the area of the optic nerve covered with GFAP⁺ astrocytes showed a similar curve. The area fraction of GFAP⁺ signal increased from day 4 to day 5 by roughly 50%. Afterwards, it dropped from day 7 to day 8 to around 50% again and even further in the following days.

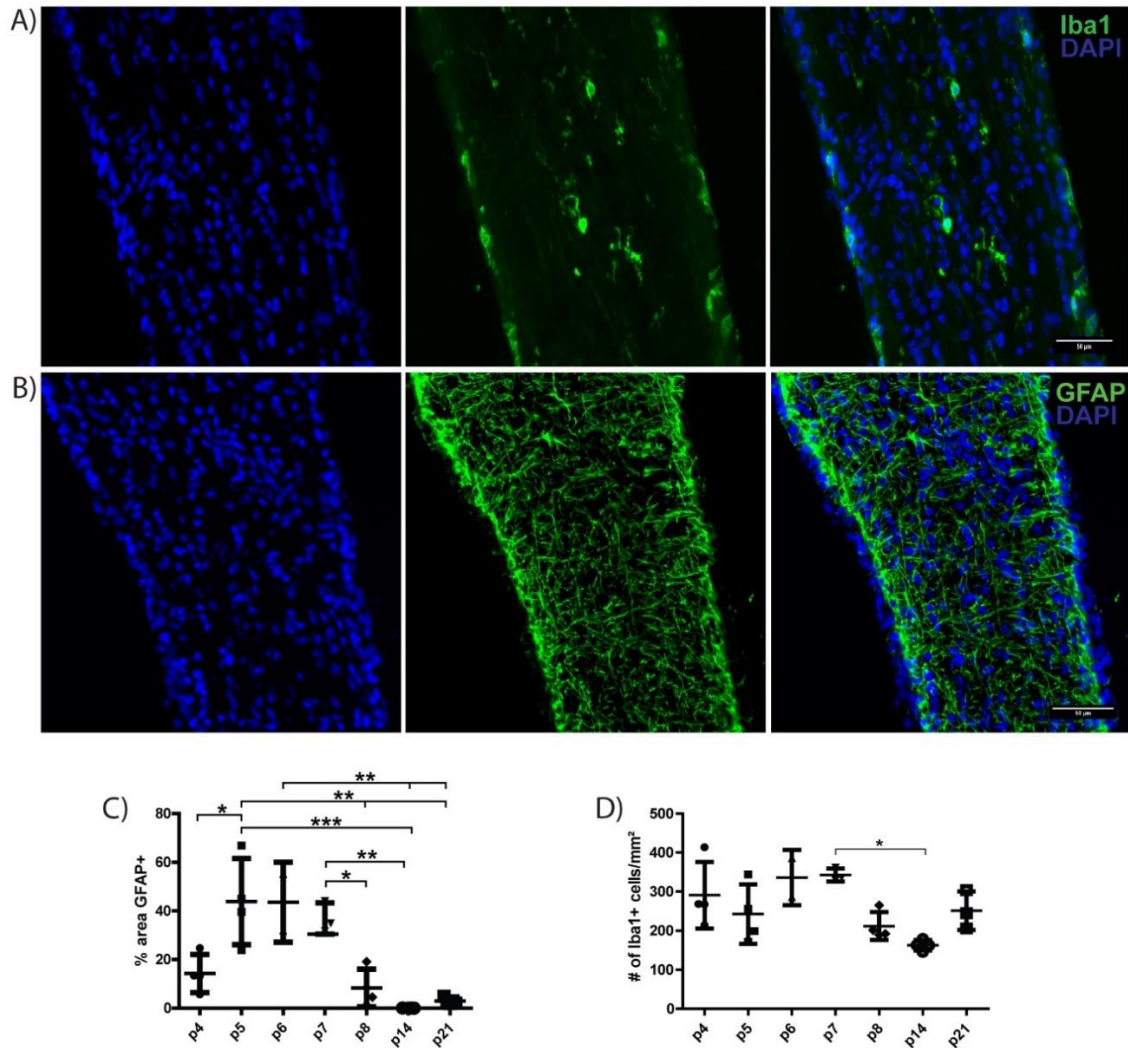


Figure 11: Astrocytes and microglia distribution in the optic nerve during development

Representative epifluorescent pictures A-B of 8 day old, stained optic nerve from C57Bl/6 wild type mice. Followed by the quantification C-D of 3-4 animals. A) Representative image of a staining against Iba1 (green) a marker for microglia counterstained with DAPI (blue) for nuclei. B) Representative image of a staining of GFAP (green) which marks processes of astrocytes. C) Percentage of area fraction covered with GFAP⁺ pixels. D) Quantification of the number of Iba⁺ cells. Shown are the mean with the standard deviation. One-way ANOVA with a Bon Ferroni Post-Hoc test was performed for statistical analysis. (p<0.05 = *, p<0.01 = **, p<0.001 = ***); Scale bar = 50 μm.

3.3 Ultrastructure of optic nerve myelination

In order to get a better understanding of the morphological changes that occur during development at an ultrastructural level, we performed, in collaboration with Dr. Hegermann and Dr. Wrede from the Medizinische Hochschule Hannover (MHH), 3D serial block face imaging (SBF-SEM). This advanced method allowed us to show the myelin ultrastructure in relation to other cells and the interaction between them not only in x/y but also in Z dimension. I manually segmented myelin sheaths with microscopy image browser and later reconstructed 3D models using Imaris. This approach allows to obtain volume information on a phenotype.

Here, I was able to detect several myelin abnormalities that are usually seen in aged mice or disease-related tissue (Bolino et al., 2004; Lampron et al., 2015; Safaiyan et al., 2016; Umehara et al., 1993), such as huge myelin outfoldings. Those are excess but still intact myelin sheets that are redirected away from the axons. In the reconstruction, one can appreciate the dimensions of the outfoldings (several μm) and that the excess myelin is usually found also far away from the normal internode (Figure 12). These observations were made at an otherwise normal appearing internode. The percentage of outfoldings was quantified in regular 2D TEM images and decreased in number as the mice matured (Figure 16), which is consistent with the data from our own laboratory (Snaidero et al., 2014).

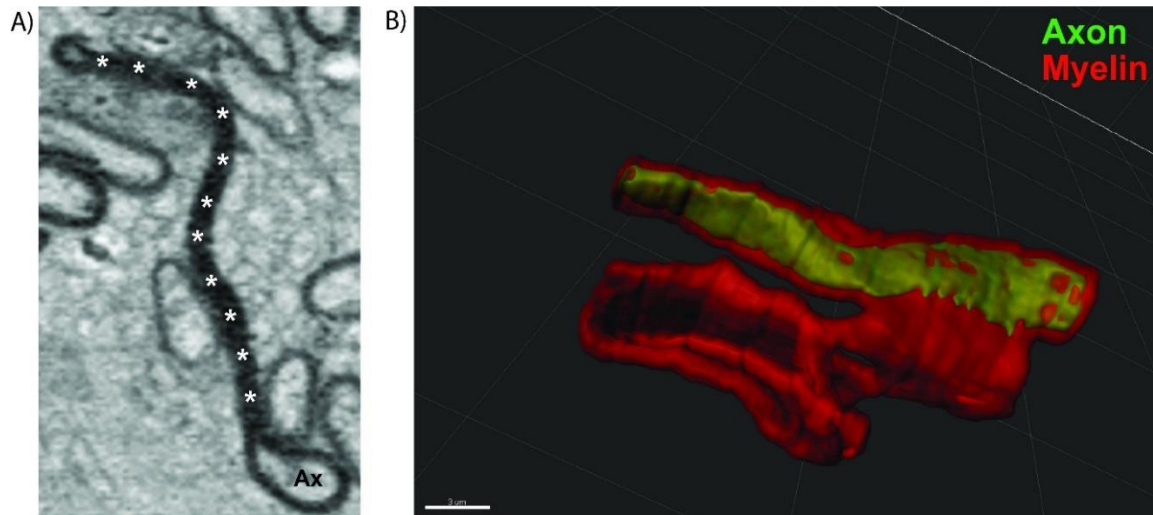


Figure 12: Myelin outfoldings occur during normal development

Wild type optic nerve of a 14 day old C57Bl/6 mouse was immersion fixed and processed for 3View imaging. A) 2D representing SEM image of the reconstruction depicted in B. Asterix marks an outfolding around the axon (Ax). B) 3D-reconstruction of myelin outfolding (red) around the axon (green) was created from the binned raw data with MIB and Imaris software. Scalebar = 3 μm.

Not only myelin outfoldings but also myelin debris attached to the internode, were found in the 3D volumes of the maturing optic nerve. Degenerated or deformed myelin was observed, which is two to three times larger than the diameter of the axon itself. Interestingly, these features were often still attached to the internode of healthy axons (Figure 13). Those findings were quantified by using TEM imaging which showed a similar decrease upon maturation (Figure 16).

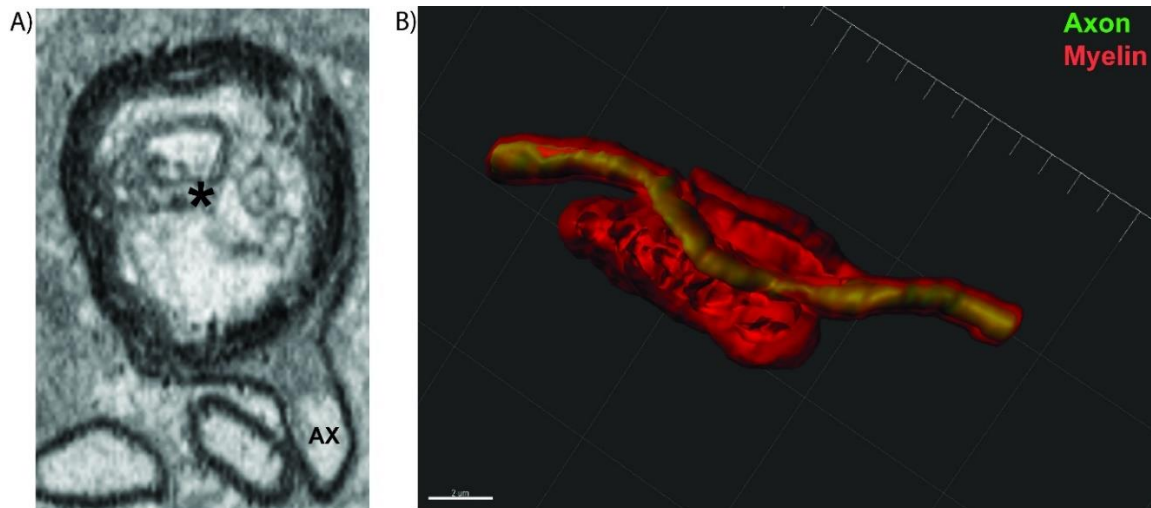


Figure 13: Myelin debris are attached to the axon during normal optic nerve development

Wild type optic nerve of 14 day old C57Bl/6 mouse was immersion fixed and processed for 3View imaging. A) 2D representing SEM image of the reconstruction depicted in B. Asterix marks degenerated myelin debris around the axon (Ax). B) 3D-reconstruction of myelin debris (red) around the axon (green) was created from the binned raw data with MIB and Imaris software. Scalebar = 2 μ m.

Another interesting finding was myelin debris that is phagocytosed by microglia cells at P8 to P60. This feature is normally observed under pathological conditions in MS lesions or demyelinating animal models (Lampron et al., 2015; Nielsen et al., 2009). Surprisingly, I found the same ultrastructural features during normal development. Extracellular myelin debris was taken up in big chunks by microglia cells (Figure 14). Additionally, myelin debris that was still attached to the axon and even the whole internode was engulfed by microglia processes (Figure 15). These observations were made in early development (P10, P14) and also at later stages (P21, P60), but to a much lesser extent.

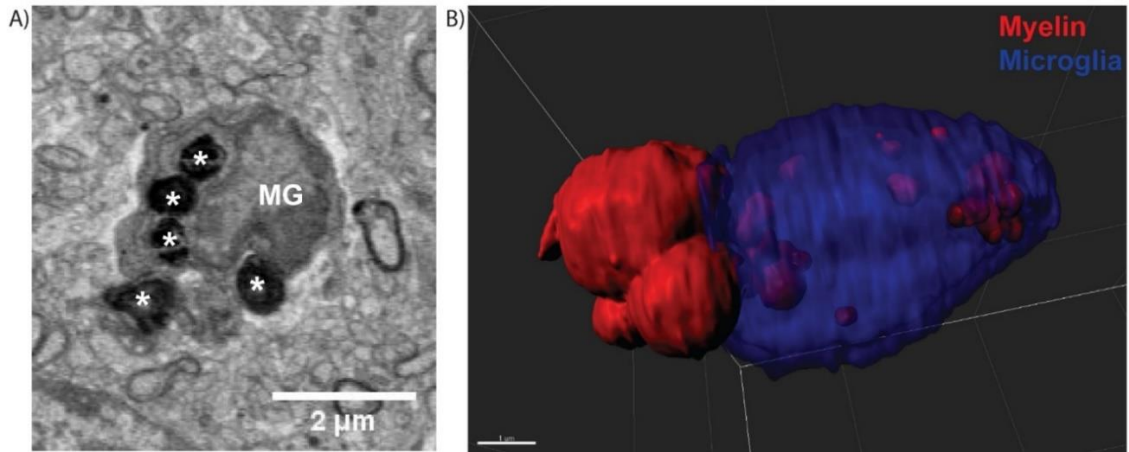


Figure 14: Microglia phagocytose myelin debris during normal development in the optic nerve

Wild type optic nerve of 10 day old C57Bl/6 mouse was immersion fixed and processed for 3View imaging. A) 2D representing SEM image of the reconstruction depicted in B. Asterix marks myelin debris inside a microglia cell (MG). B) 3D-reconstruction of myelin debris (red) partially surrounded by a microglia cell (blue) was created from the binned raw data with MIB and Imaris software. Scalebar = 1 μm .

We termed this phagocytosis of myelin “myelin pruning”, since it resembles synapse pruning, which is another important developmental process for network calibration (H. J. Kim et al., 2017; Paolicelli et al., 2011).

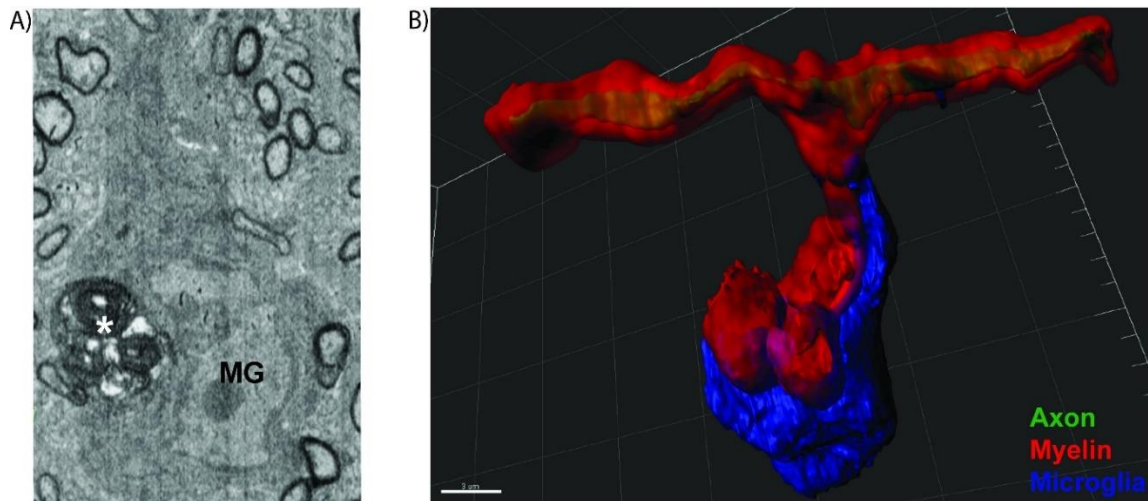


Figure 15: Microglia actively pull myelin off of internodes

Wild type optic nerve of 14 day old C57Bl/6 mouse was immersion fixed and processed for 3View imaging. A) 2D representing SEM image of the reconstruction depicted in B. Asterix marks degenerated myelin inside a microglia (MG) cell. B) 3D-reconstruction of myelin debris (red) partially surrounded by a microglia cell (blue) around the axon (green) was created from binned raw data with MIB and Imaris software. Scale bar = 3 μm .

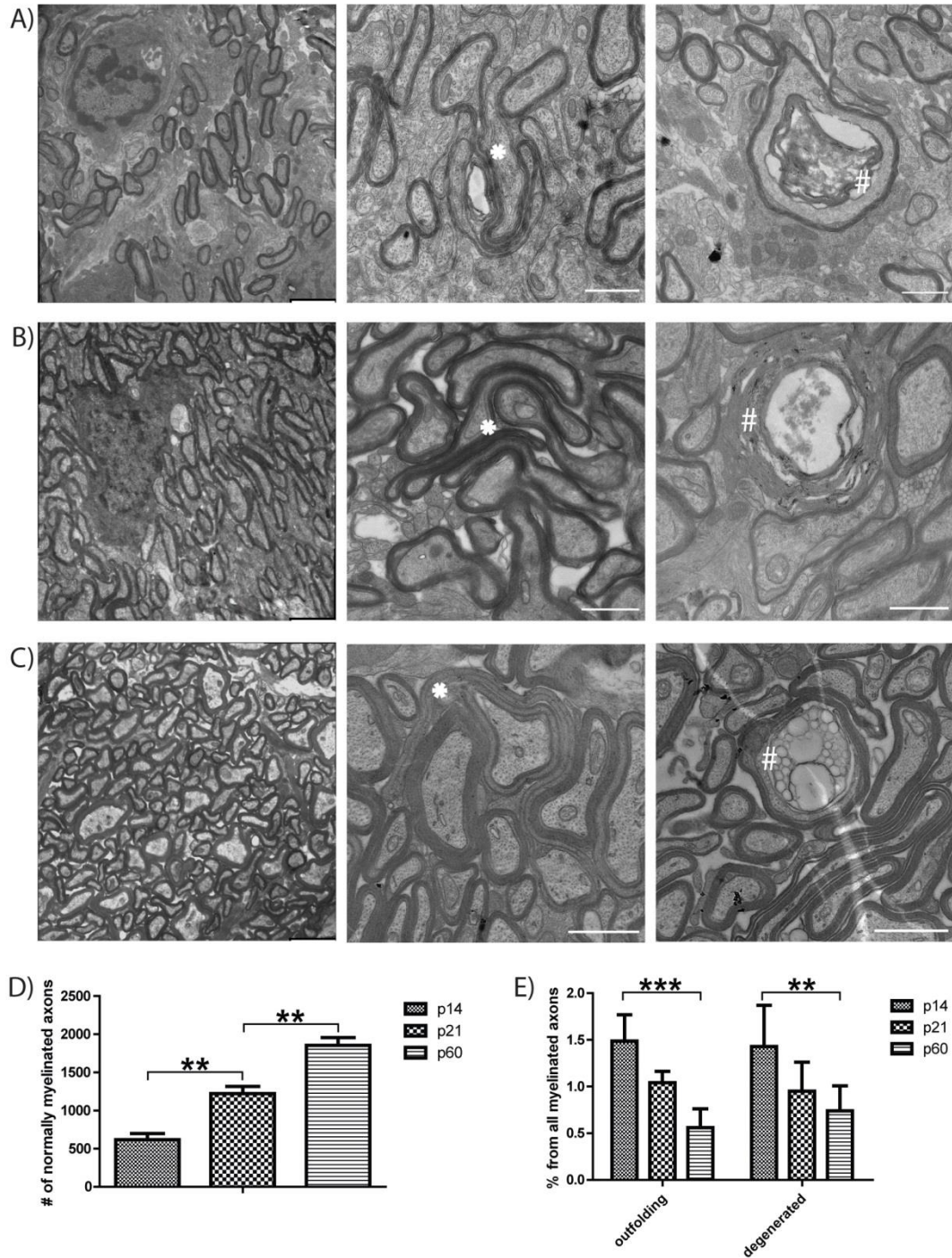


Figure 16: Increase of myelinated axons and decrease of myelin degeneration during development

Representative TEM images of optic nerve from wildtype C57Bl/6 animals 14 days old (A), 21 days old (B) and 60 days old (C). Left panel overview, middle and right panel example of outfolding and degeneration. An * marks outfoldings and # marks degenerated myelin. D) Quantification of myelinated axons at different time points in the optic nerve. Shown are means + standard error of mean. E) Quantification of the percentage of outfoldings and degenerated myelin. Shown are the means + SEM. One-way (D) and two-way (E) ANOVA with a Bon Ferroni Post-Hoc test was performed for statistical analysis.

($p < 0.05 = *$, $p < 0.01 = **$, $p < 0.001 = ***$). Scale bar in A)-C) left panel = 2 μm , middle and right panel = 1 μm .

Furthermore at the histological level, I could show that microglia (Iba1) phagocytose myelin (MBP) and degrade it through the lysosomal pathway (LAMP1). This event was rarely visible (1-2 times per whole optic nerve longitudinal section), hence only a representation is shown in Figure 17.

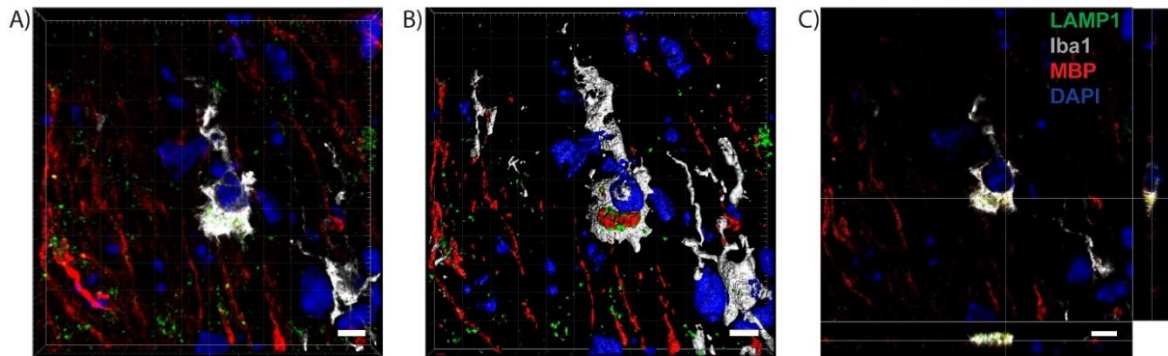


Figure 17: Myelin is phagocytosed by microglia cells during development

Optic nerve of 8 day old mouse was stained with Lamp1 (lysosomal, green), MBP (myelin, red), Iba1 (microglia, white) and DAPI (blue) for the nucleus. Shown are the native 3D-volume. (A), the reconstructed channels (B) and the orthogonal slicer view (C). Reconstruction was done with Imaris. Scale bar = 20 μm

3.4 MERTK is not a receptor responsible for myelin pruning

Since microglia are engaged in myelin pruning, I wanted to investigate which receptor is responsible for myelin recognition and uptake. Microglia have multiple receptors mediating phagocytosis and one of them, is MER Proto-Oncogene tyrosine kinase (MERTK). Hence, I also wanted to see whether deletion of this receptor would affect the amount of debris or outfoldings observed in the wild type mice.

Therefore, I prepared samples of MerTK deficient mice and age-matched litter mates for electron microscopy. When comparing the transgenic mice to the wild type control, no differences regarding number of myelinated axons, outfoldings or debris were observed at 14 days after birth or 21 days (Figure 18). Additionally, the 3D data of the knockout nerves did not show any differences compared to the control group.

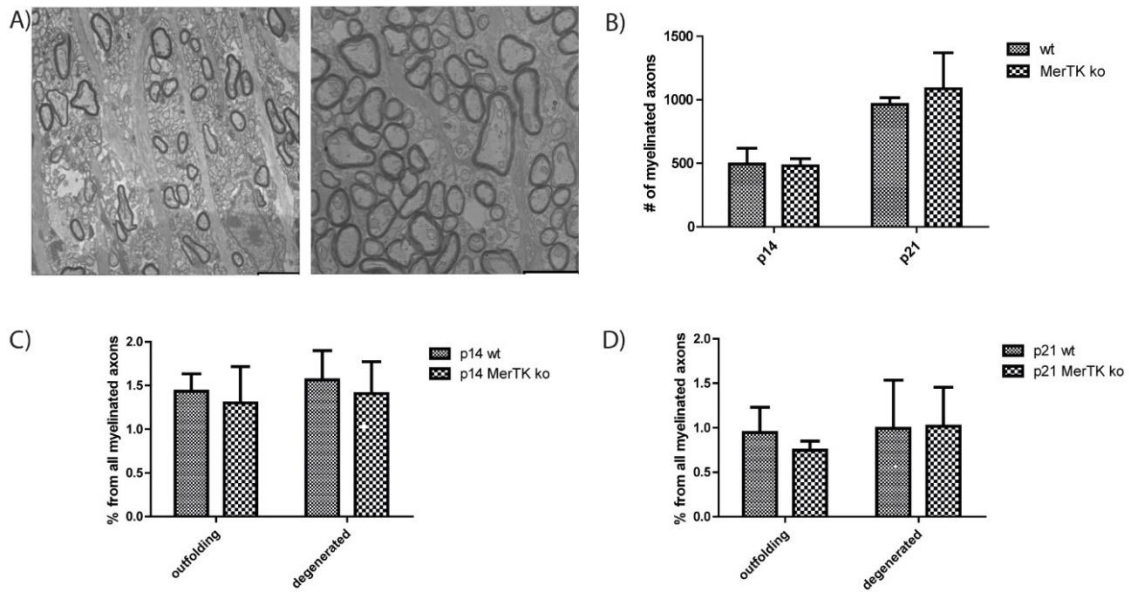


Figure 18: MerTK KO mice show no apparent difference in amount of degeneration

A) Representative TEM images of optic nerve from MertK KO mice P14 (left panel) and P21 (right panel). B) Quantification of myelinated axons at different time points and genotypes in the optic nerve. C) Quantification of the percentage of outfoldings and degenerated myelin at 14 day optic nerve from MertK KO and wildtype mice. D) Quantification of the percentage of outfoldings and degenerated myelin of P21 optic nerve from MertK KO and wildtype mice. One-way (B) and two-way (C, D) ANOVA with a Bon Ferroni Post-Hoc test were performed for statistical analysis. ($p < 0.05 = *$, $p < 0.01 = **$, $p < 0.001 = ***$). Shown are the means + SEM; Scale bar in A) = $2\mu\text{m}$.

3.5 TREM2 deficient microglia show less activation

Next I tested another candidate, namely triggering receptor expressed on myeloid cells 2 (Trem2). Trem2 is a microglial receptor important for activation, phagocytosis and cell survival (Filipello et al., 2018).

By assessing electron micrographs of optic nerves from developmental day 14 to 21, I could not identify differences in the number of normally myelinated axons at P14 or P21 in the optic nerve (Figure 19). Additionally, there were no differences in the amount of outfoldings in Trem2 KO mice compared to the wild type control. In contrast to that, the percentage of degenerated myelin compared to all myelinated axons was significantly increased from 2 to 8% at p14 and from 1 to 4% at p21 (Figure 19 C, D). Furthermore, the percentage of degenerated myelin was doubled in the younger time point compared to 7 days later.

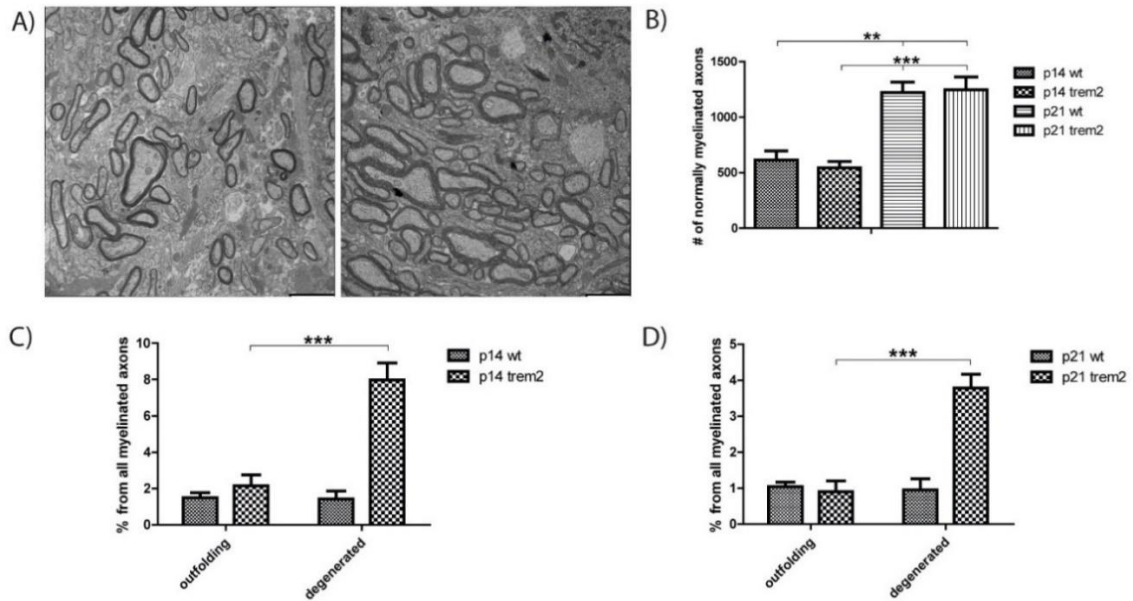


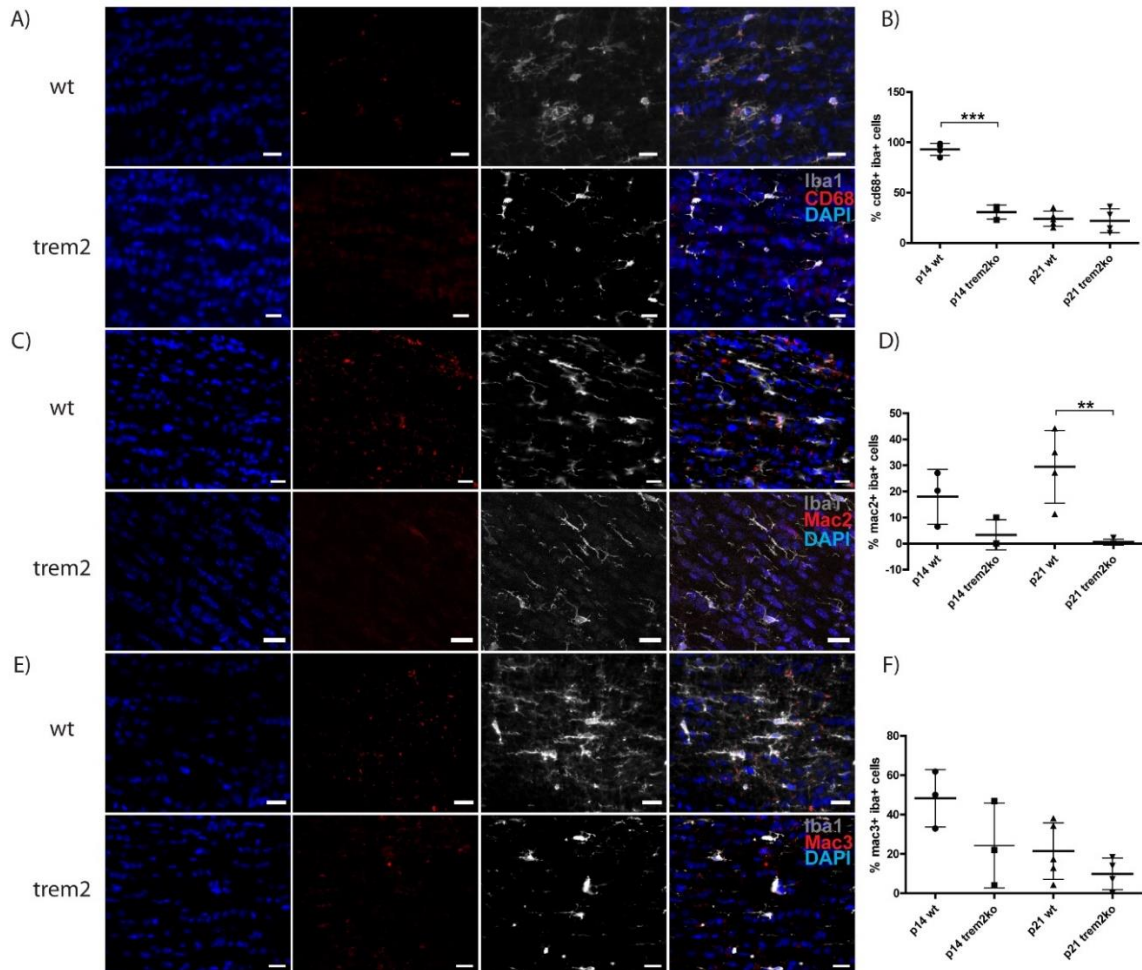
Figure 19: Trem2 KO mice show more degenerated myelin during development

A) Representative TEM images of myelinated axons from the optic nerve of Trem2 KO mice at P14 (left panel) and P21 (right panel). B) Quantification of myelinated axons at different time points and genotypes in the optic nerve. C) Quantification of the percentage of outfoldings and degenerated myelin in 14 day old Trem2 KO and wildtype optic nerves. D) Quantification of the percentage of outfoldings and degenerated myelin of 21 day old Trem2 KO and wildtype optic nerves. One-way (B) and two-way (C, D) ANOVA with a Bon Ferroni Post-Hoc test was performed for statistical analysis. ($p < 0.05 = *$, $p < 0.01 = **$, $p < 0.001 = ***$). Shown are the means + SEM; Scale bar in A) = 2 μ m.

Due to this vast increase in degenerated myelin, I wanted to analyze if Trem2-deficient mice also have a different activation profile compared to the controls. Therefore, I performed immunohistochemical stainings for CD68, which is a member of the lysosomal/endosomal-associated membrane glycoprotein (LAMP) family. There was a clear difference between Trem2 knockout and wildtype mice: microglia from control mice were almost 100% positive for CD68, whereas the Trem2-deficient microglia showed less than 25% of activation. Interestingly, this was only the case 14 days after birth, whereas at P21 microglia of Trem2 knockout showed the same amount of CD68⁺/Iba1⁺ cells compared to age matched controls.

To assess another microglia marker, I evaluated a member of the lectin family, namely MAC2/Galectin3, which is involved in activating microglia phagocytosis, on a histological level, (Reichert & Rotshenker, 1996). Almost 20% of wildtype microglia at P14 were

MAC2⁺ as compared to less than 5% MAC2⁺/Iba1⁺ in the Trem2-deficient microglia. At 21 days after birth, this difference increased to almost 30% positive microglia cells in the wildtype compared to almost no double positive microglia in the Trem2 knockout.



The last marker I investigated was Lysosomal-associated membrane protein 2 (LAMP2) also known as MAC3 which is part of the lysosomal cascade to break down cellular debris (Eskelinen et al., 2002; Hubert et al., 2016). The MAC3 positivity of microglia at p14 was at 50% for the wild type microglia and 25% for the Trem2-deficient microglia. At p21 the

double positivity dropped to around 20% for the wild type microglia and around 10% for the Trem2-deficient microglia.

3.6 RNA profile of microglia in the corpus callosum and cortex

On a histological level, I found that the Trem2 knockout mice showed less activation of microglia proteins involved in phagocytosis and degradation of debris. Using RNAseq, I wanted to further assess the microglia phenotype in these mice, as Keren-Shaul and colleagues used this method to identify a microglial subtype called DAM, which is formed in a Trem2-dependent manner (Keren-Shaul et al., 2017).

Therefore, our collaborators from the laboratory of Gesine Saher (MPI-EM) prepared cortex (ctx) and corpus callosum (cc) samples from P14 and P60 wild type mice. Two mice were pooled for n=1 and n=2 were used for sequencing each of the four groups (14 cc, 14 ctx, 60 cc, 60 ctx) (Table 4). In the following, genes that were expressed at least 2 fold higher or lower than the other group and with a p-value of less than 5% are shown. Every sample had between 8 and 12 million total reads (Figure 26) and over 80% alignment to the genome (Figure 29). The principle component analysis showed that principle component one is responsible for 58% of the variances in the samples and principle component two is responsible for 30% of variances (Figure 30). Each group was well separated from the others.

On RNAseq level, there were 649 genes upregulated and 330 genes downregulated when comparing cortex of p14 to p60 microglia. When comparing the corpus callosum of 14 and 60 day old microglia 381 genes were upregulated and 782 genes were downregulated.

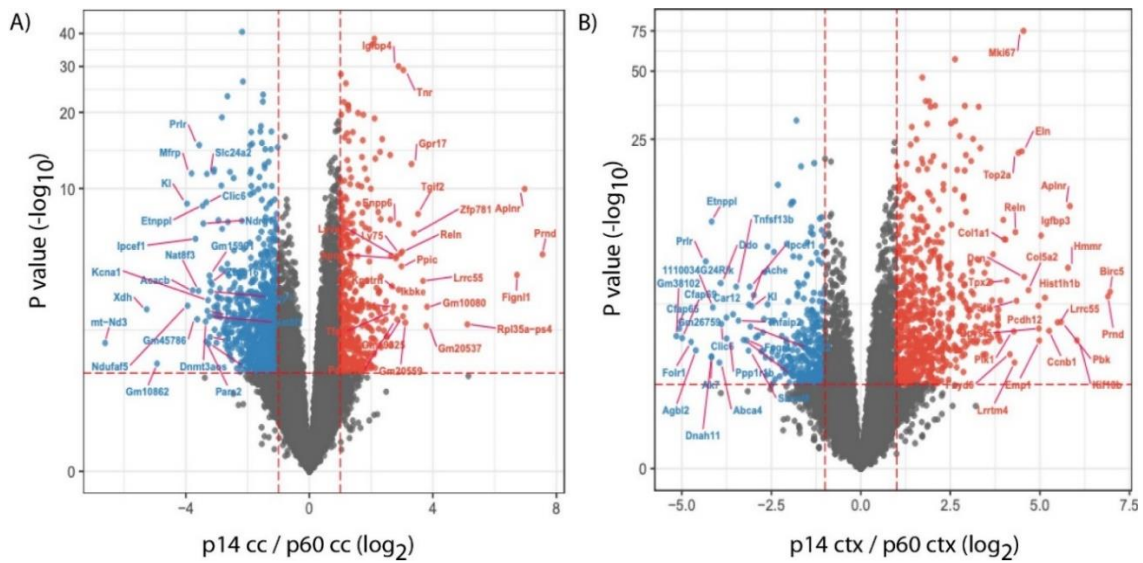


Figure 21: Microglia show differentially expressed genes in grey and white matter upon maturation

A) The p-value is plotted against the fold change of genes that are compared between P14 and P60 corpus callosum. B) Here the same values are plotted as in A) but comparing the change between P14 and P60 cortex. Genes that are upregulated in P14 compared to P60 are shown in red and downregulated genes are shown in blue. Marked genes are below a p-value of 0.05 and a logFold change above 1.

The Volcano plots in Figure 21 are showing the most regulated genes when comparing corpus callosum (A) and cortex (B) of microglia from P14 and P60 old wild type mice. Genes marked in red are upregulated in p14 compared to p60 and blue when downregulated. Most differentially changed genes when comparing the corpus callosum of P14 microglia to cortex and P60 corpus callosum and cortex revealed only small changes (Figure 32). No significance was seen, since the biological variance was too high.

The top ten regulated KEGG-pathways are shown in Figure 22. Most prominent pathways when looking at the corpus callosum upregulation in p14 compared to p60 microglia were ECM-receptor interaction, focal adhesion, PI3K-Akt signaling, cytokine-cytokine receptor interaction, protein digestion and absorption. These can all be linked to myelin pruning. The same ones were significantly regulated when comparing the cortex of p14 and p60. But the significance was higher in the cortex (B) than the corpus callosum (A). Some interesting pathways were also downregulated (C). Here, calcium signaling, complement coagulation cascades, insulin secretion, neuroactive ligand-receptor interaction and cAMP signaling were downregulated most significantly. When comparing the downregulated genes in the cortex (D) only complement and coagulation cascades pathway seemed to be interesting.

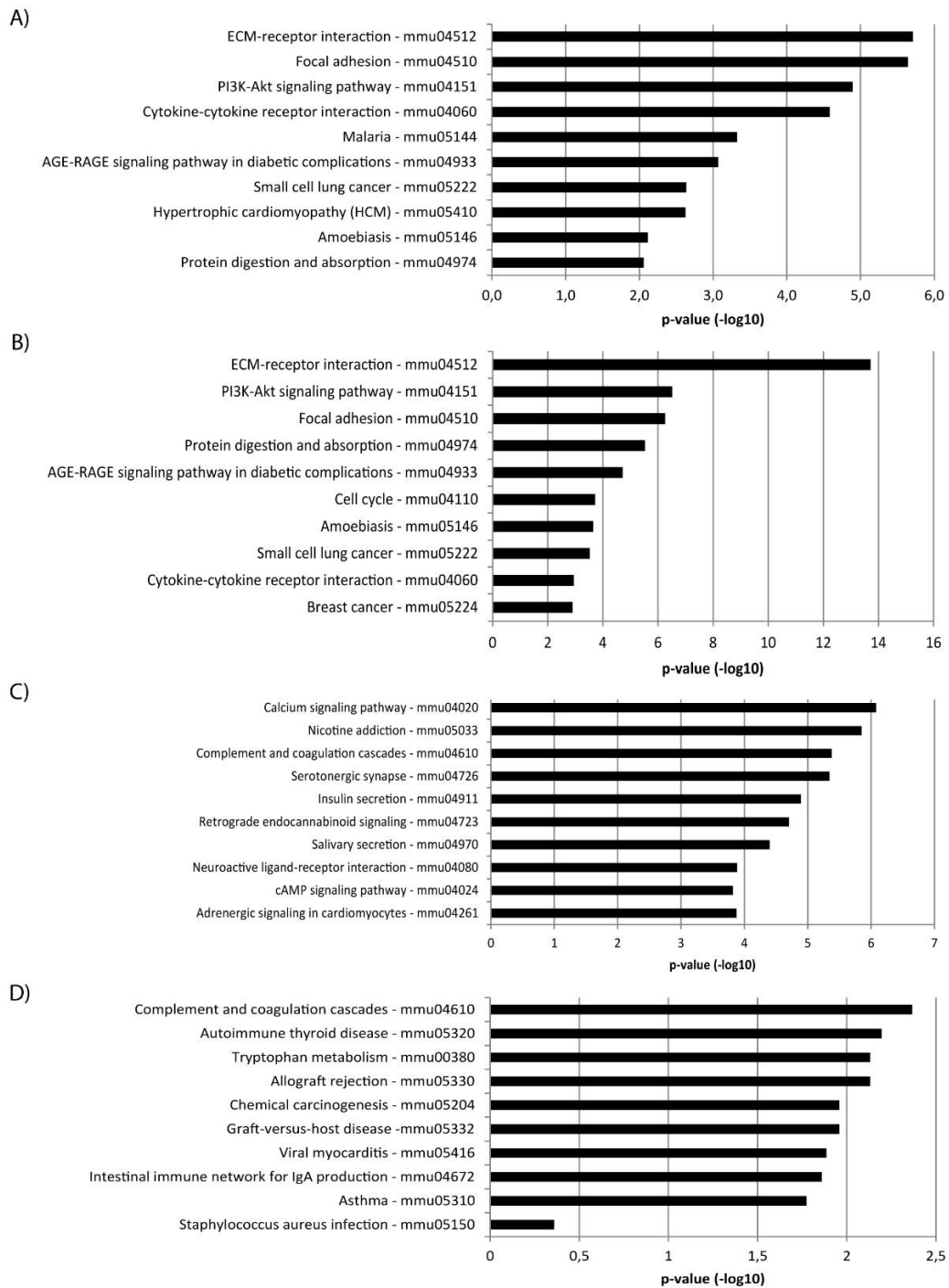


Figure 22: Top 10 regulated KEGG - Pathways

A-B) Top upregulated pathways between P14 and P60 microglia from corpus callosum (A) and cortex (B) are shown. C-D) Top downregulated pathways between P14 and P60 microglia from corpus callosum (C) and cortex (D) are illustrated. P-value from hypergeometric test from WebGestalt (<http://www.webgestalt.org>).

Lastly, we compared the gene expression profile in the context of DAM to gene expression from the literature (Keren-Shaul et al., 2017). Figure 23 A shows the top regulated genes in our samples matching the list published by Keren-Shaul *et al.* The expression level of genes that were upregulated in P14 corpus callosum were then compared to the expression levels of differently activated Trem2-deficient 5xFAD mouse line of early onset AD (B). Here the expression levels of our samples were low compared to the ones published in different DAM stages.

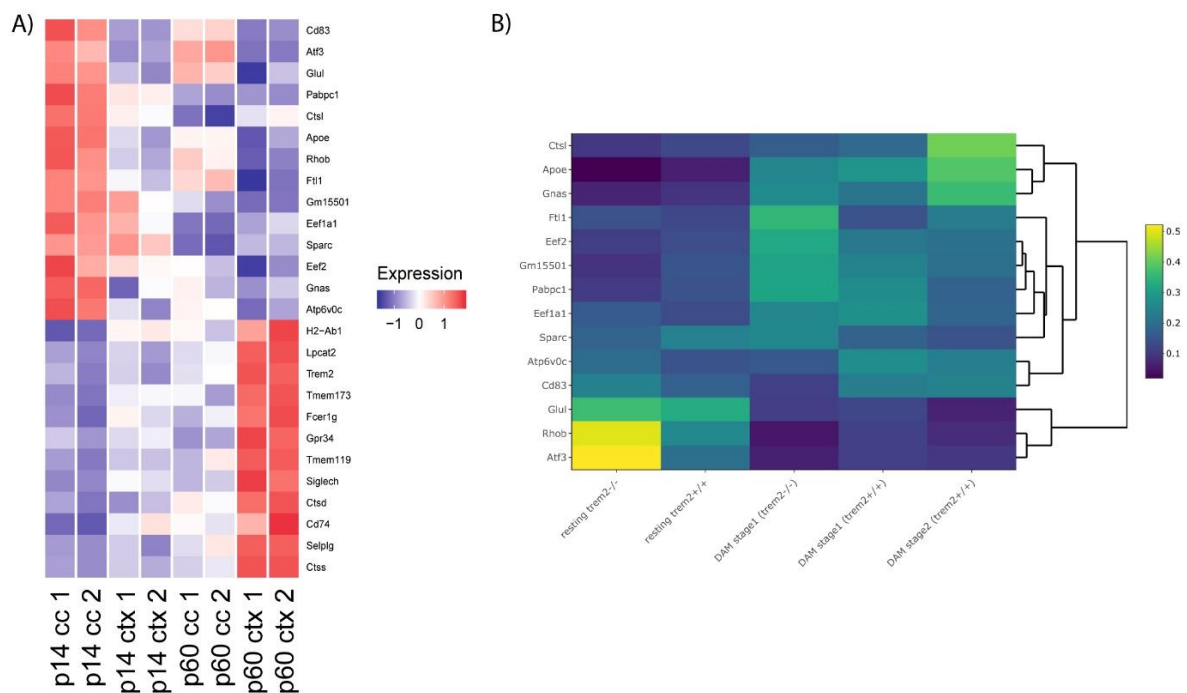


Figure 23: DAM response genes are not activated during myelinogenesis

A) Genes related to the DAM-response found in (Keren-Shaul et al., 2017), regulated in corpus callosum of P14 mice compared to the cortex and older age (P60). Color code: blue = downregulated, red = upregulated. B) Gene expression levels of genes upregulated in P14 corpus callosum (A) compared to the expression levels of the same genes found in different knockout animals published by Keren-Shaul *et al.* (2017). Color code: blue = slightly enriched, yellow mildly enriched.

4 Discussion

4.1 Effects of DNA-methylation on complex motor skill learning

Several studies have shown that increased activity of motor cortices changed the white matter landscape (as reviewed by (S. Wang & Young, 2014)). Oligodendrocytes in the corpus callosum increased proliferation after optogenetic stimulation of projection neurons in the premotor cortex. Even four weeks after stimulation increased number of EdU⁺/CC1 cells (newly born mature oligodendrocytes) was detected (Gibson et al., 2014). Moreover, the ultrastructure was changed, since myelin thickness seemed to increase with neuronal activity. Furthermore, mice that were placed on a complex running wheel showed an increased number of newly formed oligodendrocytes and the proliferation of OPCs was activated shortly after. When the transition of precursor cells to myelin forming oligodendrocytes was blocked by inhibiting the expression of myelin regulatory factor (MyRF), mice were unable to learn to run on the complex wheel (Mckenzie et al., 2014). It was later shown by the same group (L. Xiao et al., 2016) that this increase in newly formed oligodendrocytes occurred already after 2.5 hours in the corpus callosum and after 4 hours in the motor cortex. This means that changes occur already rapidly after first contact with the complex running wheel. Changes were still significantly different 8 days after running. Another study using rats found that even an enriched environment lead to enlargement of the corpus callosum as well as an increase in myelinated fibers (Zhao et al., 2012).

Supporting the hypothesis that myelin plasticity is involved in learning, experiments in which the corpus callosum was demyelinated using cuprizone treatment showed worse performance with overall decreased speed and distance traveled on the training wheel. This even intensified on the complex wheel in cuprizone treated mice compared to un-treated controls. In a second experiment, mice were tested after remyelination of the corpus callosum. The distance and running speed were again comparable to the untreated control animals. Hence the corpus callosum ventral to the motor cortices, was also important for bimanual motor coordination (Liebetanz & Merkle, 2006; Schalomon & Wahlsten, 2002). Therefore I also used the MOSS paradigm by Liebetanz *et al.* in order to detect small changes in the corpus callosum. Here, I compared two groups: MLG1 ran for two weeks on the training wheel before a complex wheel was introduced for the final third week. MLG2 ran for three weeks on the training wheel as a control group. Both groups showed an increase

in distance ran after each day and also higher maximum running speed achieved at the time analyzed (Figure 7 left panels). However, when performance was compared on the complex wheel significant changes could be detected (Figure 7 right panels). MLG1 had a dramatic reduction of maximum running speed and distance ran as expected due to the difficult task compared to MLG2. Inside the groups, there was no significant increase in distance or speed each day. Additionally, the within group ANOVA of MLG2 showed no difference of maximum running speed on the complex wheel indicating that the mice already reached the maximum running speed and that training for another week did not further increase their performance. In contrast to that MLG1 showed a significant increase in maximum running speed after 7 days suggesting that MLG1 indeed learned to run on the complex wheel after 1 week of training. They did not reach the maximum running speed as observed by MLG2 or during the training wheel period. This shows the complexity of the task, leading to the assumption that the mice might have improved their performance after a longer training period.

On day 12 on the training wheel there was a drop in both parameters in both groups. This might be a technical error or an external disturbance e.g. through noise, light during the night or storm that could have affected the animals. This was observed in both groups and afterwards the measured parameters continued their trends as before. Moreover, after a little training both groups ran between 5-8 km a night which overlaps with observations seen by other groups (Hibbits, Pannu, Wu, & Armstrong, 2009; Liebetanz et al., 2007). Hence, technical or external disturbances are considered unlikely in this study.

Analyzing the methylation profile, there was only a small amount of differentially methylated genes and regions (Figure 9), when MLG1 and non-runners were compared. I decided to compare those two groups, since I expected the most methylation changes between them. MLG1 and MLG2 might be too close in methylation profiles, since both had the exercise on the training wheel. To further analyze the data, MLG1 was compared to itself on different days: when looking at the changes of NeuN⁺ nuclei between day 0 and day 3, as well as the Olig2⁺ nuclei only one non-coding gene for neurons (C230014O12Rik) and one for oligodendrocytes (Gm9013) were identified. Notably, neither of them is involved in plasticity, as C230014O12Rik is a long non-coding RNA and Gm9013 is a pseudogene. When day 0 samples were compared to day 7 of both cell types, more genes were detected indicating a later response of myelin to exercise. A closer look at the gene

functions revealed, that only a few genes might be linked to motor learning (Table 3). Other genes did not code for functional proteins. For neuronal genes, the Neural cell adhesion molecule L1-like (Chl1) protein might be relevant, since it is involved in neurite outgrowth and positioning of pyramidal neurons, as well as defects in motor coordination (Demyanenko et al., 2004; Naus et al., 2004; Pratte, Rougon, Schachner, & Jamon, 2003). Every other gene found in the comparison of day 0 and day 3 in NeuN⁺ nuclei do not seem to be related to motor learning. There were some genes that were found in the comparison of Olig2⁺ nuclei at different training days. One was transcription factor EB (TFEB), that is a regulator of lysosomal biogenesis (Settembre et al., 2011). Furthermore, it has been shown that TFEB acts as a negative regulator of myelination by either repressing trafficking of new membrane or suppressing lipid synthesis. A study using a zebrafish model showed that Ras-related GTP Binding A (RagA) represses TFEB, which in turn represses myelination. The exact mechanism is still not completely understood yet (Meireles et al., 2018). Additionally, Barres and colleagues could show that TFEB is actually responsible for inducing programmed cell death in oligodendrocytes in unmyelinated brain regions through the PUMA-Bax-Bak pathway. This study links TFEB to a timed regulation of myelination during development (Sun et al., 2018). Concerning our experiment, this would mean that the TFEB gene is hypermethylated, which inactivates gene expression and favors myelination. Further experiments, using TFEB deficient mice could be conducted to elucidate more aspects of its connection to myelination.

In conclusion, I expected more changes in gene methylation related to either neuronal or glial plasticity due to exercise as mice are learning or at least have an enriched environment. But there are several reasons why I might not have been able to see a lot of relevant differences. One of the reasons could be that other research laboratories focused on the cerebellum or hippocampus when looking at motor learning (Abel & Rissman, 2013; Gomez-Pinilla, Zhuang, Feng, Ying, & Fan, 2011; Guo et al., 2011). Therefore, maybe the corpus callosum was just not affected as much as other regions. Here, I would like to point out that we tried to sort cells from the motor cortex, but we could not analyze the samples as we were unable to acquire sufficient material. Another reason might be the time points that we chose were not in the window of plasticity. The first time point after two weeks of training wheel functions as a baseline. This will negate the pure training effect. The next time point was 3 days after running on the complex wheel. As shown by Xiao *et al.* (2016) first changes of newly formed oligodendrocyte numbers were already seen after 2.5 hours

of running in the subcortical white matter and after 4 hours in the motor cortex. This difference increases and stays significantly, even 8 days after running with a peak at 24 hours after running. Therefore, three days after running, those changes are already so small that we were not able to detect it with the chosen MeDIP approach. Third, changes in the epigenetic landscape might be on the histone level rather than the DNA-methylation level. Some research suggests that also 24 hours after stimulation of the premotor cortex (M2) with optogenetics, the expression of histone modification markers (histone H3 lysine 9 trimethylation (H3K9me3) and histone H3 acetylation (AcH3)) on newly formed oligodendrocytes changed (Gibson et al., 2014). Three hours after stimulation no changes were apparent.

Research by other laboratories has shown that the differentiation of OPCs to myelinating oligodendrocytes is regulated by chromatin remodeler BRG1 (Smarca4), which is recruited by the transcription factor Olig2. This facilitates expression of myelin related genes (Yu et al., 2013) and therefore complex motor skill learning might be regulated on different levels and during different time points. Oligodendrocyte development depends on stage-specific transcription factors, including Olig2, Sox10, YY1, Olig1, MRF, and Zfp191, as well as small non-coding RNAs, such as miR-219 (Emery, 2010; Li et al., 2009). Those would have been expected to change in the methylome, but none of them showed significant changes. Hence, I suggest that a repetition of this experiment with earlier time points and in different cortical areas, would reveal differences in the parameters outlined above.

4.2 Optic nerve development

In another approach, I wanted to investigate the physiological myelin plasticity during development of the optic nerve (Snaidero et al., 2014). Here, myelin outfoldings during internode formation was seen, which in adult stage decreases again suggesting that the myelin outfoldings might serve as a membrane reservoir. Outfoldings are commonly known from patients or disease models, such as Charcot-Marie-Tooth disease or hereditary motor sensory neuropathy and EAE (Bolino et al., 2004; Bolis et al., 2005; Ohnishi A, Murai Y, Ikeda M, Fujita T, Furuya H, 1989; Umehara et al., 1993; Weil et al., 2016).

In order to better understand the role of myelin outfoldings in development, I wanted to establish a time course with all glia cells in the optic nerve to see if we can find a correlation

with other cell types. In accordance with others (Dangata, Findlater, & Kaufman, 1996; Foran & Peterson, 1992; Kondo et al., 2013), I also detected that the number of OPCs decreases after P8, while the maturing, myelinating oligodendrocytes start appearing (Figure 10). In the optic nerve the first MBP⁺ myelin sheets were visible 7 days after birth. Likewise the amount of APC expressing cells starts rising at p7.

Around the same time the number of microglia and astrocytes also start to decrease again (Figure 11) (Hagemeyer et al., 2017). At this time, it has been reported that programmed cell death (PCD) of oligodendrocytes is happening (Sun et al., 2018), which could explain the peak in microglia/astrocyte numbers at P8. Several papers have shown the involvement of microglia in phagocytosis of apoptotic neurons (Marín-Teva et al., 2004; Takahashi et al., 2005), but this is outside the optic nerve. Either they engulf dying neurons or they actively induce PCD by secreting factors like NGF, TNF α or ROS. Another way to regulate cell numbers is to directly monitor progenitor cell numbers by phagocytosis (Reemst, Noctor, Lucassen, & Hol, 2016). Those are all events that happen in the first two weeks after birth.

I took the optic nerve as the model system, as myelination events and distribution of other cell types are relatively more synchronous compared to different areas like the spinal cord, corpus callosum or the cerebellum. Those other areas have a more complex interplay of cell types and a less synchronized time course. Therefore, I investigated the effects at the peak of myelination around P14 (Mayoral, Etxeberria, Shen, & Chan, 2018; Winters et al., 2011). This time point allowed us to have enough myelinating oligodendrocytes, but not too much in order to see individual patches better.

4.3 Ultrastructural changes during optic nerve development

On ultrastructural level, myelin can be visualized quite efficiently through electron microscopy due to its dense structure. Traditionally 2D micrographs are produced that have a good resolution in order to describe the myelin morphology. The state of the art sample preparation, using high pressure freezing (HPF), can be applied to get a more native preservation of membrane architecture (Leunissen & Yi, 2009; Möbius, Nave, & Werner, 2016). This is achieved through the sudden drop in pressure (2000 bar) and temperature (liquid nitrogen), which avoids the formation of ice crystals harming the sample and

building artefacts. It needs to be mentioned, however, that sometimes wrong conclusions are drawn since this method lacks additional volume information of surrounding tissue and cells.

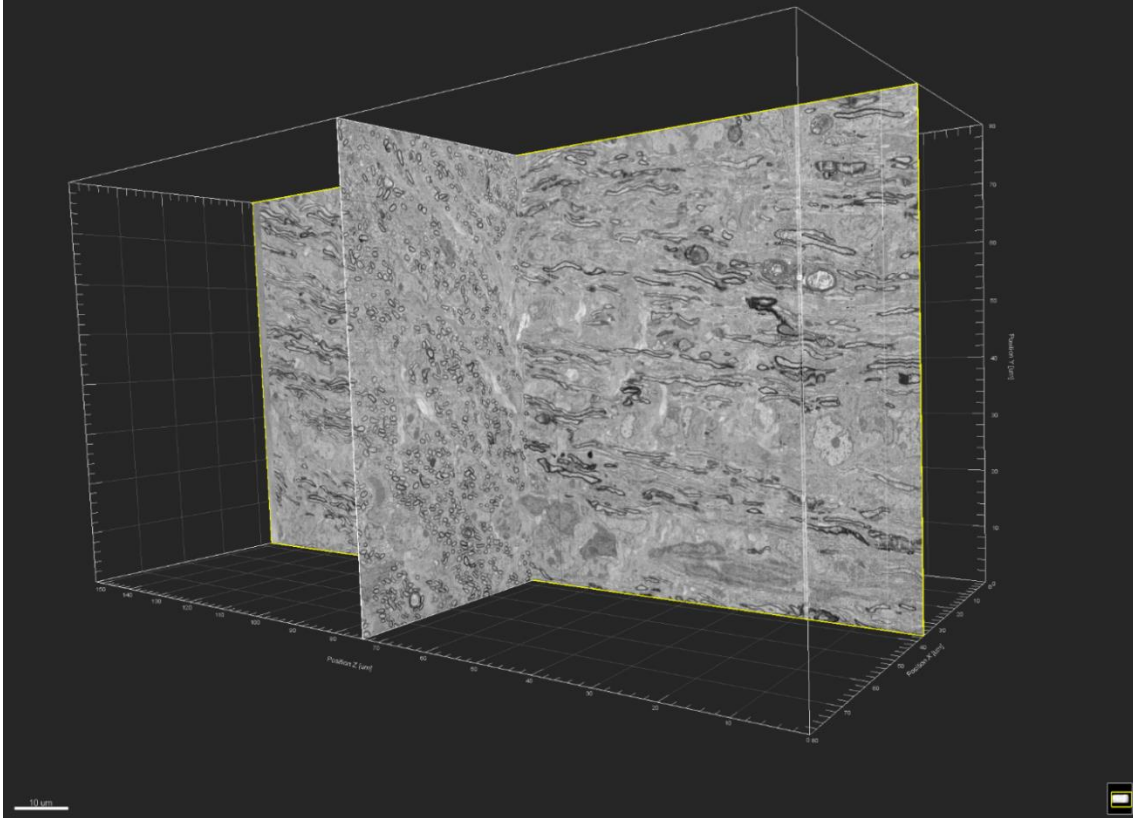


Figure 24: 3D-electron microscopy stack of 14 day old optic nerve of a wild type mouse

Visualization of a $80 \times 80 \times 150 \mu\text{m}$ volume in Imaris using two perpendicular cross sectional slices generated from image stack acquired with serial block face scanning electron microscope (SBF-SEM). Scale bar = $10 \mu\text{m}$.

Therefore, I went for a scanning electron microscopy method which combines still good resolution with 3D volume imaging called: serial block face imaging (3 View). The tissue is differently contrasted and embedded in plastic like for regular transmission electron microscopy. The gain of volume information is achieved by the setup itself using a diamond knife mounted inside the microscope itself. After each cut the surface is scanned. This allowed us to acquire datasets of several $80 \times 80 \times 150 \mu\text{m}^3$ volumes, which gave us additional information about myelin events in 3D. The volume gave me the opportunity to look at the outfoldings in more detail, which revealed several novel findings. Outfoldings were detected from P14 to P60 in decreasing rate as described already by our lab previously

in conventional TEM But in the (Snaidero et al., 2014). In the 3D reconstruction (Figure 12) one could see that the dimension of the outfoldings were several μm stretching away from the axon. The myelin seemed to be intact and still fully attached to the corresponding internode. This was seen in all time points analyzed (P10, P14, P21, P60) in various degrees of severity. Interestingly, I was able to find debris that was still attached to the internode (Figure 13). That came as a surprise, since the myelin was similar as found in demyelination models (Weil et al., 2016). Additionally, I could find microglia that engulfed and also already phagocytosed sizeable myelin clumps (Figure 14). This was unexpected in normal developing optic nerve. This redundant myelin debris is normally observed after axonal injury or damage to the tissue itself (Cantuti-Castelvetri et al., 2018; Kocur et al., 2015). My findings suggest that the outfoldings are pinched off by microglia during development. This is supported by my finding of microglia pulling at myelin debris that was still attached to an otherwise intact internode (Figure 15). Therefore I suggest a newly identified, active role for microglia in myelin pruning during development, similar to synaptic pruning (Paolicelli et al., 2011). It is possible, that the intact outfoldings have a certain threshold in length, which decides on whether they can be retracted again by the oligodendrocyte for further use, when the axons grows. If the size is over a certain limit, then there are two options to discard excess myelin again. Either the oligodendrocyte starts exposing eat-me signals like phosphatidylserine, on the outer membrane, or microglia actively start to degrade the myelin themselves. This theory of active involvement in myelin disassembly is supported by the fact, no intact myelin outfoldings have been phagocytosed by microglia. The intact outfoldings could be seen attached or aligned around the microglia but not intracellularly. Only degenerated myelin was internalized by the microglia. Sometimes there was also myelin debris visible, which was not attached to the axon but just existing in the extracellular space (like in Figure 14).

To further investigate the underlying mechanism of myelin pruning by microglia e.g. live *in vivo* imaging of myelin and microglia tagged proteins in either the zebrafish or mice model using two-photon or confocal imaging could be done, similar to approaches by (Morsch et al., 2015; Peri & Nüsslein-Volhard, 2008). However, myelin pruning it is a rather infrequent event, hence it is hard to track and to identify.

Further investigation of 2D TEM images revealed that this degenerated myelin is also decreasing as the optic nerve matures (Figure 16). This hints towards myelin pruning being

a transient process, like synaptic pruning, to establish the first mature connections for early adulthood.

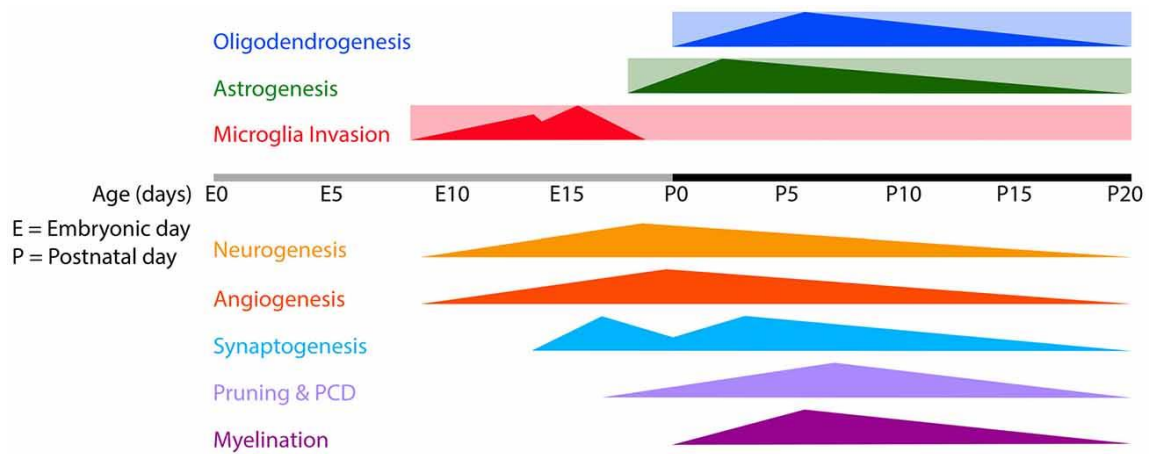


Figure 25: Developmental processes in the CNS

Shown are developmental processes involving central nervous system cell types along a time axis ranging. PCD = programmed cell death. Modified from (Reemst et al., 2016)

To further proof that microglia are indeed the cells that are involved in the pruning process of myelin internodes, I detected MBP⁺ lysosomes inside microglia as shown in Figure 17.

4.4 MerTK/TREM2 involvement in pruning

I established that microglia are involved in myelin pruning. Thus, I wanted to further investigate possible receptors involved in the recognition and phagocytosis of myelin debris. Several publications pointed to MerTK being responsible for myelin uptake, either *in vitro* with human myeloid cells or *in vivo* Schwann cells in the peripheral nervous system (Akkermann et al., 2017; Brosius Lutz et al., 2017; Healy et al., 2016, 2017). To check, whether ablation of this receptor leads to a decrease in myelin phagocytosis and an increase in myelin debris, I performed the same TEM quantification as before with optic nerves from a mouse line deficient for MerTK in microglia. Surprisingly, there were no differences detectable when looking at the number of normally myelinated axons, as well as outfoldings or debris as seen in Figure 18. This did not change, when maturing as P21 mice showed also no effect. One explanation could be that other receptors from the same family are higher expressed on microglia compensate for the loss of function of MerTK. MerTK is a member of the TAM - receptor tyrosine kinase family, with the other two members being Axl and

Tyro3. Schwann cells deficient for Axl, were not able to sufficiently clear myelin debris, after a nerve crush injury in the peripheral nervous system (Brosius Lutz et al., 2017). Furthermore, Axl-deficient mice were also not able to clear myelin in an EAE demyelinating model (Weinger et al., 2011). The same was apparent in a cuprizone induced demyelinating model, where Axl-deficient mice showed a delayed removal of myelin debris and a resulting delay in recovery (Hoehn et al., 2008). So maybe there is a compensatory effect when MerTK is deleted (Seitz, Camenisch, Lemke, Earp, & Matsushima, 2007), although Axl is known to be expressed more in aged white matter (Raj et al., 2017). Additionally, there could also be other cells that could compensate for the lack of microglia phagocytosis. Astrocytes have also been shown to be able to phagocytose myelin from the internode of developing optic nerve in *Xenopus laevis* during metamorphosis (Mills et al., 2015). In the adult forebrain of rats, astrocytes have also been shown to associated with disrupted myelin (Varela-Echevarría, Vargas-Barroso, Lozano-Flores, & Larriva-Sahd, 2017). It can also be an age effect, meaning during development maybe other receptors are involved but later on MerTK considered to be mainly responsible (X. Wang et al., 2018).

Hence, I changed the focus to another promising receptor, called Trem2. This receptor has been shown to activate microglia cells (Filipello et al., 2018) during normal development. During demyelination by cuprizone treatment, Trem2-deficiency has led to a decreased gene expression of phagocytic receptor (Axl), lipid transport and metabolism linked genes (ApoE, Lpl) or inflammatory genes (Il1b, Il6) (Poliani et al., 2015). Another study also suggests that Trem2 is responsible for the recognition of glycolipids like sphingomyelin and sulfatides, which are present on degenerated myelin (Y. Wang et al., 2015). Besides a study has shown that TREM2 protein is expressed longer in white matter regions after birth, compared to grey matter regions (Chertoff, Shrivastava, Gonzalez, Acarin, & Giménez-Llort, 2013). This suggests an involvement of TREM2 in the formation of white matter tracts.

Consequently, I went for the same approach, as described for the wild type and Mertk-deficient microglia before (Figure 16, Figure 18). The number of overall normally myelinated axons was not changed in 14 and 21 day old animals. When comparing the percentage of outfoldings observed per total number of axons, no difference was detectable. But, when comparing the percentage of degenerated myelin, there was an increase from 2 to 8% of all myelinated axons at 14 days after birth. This percentage decreased from 1 to

4% of all myelinated axons at 21 days after birth (Figure 19). So there is an overall decrease within those two time points, but an increase when wild type and trem2 deficient mice are compared. Therefore, trem2-deficiency in microglia leads to an increase in degenerated myelin during the first three weeks after birth. Suggesting impaired phagocytosis of myelin debris. Indeed, a recent study has shown that microglia are actually phagocytosing newly myelinating oligodendrocytes during development (Li et al., 2019). But this study suggests a peak of those phagocytosing amoeboid microglia cells at P8 and already a decline again at P14. In their model they suggest that those microglia, are not dependent on TREM2 signaling, since in TREM2 and APOE mutant mice, this pool of developmental, phagocytosing microglia cells was not reduced.

To further investigate the microglia behavior, I investigated whether microglia activation is altered as described by literature (Filipello et al., 2018). Here, I checked for known microglia activation markers like CD68, Galectin-3/Mac2 and Mac3 (Bodea et al., 2014; Hagemeyer et al., 2017; Reichert & Rotshenker, 1996). Here, I could see that CD68/IBA1 double positive cells were significantly reduced in the 14 day old trem2 deficient animals compared to the wild type. That drastic decrease in activation was not seen 7 days later at p21 (Figure 20). This could mean, that there is only a small window during development, when myelin pruning takes place. This observation matches with the previous findings, where the percentage of outfoldings and degenerated myelin declines upon maturation of the animal (Figure 17). Also in literature it was shown, that *in vitro* microglia devoid of trem2 are less activated and less motile than in the wild type control (Mazaheri et al., 2017). The other activation marker Galectin3/MAC-2 did show the opposite pattern. Here, there was no significant decrease at 14 days after birth, but at 21 days with a decrease of 30% to almost no double positive cells. At 14 days, a downward trend was visible. The expression at 21 days after birth in the wild type was higher compared to the 14 day old wild type which could be explained by a delayed expression of MAC-2 in white matter as shown by (Raj et al., 2017). Lastly, MAC-3 was tested as an activation marker. It did not show any significant changes between the Trem2 knock out and control animals, but there was a downward trend visible Figure 20. The biological variance was quite high, because the reproducible cutting of thin cryo-sections was quite difficult. Additional animals would be needed here, in order to detect small changes within microglial activation makers.

4.5 DAM-response during development

In the last experiment I wanted to confirm a microglia activation during peak of myelination. Therefore, we compared the cortex and corpus callosum at peak myelination (at P14) to almost complete myelination (at P60). I chose those time points since pruning should not be visible anymore when myelination is declining again at p60. If there is a microglia subtype that is responsible for myelin pruning, there should be genes that are higher expressed at p14 corpus callosum compared to either p14 grey matter or at a more adult (at p60) stage. Indeed, I could see differentially expressed genes (Figure 21, Figure 32) and pathways (Figure 22) when comparing the different tissues. The top 10 regulated pathways in p14 showed some relation to our hypothesis. First of all, the pathways that were upregulated in p14 white matter compared to p60 white matter can be linked to myelin pruning. For instance the ECM-receptor interaction might be necessary in order to activate microglia into phagocytosing the myelin debris (Milner & Campbell, 2003) or to attach the microglia to the ECM with integrins in order to migrate towards the debris (Dupuy & Caron, 2008). Another way of recognition of debris might be through cytokine signaling, but it is not clear if proteins or lipids from the myelin sheath would act as attractants (Barrette, Nave, & Edgar, 2013). Now the microglia, if being attracted towards the debris, can move by actin remodeling and anchoring via focal adhesion (Fan, Chen, Pathak, Carneiro, & Chung, 2018). This combined with the PI3k-Akt signaling then can lead to actin reorganization and therefore, cell growth and cell motility towards the debris (Chung, Funamoto, & Firtel, 2001; Horvath & DeLeo, 2009) and after phagocytosis of the debris to protein digestion (Janda, Boi, & Carta, 2018). This program of events would match our results of the pathway analysis (Madry & Attwell, 2015). It was surprising, that the same pathways are even more significantly upregulated in the cortex samples compared to the corpus callosum Figure 22. Looking closer, also more genes were involved in the pathways mentioned compared to the white matter comparison. This might be explained by the difference between the cortical areas and the corpus callosum itself: maybe in white matter those phagocytic mechanisms are important in order to accompany the overproduction of myelin by the oligodendrocyte and to aid myelination, but are also necessary in the cortical regions for removal of debris caused by apoptosis of various cell types (W. R. Kim & Sun, 2011).

Since I saw an upregulation of pathways that can be involved in myelin pruning and chemotaxis towards debris, I wanted to further investigate, if this activation is enough to

trigger a profile as described for Trem2-dependent DAM (Keren-Shaul et al., 2017; Li et al., 2019). Therefore, we compared our differentially expressed genes with the ones from supplement table no. 2 from Keren-Shaul *et al.* (2017) (Figure 23 A). Here, we could see a difference in gene expression levels, when comparing our different ages and brain regions. Unfortunately, when comparing the expression values with the level that Keren-Shaul *et al.* showed, DAM genes were not as highly expressed (Figure 23 B). Therefore, I do not think that myelin debris produced during normal myelination is a strong signal triggering the transition of microglia into a highly activated state in order to phagocytose myelin. Maybe myelin pruning is also mediated through complement receptors as shown for synaptic pruning (Schafer et al., 2012). One would need to either do slice-culture experiments, with labeled myelin debris or zebrafish live imaging experiments in order to prove the receptor involvement. Also qPCR could be done to compare actual transcript levels.

Taken together, microglia seem to be important for the proper formation and fine tuning of myelin. But further research needs to be done to identify important pathways and specific regulators, for recognition of debris and the signal transduction, which is triggered.

5 Summary

Myelin has been shown to be more than just an insulator of neuronal processes. The involvement in motor skill learning and different forms of plasticity have been in focus of research in the recent years. In this thesis, my aim was to investigate the gene regulation after motor skill learning and the myelin plasticity during development. I could show that mice are able to increase their running speed and velocity after a few days of learning. I could see no broad epigenetic (DNA-methylation) regulation of genes related to plasticity or myelination. This was true after two weeks on the training wheel, as well as 3 or 7 days after learning on the complex wheel. Only the transcription factor TFEB, which is directly linked to myelin, was differentially methylated. This factor is involved in inducing apoptosis in unmyelinated brain regions in oligodendrocytes by regulating the timing of myelination during development (Sun et al., 2018). In our experiment this would translate to a regulation of myelinating oligodendrocytes by methylation of the TFEB gene to suppress programmed cell death. This could increase OL number and myelination capabilities. Otherwise, I did see no other significant changes, but this could be because other brain regions (motor cortex, cerebellum) are mainly affected, or the timing of the samples taken was too late (Doya, 2000; L. Xiao et al., 2016).

In order to investigate myelin plasticity during optic nerve development, I investigated the ultrastructure using 2D- and 3D-electron microscopy. In the 3D volumes of optic nerves from P14, P21 and P60 wild type mice, I could observe outfoldings and degenerated myelin debris. The degenerated myelin was seen in the extracellular space, but more interestingly sometimes also still attached to the myelinated axon. This debris in the extracellular space, degenerated myelin membranes and outfoldings were often associated with microglia cells. Outfoldings and degenerated myelin was seen most at p14 and decreased later in development.

Following this engulfment of myelin debris by microglia during development, which I termed “myelin pruning”, I investigated if this process is receptor-mediated. Therefore, I investigated if certain receptors like MerTK and TREM2, which have been linked to the recognition and phagocytosis of myelin debris. Hence, I checked the same parameters using

electron microscopy in an optic nerve from a MerTK mutant mice. Here, no differences in myelin outfoldings or degenerated debris compared to the wild type were visible. This suggests that MerTK might not be responsible for developmental myelin pruning, but rather another microglial receptor.

Furthermore, I investigated another receptor called TREM2, which also has been described as being responsible for phagocytosis of apoptotic neurons and oligodendrocyte precursors during development. Here, TEM analysis showed no change in the amount of outfoldings, but a significant increase in degenerated myelin. Furthermore, immunohistochemical stainings of the optic nerve confirmed that microglia cells are less activated in TREM2 deficient animals at P14 and P21. Microglial activation markers like CD68, Mac2 and Mac3, co-expressed with Iba1 seemed to be downregulated in the knockout animals. It was recently discovered that a subpopulation of microglia, which are highly phagocytic active and were identified i.e. in AD mouse models, are formed in a Trem2- dependent manner. These cells were identified due to their distinct gene expression profile. Hence, I wanted to know if myelin pruning is also triggering a gene profile comparable to DAM (Keren-Shaul et al., 2017). Therefore, we compared the white and grey matter of 14 and 60 day old mice. Here, the corpus callosum and the cortex were sequenced separately. Classical genes that were mentioned in Alzheimer's disease, related to lipid metabolism, phagocytosis, and lysosomal pathways were not upregulated in P14 white matter compared to literature and also P60 mice (Keren-Shaul et al., 2017; Li et al., 2019). But when a pathway analysis was performed, pathways related to cell migration, cytokine signaling and extracellular matrix signaling were upregulated. This was observed in both white and grey matter and might be because of other developmental processes like synapse pruning or apoptosis of overproduced glial cells.

Taken together, microglia appear to be involved in myelin pruning during development. This might be regulated via TREM2 signaling, but does not trigger a full DAM gene profile as seen in disease models.

6 Appendix

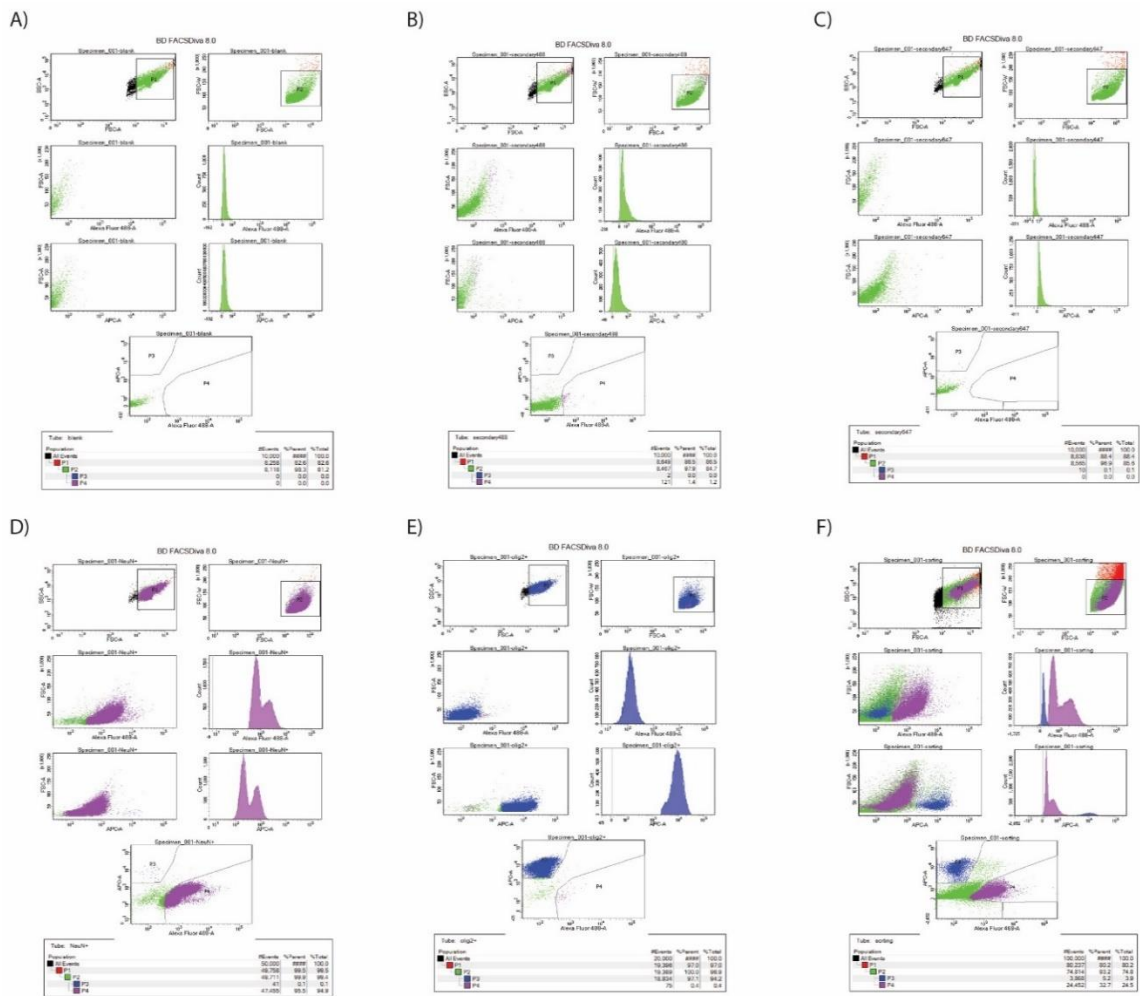


Figure 26: FACS control stainings of mouse corpus callosum

A) The blank sample did not have any antibody labeling. Gate P3 and P4 were without staining. B)-C) For the background control of the AF488 (B) and AF647 (C) the respective primary antibody was omitted and only the secondary was used. No staining was apparent in gate P3 and P4. D) Staining for NeuN with Alexa 488 as secondary antibody did not show cells in gate P3. The purity of the cells gated in P4 were above 95%. E) Staining for Olig2 with Alexa 647 did show only a small set of positive cells in the gate P4 for NeuN⁺ cells. The purity of the gated cells was above 95%. F) Double staining for NeuN⁺ and Olig2⁺ cells.

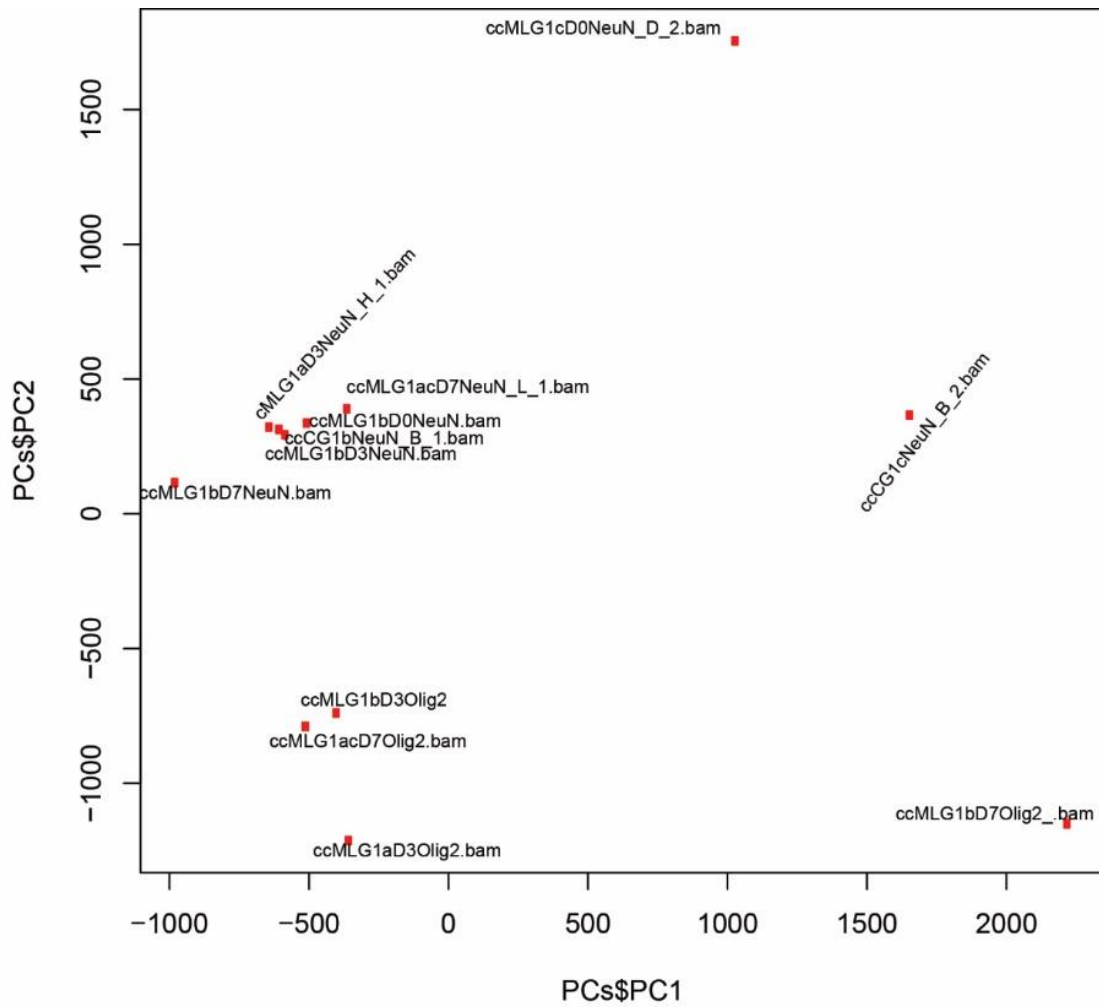


Figure 27: Principal Component Analysis of the samples tested for MeDIP sequencing

MLG1 on different days (D0, D3, D7) and the CG1 that did not run on a wheel were compared with each other. For neurons (NeuN⁺) and oligodendrocytes (Olig2⁺) nuclei were compared using the clustering of variances between samples.

Table 4: Sample barcode

Listed are the sample and their sample information, that were pooled and their given names for the sequencing.

SI	Sample Name	Genotype	Region	Age	Sex	Pool	Barcode
1	P14 cc #1	WT	CC	P14	male	1	IonXpress001
2	P14 cc #2	WT	CC	P14	male		
3	P14 cc #3	WT	CC	P14	male	2	IonXpress002
4	P14 cc #4	WT	CC	P14	male		
5	P14 ctx #1	WT	CTX	P14	male	3	IonXpress003
6	P14 ctx #2	WT	CTX	P14	male		
7	P14 ctx #3	WT	CTX	P14	male	4	IonXpress004
8	P14 ctx #4	WT	CTX	P14	male		
9	P60 cc #1	WT	CC	P60	male	5	IonXpress005
10	P60 cc #2	WT	CC	P60	male		
11	P60 cc #3	WT	CC	P60	male	6	IonXpress006
12	P60 cc #4	WT	CC	P60	male		
13	P60 ctx #5	WT	CTX	P60	male	7	IonXpress007
14	P60 ctx #6	WT	CTX	P60	male		
15	P60 ctx #7	WT	CTX	P60	male	8	IonXpress008
16	P60 ctx #8	WT	CTX	P60	male		

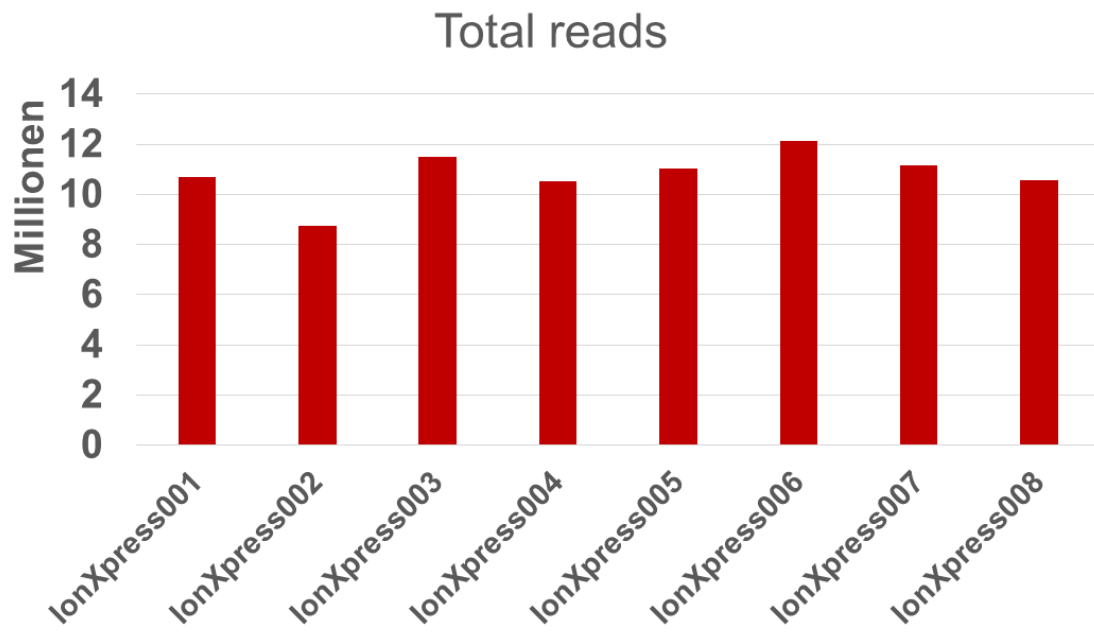


Figure 28: Sample reads

Shown are the total reads from each microglia sample. Names can be taken from Table 4.

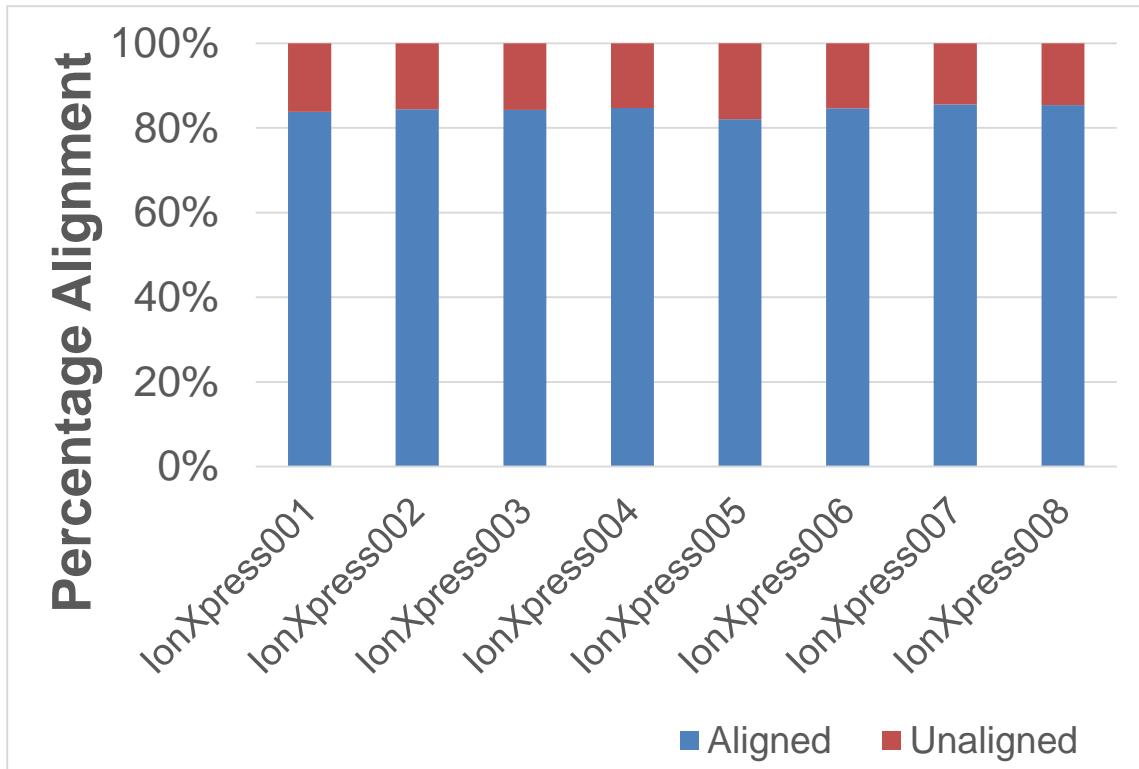


Figure 29: Alignment to genome

Shown is the alignment of the reads to the mouse genome. All the samples had over 80% alignment. Names can be taken from Table 4.

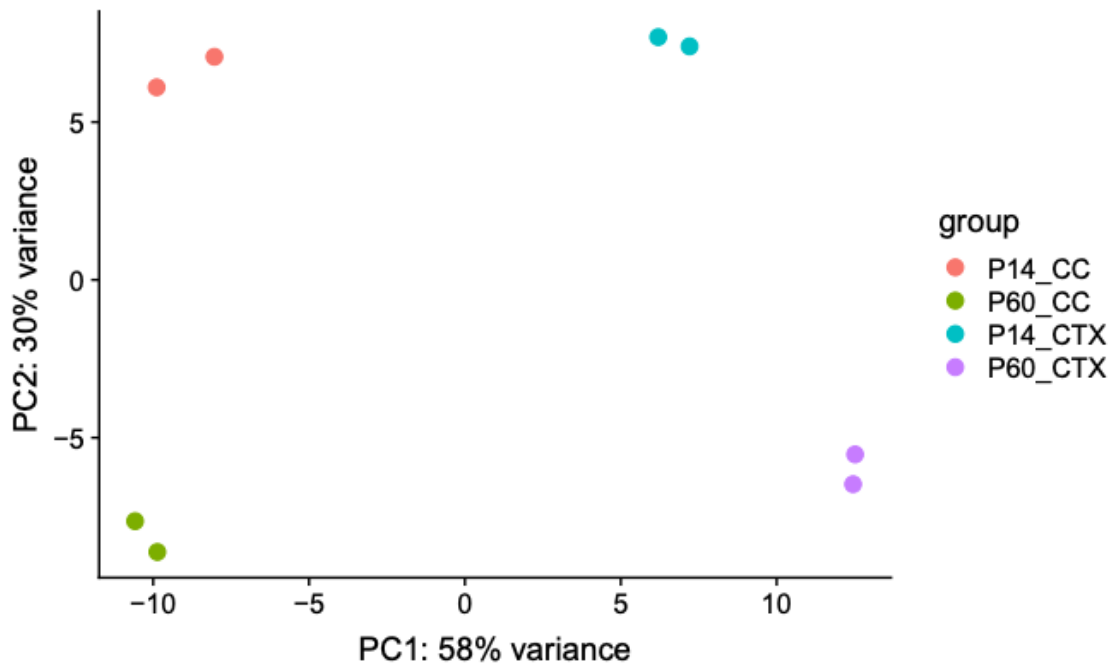


Figure 30: Principle component analysis of different microglia conditions

Shown is the principle component analysis of the samples from Table 4. Principle component 1 (PC1) accounts for 58% of the variance in the samples. Principle component 2 accounts for 30% of the variance in the samples. Each group was well separated from all other groups. cc= corpus callosum, ctx= cortex.

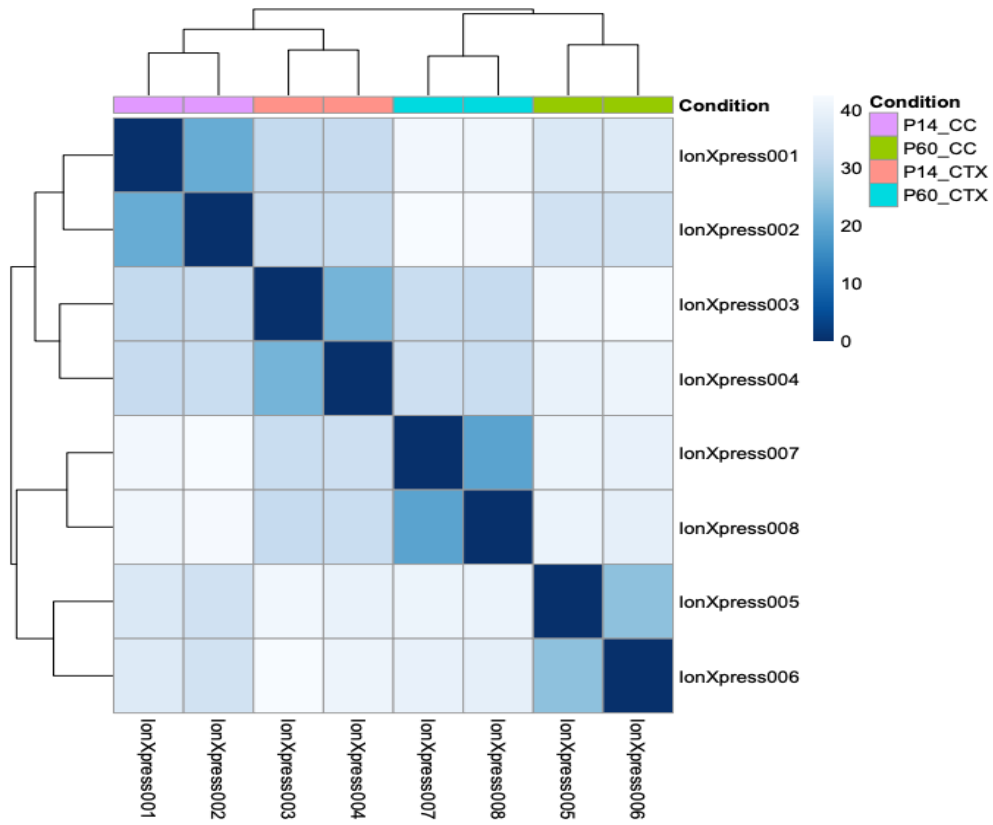


Figure 31: Sample to Sample Distance

Comparison of sample to sample distance. The color code ranges from no distance (dark blue) to big difference (white). cc= corpus callosum, ctx= cortex.

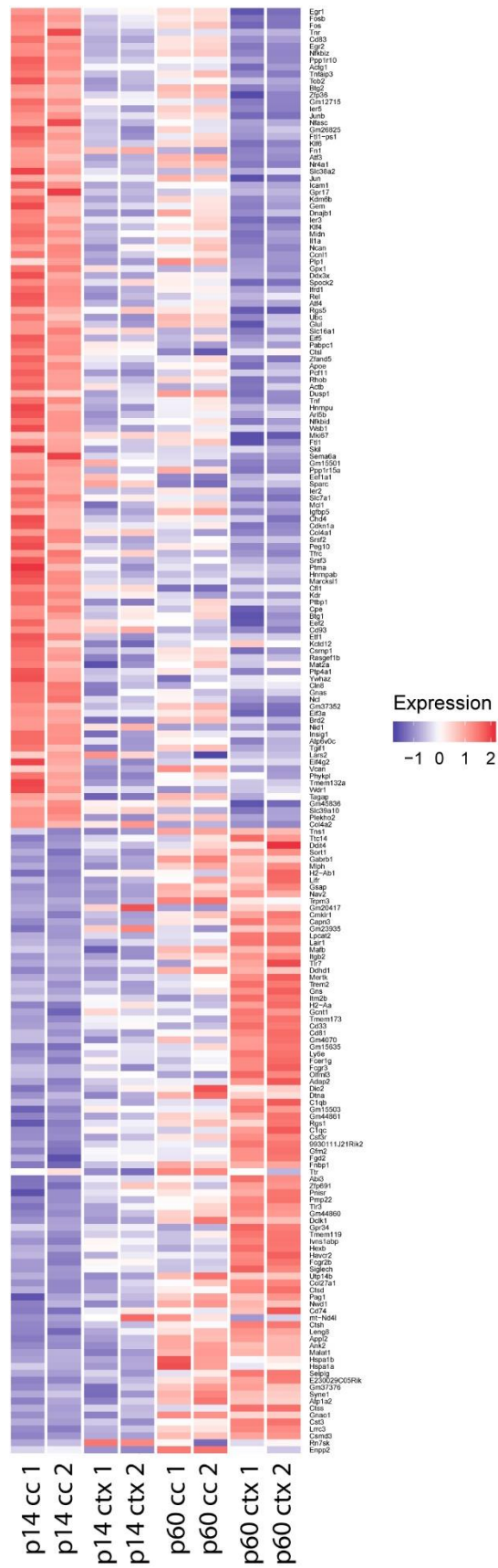


Figure 32: Most differentially expressed genes from wt mice at P14 and P60

Genes that were differentially expressed when comparing wild type mice corpus callosum at P14 to P60 and cortex. cc = corpus callosum, ctx = cortex. There were no significant differences with a p-value of 0,05 when performing a Wilcoxon rank-test.

7 Bibliography

- Abel, J. L. e. B., & Rissman, E. F. (2013). Running-induced epigenetic and gene expression changes in the adolescent brain. *International Journal of Developmental Neuroscience: The Official Journal of the International Society for Developmental Neuroscience*, 31(6), 382–390. <http://doi.org/10.1016/j.ijdevneu.2012.11.002>
- Ajami, B., Bennett, J. L., Krieger, C., Tetzlaff, W., & Rossi, F. M. V. (2007). Local self-renewal can sustain CNS microglia maintenance and function throughout adult life. *Nature Neuroscience*. <http://doi.org/10.1038/nn2014>
- Akkermann, R., Aprico, A., Perera, A. A., Bujalka, H., Cole, A. E., Xiao, J., ... Binder, M. D. (2017). The TAM receptor Tyro3 regulates myelination in the central nervous system. *Glia*, 65(4), 581–591. <http://doi.org/10.1002/glia.23113>
- Allen, N. J., & Lyons, D. A. (2018). Glia as architects of central nervous system formation and function. *Science*. <http://doi.org/10.1126/science.aat0473>
- Almeida, R. G., & Lyons, D. A. (2017). On Myelinated Axon Plasticity and Neuronal Circuit Formation and Function. *The Journal of Neuroscience*, 37(42), 10023–10034. <http://doi.org/10.1523/JNEUROSCI.3185-16.2017>
- Antony, J. M., Paquin, A., Nutt, S. L., Kaplan, D. R., & Miller, F. D. (2011). Endogenous microglia regulate development of embryonic cortical precursor cells. *Journal of Neuroscience Research*. <http://doi.org/10.1002/jnr.22533>
- Baraban, M., Koudelka, S., & Lyons, D. A. (2018). Ca²⁺ activity signatures of myelin sheath formation and growth in vivo. *Nature Neuroscience*. <http://doi.org/10.1038/s41593-017-0040-x>
- Barrera, K., Chu, P., Abramowitz, J., Steger, R., Ramos, R. L., & Brumberg, J. C. (2013). Organization of myelin in the mouse somatosensory barrel cortex and the effects of sensory deprivation. *Developmental Neurobiology*. <http://doi.org/10.1002/dneu.22060>
- Barrette, B., Nave, K. A., & Edgar, J. M. (2013). Molecular triggers of neuroinflammation in mouse models of demyelinating diseases. *Biological Chemistry*. <http://doi.org/10.1515/hsz-2013-0219>
- Bélangier, M., Allaman, I., & Magistretti, P. J. (2011). Brain energy metabolism: Focus on Astrocyte-neuron metabolic cooperation. *Cell Metabolism*, 14(6), 724–738. <http://doi.org/10.1016/j.cmet.2011.08.016>
- Bellot-Saez, A., Kékesi, O., Morley, J. W., & Buskila, Y. (2017). Astrocytic modulation of neuronal excitability through K⁺ spatial buffering. *Neuroscience and Biobehavioral Reviews*, 77, 87–97. <http://doi.org/10.1016/j.neubiorev.2017.03.002>
- Berghoff, S. A., Gerndt, N., Winchenbach, J., Stumpf, S. K., Hosang, L., Odoardi, F., ... Saher, G. (2017). Dietary cholesterol promotes repair of demyelinated lesions in the adult brain. *Nature Communications*. <http://doi.org/10.1097/MAO.0000000000001349>
- Bodea, L.-G., Wang, Y., Linnartz-Gerlach, B., Kopatz, J., Sinkkonen, L., Musgrove, R., ... Neumann, H. (2014). Neurodegeneration by Activation of the Microglial Complement-Phagosome Pathway. *Journal of Neuroscience*, 34(25), 8546–8556. <http://doi.org/10.1523/JNEUROSCI.5002-13.2014>
- Bohlen, C. J., Bennett, F. C., Tucker, A. F., Collins, H. Y., Mulinyawe, S. B., & Barres, B. A. (2017). Diverse Requirements for Microglial Survival, Specification, and Function Revealed by Defined-Medium Cultures. *Neuron*. <http://doi.org/10.1016/j.neuron.2017.04.043>
- Bolino, A., Bolis, A., Previtali, S. C., Dina, G., Bussini, S., Dati, G., ... Wrabetz, L. (2004). Disruption of Mtmr2 CMT4B1-like neuropathy with myelin unfolding and impaired

- spermatogenesis. *Journal of Cell Biology*, 167(4), 711–721. <http://doi.org/10.1083/jcb.200407010>
- Bolis, A. S. C., Simona Bussini, Giorgia Dina, C. P., Previtali, S. C., Mariachiara Malaguti, P. M., Carro, U. Del, Feltri, M. L., ... Bolino1, and A. (2005). Loss of Mtmr2 Phosphatase in Schwann Cells But Not in Motor Neurons Causes Charcot-Marie-Tooth Type 4B1 Neuropathy with Myelin Outfoldings. *Journal of Neuroscience*, 25(37), 8567–8577. <http://doi.org/10.1523/JNEUROSCI.2493-05.2005>
- Bosio, A., Binczek, E., & Stoffel, W. (1996). Functional breakdown of the lipid bilayer of the myelin membrane in central and peripheral nervous system by disrupted galactocerebroside synthesis. *Proceedings of the National Academy of Sciences*. <http://doi.org/10.1073/pnas.93.23.13280>
- Bribián, A., Barallobre, M. J., Soussi-Yanicostas, N., & de Castro, F. (2006). Anosmin-1 modulates the FGF-2-dependent migration of oligodendrocyte precursors in the developing optic nerve. *Molecular and Cellular Neuroscience*. <http://doi.org/10.1016/j.mcn.2006.05.009>
- Brosius Lutz, A., Chung, W.-S., Sloan, S. A., Carson, G. A., Zhou, L., Lovelett, E., ... Barres, B. A. (2017). Schwann cells use TAM receptor-mediated phagocytosis in addition to autophagy to clear myelin in a mouse model of nerve injury. *Proceedings of the National Academy of Sciences*. <http://doi.org/10.1073/pnas.1710566114>
- Bunge, M. B., Bunge, R. P., & Pappas, G. D. (1962). Electron microscopic demonstration of connections between glia and myelin sheaths in the developing mammalian central nervous system. *The Journal of Cell Biology*, 12, 448–453. <http://doi.org/10.1083/jcb.12.2.448>
- Butovsky, O., Jedrychowski, M. P., Moore, C. S., Cialic, R., Lanser, A. J., Gabriely, G., ... Weiner, H. L. (2014). Identification of a unique TGF- β -dependent molecular and functional signature in microglia. *Nature Neuroscience*. <http://doi.org/10.1038/nn.3599>
- Cantuti-Castelvetri, L., Fitzner, D., Bosch-Queralt, M., Weil, M. T., Su, M., Sen, P., ... Simons, M. (2018). Defective cholesterol clearance limits remyelination in the aged central nervous system. *Science*. <http://doi.org/10.1126/science.aan4183>
- Carlyle, W. C., McClain, J. B., Tzafriri, A. R., Bailey, L., Brett, G., Markham, P. M., ... Park, L. T. (2015). TREM2 maintains microglial metabolic fitness in Alzheimer's disease. *Cell*, 162(3), 561–567. <http://doi.org/10.1016/j.jconrel.2012.07.004>. Enhanced
- Chernoff, G. F. (1981). Shiverer: an autosomal recessive mutant mouse with myelin deficiency. *Journal of Heredity*. <http://doi.org/10.1093/oxfordjournals.jhered.a109442>
- Chertoff, M., Shrivastava, K., Gonzalez, B., Acarin, L., & Giménez-Llort, L. (2013). Differential modulation of TREM2 protein during postnatal brain development in mice. *PloS One*, 8(8). <http://doi.org/10.1371/journal.pone.0072083>
- Chung, C. Y., Funamoto, S., & Firtel, R. A. (2001). Signaling pathways controlling cell polarity and chemotaxis. *Trends in Biochemical Sciences*. [http://doi.org/10.1016/S0968-0004\(01\)01934-X](http://doi.org/10.1016/S0968-0004(01)01934-X)
- Coetzee, T., Fujita, N., Dupree, J., Shi, R., Blight, A., Suzuki, K., ... Popko, B. (1996). Myelination in the absence of galactocerebroside and sulfatide: Normal structure with abnormal function and regional instability. *Cell*. [http://doi.org/10.1016/S0092-8674\(00\)80093-8](http://doi.org/10.1016/S0092-8674(00)80093-8)
- Cotter, L., Ozçelik, M., Jacob, C., Pereira, J. A., Locher, V., Baumann, R., ... Tricaud, N. (2010). Dlg1-PTEN interaction regulates myelin thickness to prevent damaging peripheral nerve overmyelination. *Science*. <http://doi.org/10.1126/science.1187735>
- Dangata, Y. Y., Findlater, G. S., & Kaufman, M. H. (1996). Postnatal development of the optic nerve in (C57BL x CBA) F1 hybrid mice : general changes in morphometric parameters. *J Anat*, 117–125.
- Davalos, D., Grutzendler, J., Yang, G., Kim, J. V., Zuo, Y., Jung, S., ... Gan, W. B. (2005). ATP mediates rapid microglial response to local brain injury in vivo. *Nature Neuroscience*. <http://doi.org/10.1038/nn1472>
- Demyanenko, G. P., Schachner, M., Anton, E., Schmid, R., Feng, G., Sanes, J., & Maness, P. F.

- (2004). Close homolog of L1 modulates area-specific neuronal positioning and dendrite orientation in the cerebral cortex. *Neuron*, 44(3), 423–437. <http://doi.org/10.1016/j.neuron.2004.10.016>
- Doya, K. (2000). Complementary roles of basal ganglia and cerebellum in learning and motor control. *Current Opinion in Neurobiology*, 10, 732–739. [http://doi.org/10.1016/S0959-4388\(00\)00153-7](http://doi.org/10.1016/S0959-4388(00)00153-7)
- Dupree, J. L., Coetzee, T., Blight, a, Suzuki, K., & Popko, B. (1998). Myelin galactolipids are essential for proper node of Ranvier formation in the CNS. *The Journal of Neuroscience : The Official Journal of the Society for Neuroscience*. <http://doi.org/10.1002/jhbs>
- Dupree, J. L., Girault, J. A., & Popko, B. (1999). Axo-glial interactions regulate the localization of axonal paranodal proteins. *Journal of Cell Biology*. <http://doi.org/10.1083/jcb.147.6.1145>
- Dupuy, A. G., & Caron, E. (2008). Integrin-dependent phagocytosis - spreading from microadhesion to new concepts. *Journal of Cell Science*, 121(11), 1773–1783. <http://doi.org/10.1242/jcs.018036>
- Eskelinen, E.-L., Illert, A. L., Tanaka, Y., Schwarzmann, G., Blanz, J., Figura, K. von, & Saftig, P. (2002). Role of LAMP-2 in Lysosome Biogenesis and Autophagy. *Molecular Biology of the Cell*, 13(9), 3355–3368. <http://doi.org/10.1091/mbc.E02-02-0114>
- Espenshade, P. J., & Hughes, A. L. (2007). Regulation of Sterol Synthesis in Eukaryotes. *Annual Review of Genetics*. <http://doi.org/10.1146/annurev.genet.41.110306.130315>
- Fabrizio G. Mastronardi, Abdul Noor, D. Denise Wood, Tara Paton, M. A. M. (2007). Peptidyl Argininedeiminase 2 CpG Island in Multiple Sclerosis White Matter Is Hypomethylated. *Journal of Neuroscience Research*, 85, 2006–2016. <http://doi.org/10.1002/jnr.21329>
- Fan, Y., Chen, Z., Pathak, J. L., Carneiro, A. M. D., & Chung, C. Y. (2018). Differential Regulation of Adhesion and Phagocytosis of Resting and Activated Microglia by Dopamine. *Frontiers in Cellular Neuroscience*. <http://doi.org/10.3389/fncel.2018.00309>
- Filipello, F., Morini, R., Corradini, I., Zerbi, V., Canzi, A., Michalski, B., ... Matteoli, M. (2018). The Microglial Innate Immune Receptor TREM2 Is Required for Synapse Elimination and Normal Brain Connectivity. *Immunity*, 48(5), 979–991.e8. <http://doi.org/10.1016/j.immuni.2018.04.016>
- Foran, D. R., & Peterson, a C. (1992). Myelin acquisition in the central nervous system of the mouse revealed by an MBP-Lac Z transgene. *The Journal of Neuroscience : The Official Journal of the Society for Neuroscience*, 12(December), 4890–4897.
- Funfschilling, U., Supplie, L. M., Mahad, D., Boretius, S., Saab, a S., Edgar, J., ... Nave, K. a. (2012). Glycolytic oligodendrocytes maintain myelin and long-term axonal integrity, 0–5. <http://doi.org/10.1038/nature11007>
- Gabriel, S., Njunting, M., Pomper, J. K., Merschhemke, M., Sanabria, E. R. G., Eilers, A., ... Lehmann, T.-N. (2004). Stimulus and Potassium-Induced Epileptiform Activity in the Human Dentate Gyrus from Patients with and without Hippocampal Sclerosis. *Journal of Neuroscience*, 24(46), 10416–10430. <http://doi.org/10.1523/JNEUROSCI.2074-04.2004>
- Gautier, H. O. B., Evans, K. A., Volbracht, K., James, R., Sitnikov, S., Lundgaard, I., ... Káradóttir, R. T. (2015). Neuronal activity regulates remyelination via glutamate signalling to oligodendrocyte progenitors. *Nature Communications*. <http://doi.org/10.1038/ncomms9518>
- Gibson, E. M., Purger, D., Mount, C. W., Goldstein, A. K., Lin, G. L., Wood, L. S., ... Monje, M. (2014). Neuronal activity promotes oligodendrogenesis and adaptive myelination in the mammalian brain. *Science (New York, N.Y.)*, 344, 1252304. <http://doi.org/10.1126/science.1252304>
- Ginhoux, F., Greter, M., Leboeuf, M., Nandi, S., See, P., Mehler, M. F., ... Merad, M. (2010). Fate Mapping Analysis Reveals That Adult Microglia Derive from Primitive Macrophages Florent. *Science*, 330(6005), 841–845. <http://doi.org/10.1126/science.1194637>

- Goebbels, S., Oltrogge, J. H., Kemper, R., Heilmann, I., Bormuth, I., Wolfer, S., ... Nave, K.-A. (2010). Elevated Phosphatidylinositol 3,4,5-Trisphosphate in Glia Triggers Cell-Autonomous Membrane Wrapping and Myelination. *Journal of Neuroscience*. <http://doi.org/10.1523/JNEUROSCI.0219-10.2010>
- Goebbels, S., Oltrogge, J. H., Wolfer, S., Wieser, G. L., Nientiedt, T., Pieper, A., ... Nave, K. A. (2012). Genetic disruption of Pten in a novel mouse model of tomaculous neuropathy. *EMBO Molecular Medicine*. <http://doi.org/10.1002/emmm.201200227>
- Goldmann, T., Wieghofer, P., Müller, P. F., Wolf, Y., Varol, D., Yona, S., ... Prinz, M. (2013). A new type of microglia gene targeting shows TAK1 to be pivotal in CNS autoimmune inflammation. *Nature Neuroscience*. <http://doi.org/10.1038/nn.3531>
- Gomez-Pinilla, F., Zhuang, Y., Feng, J., Ying, Z., & Fan, G. (2011). Exercise impacts brain-derived neurotrophic factor plasticity by engaging mechanisms of epigenetic regulation. *European Journal of Neuroscience*, 33(August 2010), 383–390. <http://doi.org/10.1111/j.1460-9568.2010.07508.x>
- Gordon, G. R. J., Choi, H. B., Ellis-Davies, G. C. R., & MacVicar, B. A. (2012). Brain metabolic state dictates the polarity of astrocyte control over the cerebrovasculature. *Nature*, 29(7223), 997–1003. <http://doi.org/10.1126/scisignal.2001449.Engineering>
- Gudz, T. I. (2006). Glutamate Stimulates Oligodendrocyte Progenitor Migration Mediated via an Integrin/Myelin Proteolipid Protein Complex. *Journal of Neuroscience*. <http://doi.org/10.1523/JNEUROSCI.4054-05.2006>
- Guerreiro, R., Wojtas, A., Bras, J., Carrasquillo, M., Rogaeva, E., Majounie, E., ... Hardy, J. (2013). *TREM2* Variants in Alzheimer's Disease. *New England Journal of Medicine*. <http://doi.org/10.1056/NEJMoa1211851>
- Guo, J. U., Ma, D. K., Mo, H., Ball, M. P., Jang, M.-H., Bonaguidi, M. a, ... Song, H. (2011). Neuronal activity modifies the DNA methylation landscape in the adult brain. *Nature Neuroscience*, 14(10), 1345–1351. <http://doi.org/10.1038/nn.2900>
- Hagemeyer, N., Hanft, K. M., Akriditou, M. A., Unger, N., Park, E. S., Stanley, E. R., ... Prinz, M. (2017). Microglia contribute to normal myelinogenesis and to oligodendrocyte progenitor maintenance during adulthood. *Acta Neuropathologica*, 134(3), 441–458. <http://doi.org/10.1007/s00401-017-1747-1>
- Halder, R., Hennion, M., Vidal, R. O., Shomroni, O., Rahman, R. U., Rajput, A., ... Bonn, S. (2015). DNA methylation changes in plasticity genes accompany the formation and maintenance of memory. *Nature Neuroscience*, 19(1), 102–110. <http://doi.org/10.1038/nn.4194>
- Hartline, D. K., & Colman, D. R. (2007). Rapid Conduction and the Evolution of Giant Axons and Myelinated Fibers. *Current Biology*, 17(1), 29–35. <http://doi.org/10.1016/j.cub.2006.11.042>
- Healy, L. M., Jang, J. H., Won, S. Y., Lin, Y. H., Touil, H., Aljarallah, S., ... Antel, J. P. (2017). MerTK-mediated regulation of myelin phagocytosis by macrophages generated from patients with MS. *Neurology: Neuroimmunology and NeuroInflammation*, 4(6). <http://doi.org/10.1212/NXI.0000000000000402>
- Healy, L. M., Perron, G., Won, S.-Y., Michell-Robinson, M. A., Rezk, A., Ludwin, S. K., ... Antel, J. P. (2016). MerTK Is a Functional Regulator of Myelin Phagocytosis by Human Myeloid Cells. *The Journal of Immunology*, 196(8), 3375–3384. <http://doi.org/10.4049/jimmunol.1502562>
- Hibbits, N., Pannu, R., Wu, T. J., & Armstrong, R. C. (2009). Cuprizone demyelination of the corpus callosum in mice correlates with altered social interaction and impaired bilateral sensorimotor coordination. *ASN Neuro*, 1(3), 153–164. <http://doi.org/10.1042/AN20090032>
- Hill, R. A., Li, A. M., & Grutzendler, J. (2018). Lifelong cortical myelin plasticity and age-related degeneration in the live mammalian brain. *Nature Neuroscience*, 21(5), 683–695. <http://doi.org/10.1038/s41593-018-0120-6>

- Hoehn, H. J., Kress, Y., Sohn, A., Brosnan, C. F., Bourdon, S., & Shafit-Zagardo, B. (2008). Ax1^{-/-} mice have delayed recovery and prolonged axonal damage following cuprizone toxicity. *Brain Research*. <http://doi.org/10.1016/j.brainres.2008.08.076>
- Honke, K., Hirahara, Y., Dupree, J., Suzuki, K., Popko, B., Fukushima, K., ... Taniguchi, N. (2002). Paranodal junction formation and spermatogenesis require sulfoglycolipids. *Proceedings of the National Academy of Sciences*. <http://doi.org/10.1073/pnas.032068299>
- Horvath, R. J., & DeLeo, J. A. (2009). Morphine Enhances Microglial Migration through Modulation of P2X4 Receptor Signaling. *Journal of Neuroscience*. <http://doi.org/10.1523/JNEUROSCI.4595-08.2009>
- Hubert, V., Peschel, A., Langer, B., Gröger, M., Rees, A., & Kain, R. (2016). LAMP-2 is required for incorporating syntaxin-17 into autophagosomes and for their fusion with lysosomes. *Biology Open*, 5(10), 1516–1529. <http://doi.org/10.1242/bio.018648>
- Hughes, E. G., Orthmann-Murphy, J. L., Langseth, A. J., & Bergles, D. E. (2018). Myelin remodeling through experience-dependent oligodendrogenesis in the adult somatosensory cortex. *Nature Neuroscience*. <http://doi.org/10.1038/s41593-018-0121-5>
- Humphrey, M. B., Ogasawara, K., Yao, W., Spusta, S. C., Daws, M. R., Lane, N. E., ... Nakamura, M. C. (2004). The Signaling Adapter Protein DAP12 Regulates Multinucleation during Osteoclast Development. *Journal of Bone and Mineral Research*. <http://doi.org/10.1359/JBMR.0301234>
- Huxley, B. Y. A. F., & Stampfli, A. D. R. (1949). EVIDENCE FOR SALTATORY CONDUCTION IN PERIPHERAL MYELINATED NERVE FIBRES. *Journal of Physiology*, 108(1946), 315–339.
- Ishibashi, T., Dupree, J. L., Ikenaka, K., Hirahara, Y., Honke, K., Peles, E., ... Baba, H. (2002). A myelin galactolipid, sulfatide, is essential for maintenance of ion channels on myelinated axon but not essential for initial cluster formation. *The Journal of Neuroscience: The Official Journal of the Society for Neuroscience*. <http://doi.org/20026705>
- Janda, E., Boi, L., & Carta, A. R. (2018). Microglial Phagocytosis and Its Regulation: A Therapeutic Target in Parkinson's Disease? *Frontiers in Molecular Neuroscience*. <http://doi.org/10.3389/fnmol.2018.00144>
- Johns, T. G., & Bernard, C. C. A. (1999). The structure and function of myelin oligodendrocyte glycoprotein. *Journal of Neurochemistry*. <http://doi.org/10.1046/j.1471-4159.1999.0720001.x>
- Jonsson, T., Stefansson, H., Steinberg, S., Jonsdottir, I., Jonsson, P. V., Snaedal, J., ... Stefansson, K. (2013). Variant of *TREM2* Associated with the Risk of Alzheimer's Disease. *New England Journal of Medicine*. <http://doi.org/10.1056/NEJMoa1211103>
- Keren-Shaul, H., Spinrad, A., Weiner, A., Matcovitch-Natan, O., Dvir-Szternfeld, R., Ulland, T. K., ... Amit, I. (2017). A Unique Microglia Type Associated with Restricting Development of Alzheimer's Disease. *Cell*, 169(7), 1276–1290.e17. <http://doi.org/10.1016/j.cell.2017.05.018>
- Kessaris, N., Fogarty, M., Iannarelli, P., Grist, M., Wegner, M., & Richardson, W. D. (2006). Competing waves of oligodendrocytes in the forebrain and postnatal elimination of an embryonic lineage. *Nature Neuroscience*. <http://doi.org/10.1038/nn1620>
- Kim, H. J., Cho, M. H., Shim, W. H., Kim, J. K., Jeon, E. Y., Kim, D. H., & Yoon, S. Y. (2017). Deficient autophagy in microglia impairs synaptic pruning and causes social behavioral defects. *Molecular Psychiatry*, 22(11), 1576–1584. <http://doi.org/10.1038/mp.2016.103>
- Kim, W. R., & Sun, W. (2011). Programmed cell death during postnatal development of the rodent nervous system. *Development Growth and Differentiation*. <http://doi.org/10.1111/j.1440-169X.2010.01226.x>
- Klingseisen, A., & Lyons, D. A. (2018). Axonal Regulation of Central Nervous System Myelination: Structure and Function. *Neuroscientist*, 24(1), 7–21. <http://doi.org/10.1177/1073858417703030>

- Klugmann, M., Schwab, M. H., Pühlhofer, A., Schneider, A., Zimmermann, F., Griffiths, I. R., & Nave, K. A. (1997). Assembly of CNS myelin in the absence of proteolipid protein. *Neuron*. [http://doi.org/10.1016/S0896-6273\(01\)80046-5](http://doi.org/10.1016/S0896-6273(01)80046-5)
- Kocur, M., Schneider, R., Pulm, A. K., Bauer, J., Kropp, S., Gliem, M., ... Scheu, S. (2015). IFN β secreted by microglia mediates clearance of myelin debris in CNS autoimmunity. *Acta Neuropathologica Communications*. <http://doi.org/10.1186/s40478-015-0192-4>
- Kondo, Y., Ramaker, J. M., Radcliff, A. B., Baldassari, S., Mayer, J. A., Ver Hoeve, J. N., ... Duncan, I. D. (2013). Spontaneous Optic Nerve Compression in the Osteopetrotic (op/op) Mouse: A Novel Model of Myelination Failure. *Journal of Neuroscience*, 33(8), 3514–3525. <http://doi.org/10.1523/JNEUROSCI.4849-12.2013>
- Krasemann, S., Madore, C., Cialic, R., Baufeld, C., Calcagno, N., El Fatimy, R., ... Butovsky, O. (2017). The TREM2-APOE Pathway Drives the Transcriptional Phenotype of Dysfunctional Microglia in Neurodegenerative Diseases. *Immunity*, 47(3), 566–581.e9. <http://doi.org/10.1016/j.immuni.2017.08.008>
- Krasnow, A. M., Ford, M. C., Valdivia, L. E., Wilson, S. W., & Attwell, D. (2018). Regulation of developing myelin sheath elongation by oligodendrocyte calcium transients in vivo. *Nature Neuroscience*. <http://doi.org/10.1038/s41593-017-0031-y>
- Lampron, A., Laroche, A., Laflamme, N., Préfontaine, P., Plante, M.-M., Sánchez, M. G., ... Rivest, S. (2015). Inefficient clearance of myelin debris by microglia impairs remyelinating processes. *The Journal of Experimental Medicine*, 212(4), 481–495. <http://doi.org/10.1084/jem.20141656>
- Lawson, L. J., Perry, V. H., & Gordon, S. (1992). Turnover of resident microglia in the normal adult mouse brain. *Neuroscience*. [http://doi.org/10.1016/0306-4522\(92\)90500-2](http://doi.org/10.1016/0306-4522(92)90500-2)
- Lee, J., Gravel, M., Zhang, R., Thibault, P., & Braun, P. E. (2005). Process outgrowth in oligodendrocytes is mediated by CNP, a novel microtubule assembly myelin protein. *Journal of Cell Biology*. <http://doi.org/10.1083/jcb.200411047>
- Lee, Y., Morrison, B. M., Li, Y., Lengacher, S., Farah, M. H., Hoffman, P. N., ... Rothstein, J. D. (2012). Oligodendroglia metabolically support axons and contribute to neurodegeneration. *Nature*, 487(7408), 443–448. <http://doi.org/10.1038/nature11314>. Oligodendroglia
- Leis, J. A., Bekar, L. K., & Walz, W. (2005). Potassium homeostasis in the ischemic brain. *GLIA*. <http://doi.org/10.1002/glia.20145>
- Leunissen, J. L. M., & Yi, H. (2009). Self-pressurized rapid freezing (SPRF): A novel cryofixation method for specimen preparation in electron microscopy. *Journal of Microscopy*. <http://doi.org/10.1111/j.1365-2818.2009.03178.x>
- Li, Q., Cheng, Z., Zhou, L., Darmanis, S., Neff, N., Okamoto, J., ... Barres, B. A. (2019). Developmental heterogeneity of microglia and brain myeloid cells revealed by deep single-cell RNA sequencing. *Neuron*, 101(2), 207–223. <http://doi.org/10.1101/406363>
- Liebetanz, D., Baier, P. C., Paulus, W., Meuer, K., Bähr, M., & Weishaupt, J. H. (2007). A highly sensitive automated complex running wheel test to detect latent motor deficits in the mouse MPTP model of Parkinson's disease. *Experimental Neurology*, 205, 207–213. <http://doi.org/10.1016/j.expneurol.2007.01.030>
- Liebetanz, D., & Merkler, D. (2006). Effects of commissural de- and remyelination on motor skill behaviour in the cuprizone mouse model of multiple sclerosis. *Experimental Neurology*, 202, 217–224. <http://doi.org/10.1016/j.expneurol.2006.05.032>
- Lin, S. T., Heng, M. Y., Ptáček, L. J., & Fu, Y. H. (2014). Regulation of myelination in the central nervous system by nuclear lamin B1 and Non-coding RNAs. *Translational Neurodegeneration*. <http://doi.org/10.1186/2047-9158-3-4>
- Liu, J., Moyon, S., Hernandez, M., & Casaccia, P. (2016). Epigenetic control of oligodendrocyte development: Adding new players to old keepers. *Current Opinion in Neurobiology*, 39, 133–

138. <http://doi.org/10.1016/j.conb.2016.06.002>
- Liu, P., Du, J., & He, C. (2013). Developmental pruning of early-stage myelin segments during CNS myelination in vivo. *Cell Research*, *23*(7), 962–964. <http://doi.org/10.1038/cr.2013.62>
- Lively, S., Lam, D., Wong, R., & Schlichter, L. C. (2018). Comparing effects of transforming growth factor β 1 on microglia from rat and mouse: Transcriptional profiles and potassium channels. *Frontiers in Cellular Neuroscience*. <http://doi.org/10.3389/fncel.2018.00115>
- Love, M. I., Huber, W., & Anders, S. (2014). Moderated estimation of fold change and dispersion for RNA-seq data with DESeq2. *Genome Biology*, *15*(12), 1–21. <http://doi.org/10.1186/s13059-014-0550-8>
- Lundgaard, I., Luzhynskaya, A., Stockley, J. H., Wang, Z., Evans, K. a., Swire, M., ... Káradóttir, R. T. (2013). Neuregulin and BDNF Induce a Switch to NMDA Receptor-Dependent Myelination by Oligodendrocytes. *PLoS Biology*, *11*(12). <http://doi.org/10.1371/journal.pbio.1001743>
- Luo, C., Jian, C., Liao, Y., Huang, Q., Wu, Y., Liu, X., ... Wu, Y. (2017). The role of microglia in multiple sclerosis. *Neuropsychiatric Disease and Treatment*. <http://doi.org/10.2147/NDT.S140634>
- Lyahyai, J., Oulad Amar Bencheikh, B., Elalaoui, S. C., Mansouri, M., Boualla, L., Dionne-Laporte, A., ... Sefiani, A. (2018). Exome sequencing reveals a novel PLP1 mutation in a Moroccan family with connatal Pelizaeus-Merzbacher disease: A case report. *BMC Pediatrics*. <http://doi.org/10.1186/s12887-018-1063-5>
- Ma, B., Buckalew, R., Du, Y., Kiyoshi, C. M., Alford, C. C., Wang, W., ... Zhou, M. (2016). Gap junction coupling confers isopotentiality on astrocyte syncytium. *GLIA*. <http://doi.org/10.1002/glia.22924>
- Madry, C., & Attwell, D. (2015). Receptors, ion channels, and signaling mechanisms underlying Microglial dynamics. *Journal of Biological Chemistry*, *290*(20), 12443–12450. <http://doi.org/10.1074/jbc.R115.637157>
- Maglione, M., Tress, O., Haas, B., Karram, K., Trotter, J., Willecke, K., & Kettenmann, H. (2010). Oligodendrocytes in mouse corpus callosum are coupled via gap junction channels formed by Connexin47 and Connexin32. *GLIA*. <http://doi.org/10.1002/glia.20991>
- Makinodan, M., Rosen, K. M., Ito, S., & Corfas, G. (2012). A critical period for social experience-dependent oligodendrocyte maturation and myelination. *Science*. <http://doi.org/10.1126/science.1220845>
- Marín-Teva, J. L., Dusart, I., Colin, C., Gervais, A., Van Rooijen, N., & Mallat, M. (2004). Microglia Promote the Death of Developing Purkinje Cells. *Neuron*, *41*(4), 535–547. [http://doi.org/10.1016/S0896-6273\(04\)00069-8](http://doi.org/10.1016/S0896-6273(04)00069-8)
- Mathews, E. S., Mawdsley, D. J., Walker, M., Hines, J. H., Pozzoli, M., & Appel, B. (2014). Mutation of 3-Hydroxy-3-Methylglutaryl CoA Synthase I Reveals Requirements for Isoprenoid and Cholesterol Synthesis in Oligodendrocyte Migration Arrest, Axon Wrapping, and Myelin Gene Expression. *Journal of Neuroscience*. <http://doi.org/10.1523/JNEUROSCI.4587-13.2014>
- Mayoral, S. R., Etxeberria, A., Shen, Y.-A. A., & Chan, J. R. (2018). Initiation of CNS Myelination in the Optic Nerve Is Dependent on Axon Caliber. *Cell Reports*, *25*(3), 544–550.e3. <http://doi.org/10.1016/j.celrep.2018.09.052>
- Mazaheri, F., Snaidero, N., Kleinberger, G., Madore, C., Daria, A., Werner, G., ... Haass, C. (2017). TREM2 deficiency impairs chemotaxis and microglial responses to neuronal injury. *EMBO Reports*, *18*(7), 1186–1198. <http://doi.org/10.15252/embr.201743922>
- Mckenzie, I. A., Ohayon, D., Li, H., Faria, J. P. De, Emery, B., Tohyama, K., & Richardson, W. D. (2014). Motor skill learning requires active central myelination. *Science*, *346*(6207), 318–322.
- Meireles, A. M., Shen, K., Zoupi, L., Iyer, H., Bouchard, E. L., Williams, A., ... Williams, A. (2018).

- The Lysosomal Transcription Factor TFEB Represses Myelination Downstream of the Rag-Ragulator Complex Article The Lysosomal Transcription Factor TFEB Represses Myelination Downstream of the Rag-Ragulator Complex. *Developmental Cell*, 47(3), 1–12. <http://doi.org/10.1016/j.devcel.2018.10.003>
- Meyer, N., Richter, N., Fan, Z., Siemonsmeier, G., Pivneva, T., Jordan, P., ... Kettenmann, H. (2018). Oligodendrocytes in the Mouse Corpus Callosum Maintain Axonal Function by Delivery of Glucose. *Cell Reports*, 22(9), 2455–2468. <http://doi.org/10.1016/j.celrep.2018.02.022>
- Mikula, S., Binding, J., & Denk, W. (2012). Staining and embedding the whole mouse brain for electron microscopy. *Nature Methods*, 9(12), 1198–1201. <http://doi.org/10.1038/nmeth.2213>
- Mills, E. A., Davis, C. O., Bushong, E. A., Boassa, D., Kim, K.-Y., Ellisman, M. H., & Marsh-Armstrong, N. (2015). Astrocytes phagocytose focal dystrophies from shortening myelin segments in the optic nerve of *Xenopus laevis* at metamorphosis. *Proceedings of the National Academy of Sciences*, 112(33), 10509–10514. <http://doi.org/10.1073/pnas.1506486112>
- Milner, R., & Campbell, I. L. (2003). The Extracellular Matrix and Cytokines Regulate Microglial Integrin Expression and Activation. *The Journal of Immunology*, 170(0), 3850–3858. <http://doi.org/10.4049/jimmunol.170.7.3850>
- Milner, R., Edwards, G., Streuli, C., & French-Constant, C. (1996). A Role in Migration for the $\alpha\beta 1$ Integrin Expressed on Oligodendrocyte Precursors. *The Journal of Neuroscience*, 16(22), 7240–7252. <http://doi.org/10.1523/JNEUROSCI.16-22-07240.1996>
- Miron, V. E., Boyd, A., Zhao, J. W., Yuen, T. J., Ruckh, J. M., Shadrach, J. L., ... French-Constant, C. (2013). M2 microglia and macrophages drive oligodendrocyte differentiation during CNS remyelination. *Nature Neuroscience*, 16(9), 1211–1218. <http://doi.org/10.1038/nn.3469>
- Möbius, W., Nave, K. A., & Werner, H. B. (2016). Electron microscopy of myelin: Structure preservation by high-pressure freezing. *Brain Research*. <http://doi.org/10.1016/j.brainres.2016.02.027>
- Morell, P., & Quarles, R. (1999). Characteristic composition of myelin. In *Basic Neurochemistry: Molecular, Cellular and Medical Aspects*. <http://doi.org/10.1172/JCI64124>
- Morsch, M., Radford, R., Lee, A., Don, E. K., Badrock, A. P., Hall, T. E., ... Chung, R. (2015). In vivo characterization of microglial engulfment of dying neurons in the zebrafish spinal cord. *Frontiers in Cellular Neuroscience*, 9(August), 1–11. <http://doi.org/10.3389/fncel.2015.00321>
- Moscarello, M. a., Mastronardi, F. G., & Wood, D. D. (2007). The role of citrullinated proteins suggests a novel mechanism in the pathogenesis of multiple sclerosis. *Neurochemical Research*, 32, 251–256. <http://doi.org/10.1007/s11064-006-9144-5>
- Moyon, S., Huynh, J. L., Dutta, D., Zhang, F., Ma, D., Yoo, S., ... Casaccia, P. (2016). Functional Characterization of DNA Methylation in the Oligodendrocyte Lineage. *Cell Reports*, 15(4), 748–760. <http://doi.org/10.1016/j.celrep.2016.03.060>
- Moyon, S., Ma, D., Huynh, J. L., Coutts, D. J. C., Zhao, C., Casaccia, P., & Franklin, R. J. M. (2017). Efficient Remyelination Requires DNA Methylation. *Eneuro*, 4(2), ENEURO.0336-16.2017. <http://doi.org/10.1523/ENEURO.0336-16.2017>
- Mueller, K. L. O., Marion, S. D., Paul, L. K., & Brown, W. S. (2009). Bimanual motor coordination in agenesis of the corpus callosum. *Behavioral Neuroscience*, 123(5), 1000–1011. <http://doi.org/10.1037/a0016868>
- Musse, A. A., Gao, W., Homchaudhuri, L., Boggs, J. M., & Harauz, G. (2008). Myelin basic protein as a “PI(4,5)P2-modulin”: A new biological function for a major central nervous system protein. *Biochemistry*. <http://doi.org/10.1021/bi801302b>
- Naruse, M., Ishino, Y., Kumar, A., Ono, K., Takebayashi, H., Yamaguchi, M., ... Hitoshi, S. (2016). The Dorsoventral Boundary of the Germinal Zone is a Specialized Niche for the Generation of Cortical Oligodendrocytes during a Restricted Temporal Window. *Cerebral Cortex*, 26(6),

2800–2810. <http://doi.org/10.1093/cercor/bhv141>

- Naruse, M., Ishizaki, Y., Ikenaka, K., Tanaka, A., & Hitoshi, S. (2017). Origin of oligodendrocytes in mammalian forebrains: a revised perspective. *Journal of Physiological Sciences*, 67(1), 63–70. <http://doi.org/10.1007/s12576-016-0479-7>
- Naus, S., Richter, M., Wildeboer, D., Moss, M., Schachner, M., & Bartsch, J. W. (2004). Ectodomain Shedding of the Neural Recognition Molecule CHL1 by the Metalloprotease-disintegrin ADAM8 Promotes Neurite Outgrowth and Suppresses Neuronal Cell Death. *Journal of Biological Chemistry*, 279(16), 16083–16090. <http://doi.org/10.1074/jbc.M400560200>
- Nave, K.-A. (2010). Myelination and the trophic support of long axons. *Nature Reviews. Neuroscience*, 11, 275–283. <http://doi.org/10.1038/nrn2797>
- Nave, K.-A., & Werner, H. B. (2014). Myelination of the Nervous System: Mechanisms and Functions. *Annual Review of Cell and Developmental Biology*, 30(1), 503–533. <http://doi.org/10.1146/annurev-cellbio-100913-013101>
- Nawaz, S., Kippert, A., Saab, A. S., Werner, H. B., Lang, T., Nave, K.-A., & Simons, M. (2009). Phosphatidylinositol 4,5-bisphosphate-dependent interaction of myelin basic protein with the plasma membrane in oligodendroglial cells and its rapid perturbation by elevated calcium. *The Journal of Neuroscience : The Official Journal of the Society for Neuroscience*, 29(15), 4794–4807. <http://doi.org/10.1523/JNEUROSCI.3955-08.2009>
- Neumann, H., Kotter, M. R., & Franklin, R. J. M. (2009). Debris clearance by microglia: An essential link between degeneration and regeneration. *Brain*, 132(2), 288–295. <http://doi.org/10.1093/brain/awn109>
- Nielsen, H. H., Ladeby, R., Fenger, C., Toft-Hansen, H., Babcock, A. A., Owens, T., & Finsen, B. (2009). Enhanced microglial clearance of myelin debris in T cell-infiltrated central nervous system. *Journal of Neuropathology and Experimental Neurology*, 68(8), 845–856. <http://doi.org/10.1097/NEN.0b013e3181ae0236>
- Nimmerjahn, A., Kirchhoff, F., & Helmchen, F. (2005). Neuroscience: Resting microglial cells are highly dynamic surveillants of brain parenchyma in vivo. *Science*. <http://doi.org/10.1126/science.1110647>
- Ohnishi A, Murai Y, Ikeda M, Fujita T, Furuya H, K. Y. (1989). Autosomal recessive motor and sensory neuropathy with excessive myelin unfolding, (July), 568–575.
- Öhrfelt, A., Axelsson, M., Malmeström, C., Novakova, L., Heslegrave, A., Blennow, K., ... Zetterberg, H. (2016). Soluble TREM-2 in cerebrospinal fluid from patients with multiple sclerosis treated with natalizumab or mitoxantrone. *Multiple Sclerosis*. <http://doi.org/10.1177/1352458515624558>
- Okada, A., Tominaga, M., Horiuchi, M., & Tomooka, Y. (2007). Plexin-A4 is expressed in oligodendrocyte precursor cells and acts as a mediator of semaphorin signals. *Biochemical and Biophysical Research Communications*. <http://doi.org/10.1016/j.bbrc.2006.10.176>
- Olson, J. K., & Miller, S. D. (2004). Microglia Initiate Central Nervous System Innate and Adaptive Immune Responses through Multiple TLRs. *The Journal of Immunology*. <http://doi.org/10.4049/jimmunol.173.6.3916>
- Osório, M. J., & Goldman, S. A. (2018). Neurogenetics of Pelizaeus–Merzbacher disease. In *Handbook of Clinical Neurology*. <http://doi.org/10.1016/B978-0-444-64076-5.00045-4>
- Paloneva, J., Kestilä, M., Wu, J., Salminen, A., Böhling, T., Ruotsalainen, V., ... Peltonen, L. (2000). Loss-of-function mutations in TYROBP (DAP12) result in a presenile dementia with bone cysts. *Nature Genetics*. <http://doi.org/10.1038/77153>
- Paloneva, J., Manninen, T., Christman, G., Hovanes, K., Mandelin, J., Adolfsson, R., ... Peltonen, L. (2002). Mutations in Two Genes Encoding Different Subunits of a Receptor Signaling Complex Result in an Identical Disease Phenotype. *The American Journal of Human Genetics*.

<http://doi.org/10.1086/342259>

- Paolicelli, R. C., Bolasco, G., Pagani, F., Maggi, L., Scianni, M., Panzanelli, P., ... Gross, C. T. (2011). Synaptic Pruning by Microglia Is Necessary for Normal Brain Development. *Science*, 333(6048), 1456–1458. <http://doi.org/10.1126/science.1202529>
- Parhizkar, S., Arzberger, T., Brendel, M., Kleinberger, G., Deussing, M., Focke, C., ... Haass, C. (2019). Loss of TREM2 function increases amyloid seeding but reduces plaque-associated ApoE. *Nature Neuroscience*, 22(2), 191–204. <http://doi.org/10.1038/s41593-018-0296-9>
- Peri, F., & Nüsslein-Volhard, C. (2008). Live Imaging of Neuronal Degradation by Microglia Reveals a Role for v0-ATPase a1 in Phagosomal Fusion In Vivo. *Cell*, 133(5), 916–927. <http://doi.org/10.1016/j.cell.2008.04.037>
- Piccio, L., Buonsanti, C., Cella, M., Tassi, I., Schmidt, R. E., Fenoglio, C., ... Cross, A. H. (2008). Identification of soluble TREM-2 in the cerebrospinal fluid and its association with multiple sclerosis and CNS inflammation. *Brain*. <http://doi.org/10.1093/brain/awn217>
- Poliani, P. L., Wang, Y., Fontana, E., Robinette, M. L., Yamanishi, Y., Gilfillan, S., & Colonna, M. (2015). TREM2 sustains microglial expansion during aging and response to demyelination. *Journal of Clinical Investigation*, 125(5), 2161–2170. <http://doi.org/10.1172/JCI77983>
- Pratte, M., Rougon, G., Schachner, M., & Jamon, M. (2003). Mice deficient for the close homologue of the neural adhesion cell L1 (CHL1) display alterations in emotional reactivity and motor coordination. *Behavioural Brain Research*, 147(1–2), 31–39. [http://doi.org/10.1016/S0166-4328\(03\)00114-1](http://doi.org/10.1016/S0166-4328(03)00114-1)
- Raasakka, A., Ruskamo, S., Kowal, J., Barker, R., Baumann, A., Martel, A., ... Kursula, P. (2017). Membrane Association Landscape of Myelin Basic Protein Portrays Formation of the Myelin Major Dense Line. *Scientific Reports*. <http://doi.org/10.1038/s41598-017-05364-3>
- Raj, D., Yin, Z., Breur, M., Doorduyn, J., Holtman, I. R., Olah, M., ... Boddeke, E. (2017). Increased White Matter Inflammation in Aging- and Alzheimer's Disease Brain. *Frontiers in Molecular Neuroscience*, 10(June), 1–18. <http://doi.org/10.3389/fnmol.2017.00206>
- Ranvier, L.-A. (1878). *Leçons sur l'histologie du système nerveux*. Librairie F. Savy.
- Reemst, K., Noctor, S. C., Lucassen, P. J., & Hol, E. M. (2016). The Indispensable Roles of Microglia and Astrocytes during Brain Development. *Frontiers in Human Neuroscience*, 10(November), 1–28. <http://doi.org/10.3389/fnhum.2016.00566>
- Reichert, F., & Rotshenker, S. (1996). Deficient activation of microglia during optic nerve degeneration. *Journal of Neuroimmunology*, 70(2), 153–161. [http://doi.org/10.1016/S0165-5728\(96\)00112-9](http://doi.org/10.1016/S0165-5728(96)00112-9)
- Rigato, C., Buckinx, R., Le-Corronc, H., Rigo, J. M., & Legendre, P. (2011). Pattern of invasion of the embryonic mouse spinal cord by microglial cells at the time of the onset of functional neuronal networks. *GLIA*. <http://doi.org/10.1002/glia.21140>
- Safaiyan, S., Kannaiyan, N., Snaidero, N., Brioschi, S., Biber, K., Yona, S., ... Simons, M. (2016). Age-related myelin degradation burdens the clearance function of microglia during aging. *Nature Neuroscience*, 19(8), 995–998. <http://doi.org/10.1038/nn.4325>
- Saher, G., Brügger, B., Lappe-Siefke, C., Möbius, W., Tozawa, R. I., Wehr, M. C., ... Nave, K. A. (2005). High cholesterol level is essential for myelin membrane growth. *Nature Neuroscience*. <http://doi.org/10.1038/nn1426>
- Saher, G., Rudolphi, F., Corthals, K., Ruhwedel, T., Schmidt, K. F., Löwel, S., ... Nave, K. A. (2012). Therapy of Pelizaeus-Merzbacher disease in mice by feeding a cholesterol-enriched diet. *Nature Medicine*. <http://doi.org/10.1038/nm.2833>
- Sato, a., Sato, Y., & Suzuki, H. (1985). Aging effects on conduction velocities on myelinated and unmyelinated fibers of peripheral nerves. *Neuroscience Letters*, 53, 15–20. [http://doi.org/10.1016/0304-3940\(85\)90090-4](http://doi.org/10.1016/0304-3940(85)90090-4)

- Schafer, D. P., Lehrman, E. K., Kautzman, A. G., Koyama, R., Mardinly, A. R., Yamasaki, R., ... Stevens, B. (2012). Microglia Sculpt Postnatal Neural Circuits in an Activity and Complement-Dependent Manner. *Neuron*. <http://doi.org/10.1016/j.neuron.2012.03.026>
- Schalomon, P. M., & Wahlsten, D. (2002). Wheel running behavior is impaired by both surgical section and genetic absence of the mouse corpus callosum. *Brain Research Bulletin*, 57(1), 27–33. [http://doi.org/10.1016/S0361-9230\(01\)00633-5](http://doi.org/10.1016/S0361-9230(01)00633-5)
- Schmithorst, V. J., & Wilke, M. (2002). Differences in white matter architecture between musicians and non-musicians: A diffusion tensor imaging study. *Neuroscience Letters*. [http://doi.org/10.1016/S0304-3940\(02\)00054-X](http://doi.org/10.1016/S0304-3940(02)00054-X)
- Schnaar, R. L., Collins, B. E., Wright, L. P., Kiso, M., Tropak, M. B., Roder, J. C., & Crocker, P. R. (1998). Myelin-associated glycoprotein binding to gangliosides. Structural specificity and functional implications. *Ann N Y Acad Sci*. <http://doi.org/10.2190/AG.71.3.d>
- Scholz, J., Klein, M. C., Behrens, T. E. J., & Johansen-Berg, H. (2009). Training induces changes in white-matter architecture. *Nature Neuroscience*, 12(11), 1370–1371. <http://doi.org/10.1038/nn.2412>
- Schultz, R. L., & Karlsson, U. (1965). Fixation of the central nervous system for electron microscopy by aldehyde perfusion. II. Effect of osmolarity, pH of perfusate, and fixative concentration. *Journal of Ultrastructure Research*. [http://doi.org/10.1016/S0022-5320\(65\)80015-6](http://doi.org/10.1016/S0022-5320(65)80015-6)
- Schwarz, A. J., Yu, P., Miller, B. B., Shcherbinin, S., Dickson, J., Navitsky, M., ... Mintun, M. S. (2016). Regional profiles of the candidate tau PET ligand 18F-AV-1451 recapitulate key features of Braak histopathological stages. *Brain*. <http://doi.org/10.1093/brain/aww023>
- Seitz, H. M., Camenisch, T. D., Lemke, G., Earp, H. S., & Matsushima, G. K. (2007). Macrophages and Dendritic Cells Use Different Axl/Mertk/Tyro3 Receptors in Clearance of Apoptotic Cells. *The Journal of Immunology*, 178(9), 5635–5642. <http://doi.org/10.4049/jimmunol.178.9.5635>
- Settembre, C., Malta, C. Di, Polito, A., Arencibia, M. G., Vetrini, F., Erdin, S., ... Ballabio, A. (2011). TFEB Links Autophagy to Lysosomal Biogenesis. *Source: Science, New Series*, 332(6036), 1429–1433. <http://doi.org/10.1126/science.1207020>
- Shen, X. Y., Billings-Gagliardi, S., Sidman, R. L., & Wolf, M. K. (1985). Myelin deficient (shimld) mutant allele: Morphological comparison with shiverer (shi) allele on a B6C3 mouse stock. *Brain Research*. [http://doi.org/10.1016/0006-8993\(85\)91239-9](http://doi.org/10.1016/0006-8993(85)91239-9)
- Simons, M., Krämer, E. M., Thiele, C., Stoffel, W., & Trotter, J. (2000). Assembly of myelin by association of proteolipid protein with cholesterol- and galactosylceramide-rich membrane domains. *Journal of Cell Biology*. <http://doi.org/10.1083/jcb.151.1.143>
- Snaidero, N., Möbius, W., Czopka, T., Hekking, L. H. P., Mathisen, C., Verkleij, D., ... Simons, M. (2014). Myelin membrane wrapping of CNS axons by PI(3,4,5)P3-dependent polarized growth at the inner tongue. *Cell*, 156(1–2), 277–290. <http://doi.org/10.1016/j.cell.2013.11.044>
- Snaidero, N., Velte, C., Myllykoski, M., Raasakka, A., Ignatov, A., Werner, H. B., ... Simons, M. (2017). Antagonistic Functions of MBP and CNP Establish Cytosolic Channels in CNS Myelin. *Cell Reports*. <http://doi.org/10.1016/j.celrep.2016.12.053>
- Stridh, L., Mottahedin, A., Johansson, M. E., Valdez, R. C., Northington, F., Wang, X., & Mallard, C. (2013). Toll-Like Receptor-3 Activation Increases the Vulnerability of the Neonatal Brain to Hypoxia-Ischemia. *Journal of Neuroscience*. <http://doi.org/10.1523/JNEUROSCI.0673-13.2013>
- Sturrock, R. R. (1980). Myelination of the Mouse Corpus Callosum. *Neuropathology and Applied Neurobiology*, 6, 415–420.
- Suárez-Calvet, M., Morenas-Rodríguez, E., Kleinberger, G., Schlepckow, K., Araque Caballero, M. Á., Franzmeier, N., ... Haass, C. (2019). Early increase of CSF sTREM2 in Alzheimer's disease is associated with tau related-neurodegeneration but not with amyloid-β pathology. *Molecular Neurodegeneration*, 5, 1–14. <http://doi.org/10.1186/s13024-018-0301-5>

- Sun, L. O., Mulinyawe, S. B., Collins, H. Y., Ibrahim, A., Li, Q., Simon, D. J., ... Barres, B. A. (2018). Spatiotemporal Control of CNS Myelination by Oligodendrocyte Programmed Cell Death through the TFEB-PUMA Axis. *Cell*, 175(7), 1811–1826.e21. <http://doi.org/10.1016/j.cell.2018.10.044>
- Swinnen, N., Smolders, S., Avila, A., Notelaers, K., Paesen, R., Ameloot, M., ... Rigo, J. M. (2013). Complex invasion pattern of the cerebral cortex by microglial cells during development of the mouse embryo. *GLIA*. <http://doi.org/10.1002/glia.22421>
- Takahashi, K., Prinz, M., Stagi, M., Chechneva, O., & Neumann, H. (2007). TREM2-transduced myeloid precursors mediate nervous tissue debris clearance and facilitate recovery in an animal model of multiple sclerosis. *PLoS Medicine*. <http://doi.org/10.1371/journal.pmed.0040124>
- Takahashi, K., Rochford, C. D. P., & Neumann, H. (2005). Clearance of apoptotic neurons without inflammation by microglial triggering receptor expressed on myeloid cells-2. *The Journal of Experimental Medicine*. <http://doi.org/10.1084/jem.20041611>
- Takano, T., Tian, G. F., Peng, W., Lou, N., Libionka, W., Han, X., & Nedergaard, M. (2006). Astrocyte-mediated control of cerebral blood flow. *Nature Neuroscience*. <http://doi.org/10.1038/nn1623>
- Tekkök, S. B., Brown, A. M., Westenbroek, R., Pellerin, L., & Ransom, B. R. (2005). Transfer of glycogen-derived lactate from astrocytes to axons via specific monocarboxylate transporters supports mouse optic nerve activity. *Journal of Neuroscience Research*. <http://doi.org/10.1002/jnr.20573>
- Tomassy, G. S., Berger, D. R., Chen, H.-H., Kasthuri, N., Hayworth, K. J., Vercelli, A., ... Arlotta, P. (2014). Distinct profiles of myelin distribution along single axons of pyramidal neurons in the neocortex. *Science (New York, N.Y.)*, 344(June), 319–24. <http://doi.org/10.1126/science.1249766>
- Tsai, H.-H., Niu, J., Munji, R., Davalos, D., Chang, J., Zhang, H., ... Fancy, S. P. J. (2016). Oligodendrocyte precursors migrate along vasculature in the developing nervous system. *Science*, 351(6271), 379–384. <http://doi.org/10.1097/NCN.0b013e3181a91b58>. Exploring
- Turnbull, I. R., Gilfillan, S., Cella, M., Aoshi, T., Miller, M., Piccio, L., ... Colonna, M. (2006). Cutting Edge: TREM-2 Attenuates Macrophage Activation. *The Journal of Immunology*. <http://doi.org/10.4049/jimmunol.177.6.3520>
- Ueno, M., Fujita, Y., Tanaka, T., Nakamura, Y., Kikuta, J., Ishii, M., & Yamashita, T. (2013). Layer v cortical neurons require microglial support for survival during postnatal development. *Nature Neuroscience*. <http://doi.org/10.1038/nn.3358>
- Umehara, F., Takenaga, S., Nakagawa, M., Takahashi, K., Izumo, S., Matsumuro, K., ... Osame, M. (1993). Dominantly inherited motor and sensory neuropathy with excessive myelin folding complex. *Acta Neuropathologica*, 86(6), 602–608. <http://doi.org/10.1007/BF00294299>
- van Tilborg, E., de Theije, C. G. M., van Hal, M., Wagenaar, N., de Vries, L. S., Benders, M. J., ... Nijboer, C. H. (2018). Origin and dynamics of oligodendrocytes in the developing brain: Implications for perinatal white matter injury. *Glia*, 66(2), 221–238. <http://doi.org/10.1002/glia.23256>
- Varela-Echevarría, A., Vargas-Barroso, V., Lozano-Flores, C., & Larriva-Sahd, J. (2017). Is There Evidence for Myelin Modeling by Astrocytes in the Normal Adult Brain? *Frontiers in Neuroanatomy*, 11(September), 1–23. <http://doi.org/10.3389/fnana.2017.00075>
- Virchow, R. (1854). Ueber das ausgebreitete Vorkommen einer dem Nervenmark analogen Substanz in den thierischen Geweben. *Archiv Für Pathologische Anatomie Und Physiologie Und Für Klinische Medicin*, 6(4), 562–572. <http://doi.org/10.1007/BF02116709>
- Wake, H., Lee, P. R., & Fields, R. D. (2011). Control of local protein synthesis and initial events in myelination by action potentials. *Science*. <http://doi.org/10.1126/science.1206998>
- Wakselman, S., Bechade, C., Roumier, A., Bernard, D., Triller, A., & Bessis, A. (2008).

- Developmental Neuronal Death in Hippocampus Requires the Microglial CD11b Integrin and DAP12 Immunoreceptor. *Journal of Neuroscience*, 28(32), 8138–8143. <http://doi.org/10.1523/JNEUROSCI.1006-08.2008>
- Wallraff, A., Köhling, R., Heinemann, U., Theis, M., Willecke, K., & Steinhäuser, C. (2006). The Impact of Astrocytic Gap Junctional Coupling on Potassium Buffering in the Hippocampus. *Journal of Neuroscience*, 26(20), 5438–5447. <http://doi.org/10.1523/JNEUROSCI.0037-06.2006>
- Wang, C., Pralong, W.-F., Schulz, M.-F., Rougon, G., Aubry, J.-M., Pagliusi, S., ... Kiss, J. Z. (1996). Functional N-Methyl-D-Aspartate Receptors in O-2A Glial Precursor Cells: A Critical Role in Regulating Polysialic Acid-Neural Cell Adhesion Molecule Expression and Cell Migration. *The Journal of Cell Biology*, 135(6), 1565–1581 1565. <http://doi.org/10.1007/s12517-015-1933-1>
- Wang, J., Vasaikar, S., Shi, Z., Greer, M., & Zhang, B. (2017). WebGestalt 2017: A more comprehensive, powerful, flexible and interactive gene set enrichment analysis toolkit. *Nucleic Acids Research*, 45(W1), W130–W137. <http://doi.org/10.1093/nar/gkx356>
- Wang, S., & Young, K. M. (2014). White matter plasticity in adulthood. *Neuroscience*, 276, 148–160. <http://doi.org/10.1016/j.neuroscience.2013.10.018>
- Wang, X., Malawista, A., Qian, F., Ramsey, C., Allore, H. G., & Montgomery, R. R. (2018). Age-related changes in expression and signaling of TAM receptor inflammatory regulators in monocytes. *Oncotarget*, 9(11), 9572–9580. <http://doi.org/10.18632/oncotarget.23851>
- Wang, Y., Cella, M., Mallinson, K., Ulrich, J. D., Young, K. L., Robinette, M. L., ... Colonna, M. (2015). TREM2 lipid sensing sustains the microglial response in an Alzheimer's disease model. *Cell*, 160(6), 1061–1071. <http://doi.org/10.1016/j.cell.2015.01.049>
- Wang, Y., Ulland, T. K., Ulrich, J. D., Song, W., Tzaferis, J. A., Hole, J. T., ... Colonna, M. (2016). TREM2-mediated early microglial response limits diffusion and toxicity of amyloid plaques. *The Journal of Experimental Medicine*. <http://doi.org/10.1084/jem.20151948>
- Weil, M. T., Möbius, W., Winkler, A., Ruhwedel, T., Wrzos, C., Romanelli, E., ... Simons, M. (2016). Loss of Myelin Basic Protein Function Triggers Myelin Breakdown in Models of Demyelinating Diseases. *Cell Reports*, 16(2), 314–322. <http://doi.org/10.1016/j.celrep.2016.06.008>
- Weinger, J. G., Brosnan, C. F., Loudig, O., Goldberg, M. F., Macian, F., Arnett, H. A., ... Shafit-Zagardo, B. (2011). Loss of the receptor tyrosine kinase Axl leads to enhanced inflammation in the CNS and delayed removal of myelin debris during Experimental Autoimmune Encephalomyelitis. *Journal of Neuroinflammation*, 8, 1–18. <http://doi.org/10.1186/1742-2094-8-49>
- Winters, J. J., Ferguson, C. J., Lenk, G. M., Giger-Mateeva, V. I., Shrager, P., Meisler, M. H., & Giger, R. J. (2011). Congenital CNS Hypomyelination in the Fig4 Null Mouse Is Rescued by Neuronal Expression of the PI(3,5)P2 Phosphatase Fig4. *Journal of Neuroscience*, 31(48), 17736–17751. <http://doi.org/10.1523/JNEUROSCI.1482-11.2011>
- Wu, K., Byers, D. E., Jin, X., Agapov, E., Alexander-Brett, J., Patel, A. C., ... Holtzman, M. J. (2015). TREM-2 promotes macrophage survival and lung disease after respiratory viral infection. *The Journal of Experimental Medicine*. <http://doi.org/10.1084/jem.20141732>
- Xiao, L., Ohayon, D., Mckenzie, I. A., Sinclair-Wilson, A., Wright, J. L., Fudge, A. D., ... Richardson, W. D. (2016). Rapid production of new oligodendrocytes is required in the earliest stages of motor-skill learning. *Nature Neuroscience*, 19(9), 1210–1217. <http://doi.org/10.1038/nn.4351>
- Xiao, Y. Q., Freire-de-Lima, C. G., Schiemann, W. P., Bratton, D. L., Vandivier, R. W., & Henson, P. M. (2008). Transcriptional and Translational Regulation of TGF- Production in Response to Apoptotic Cells. *The Journal of Immunology*. <http://doi.org/10.4049/jimmunol.181.5.3575>

- Xu, C., Sakai, N., Taniike, M., Inui, K., & Ozono, K. (2006). Six novel mutations detected in the GALC gene in 17 Japanese patients with Krabbe disease, and new genotype-phenotype correlation. *Journal of Human Genetics*. <http://doi.org/10.1007/s10038-006-0396-3>
- Yamasaki, R., Lu, H., Butovsky, O., Ohno, N., Rietsch, A. M., Cialic, R., ... Ransohoff, R. M. (2014). Differential roles of microglia and monocytes in the inflamed central nervous system. *The Journal of Experimental Medicine*. <http://doi.org/10.1084/jem.20132477>
- Yao, L., Kan, E. M., Lu, J., Hao, A., Dheen, S. T., Kaur, C., & Ling, E. A. (2013). Toll-like receptor 4 mediates microglial activation and production of inflammatory mediators in neonatal rat brain following hypoxia: Role of TLR4 in hypoxic microglia. *Journal of Neuroinflammation*. <http://doi.org/10.1186/1742-2094-10-23>
- Ye, F., Chen, Y., Hoang, T., Montgomery, R. L., Zhao, X. H., Bu, H., ... Lu, Q. R. (2009). HDAC1 and HDAC2 regulate oligodendrocyte differentiation by disrupting the B-catenin-TCF interaction. *Nature Neuroscience*. <http://doi.org/10.1038/nn.2333>
- Yeh, F. L., Wang, Y., Tom, I., Gonzalez, L. C., & Sheng, M. (2016). TREM2 Binds to Apolipoproteins, Including APOE and CLU/APOJ, and Thereby Facilitates Uptake of Amyloid-Beta by Microglia. *Neuron*. <http://doi.org/10.1016/j.neuron.2016.06.015>
- Yokota, S., & Okada, Y. (1996). Effect of Fixation Catalase with and Reduced Erythrocyte Osmium Esterase Tetroxide upon the Antigenicity of Liver Sadaki Yokota1 and Yoshiie Okada2 of Anatomy and 2Department 1 of Biochemistry , Yamanashi Medical Received for publication December 11 , 199. *Acta Histochem. Cytochem.*, 29(4), 335–338.
- Yool, D. A., Edgar, J. M., Montague, P., & Malcolm, S. (2000). The proteolipid protein gene and myelin disorders in man and animal models. *Human Molecular Genetics Review*. <http://doi.org/10.1093/hmg/9.6.987>
- Yu, Y., Chen, Y., Kim, B., Wang, H., Zhao, C., He, X., ... Lu, Q. R. (2013). Olig2 targets chromatin remodelers to enhancers to initiate oligodendrocyte differentiation. *Cell*, 152(1–2), 248–261. <http://doi.org/10.1016/j.cell.2012.12.006>
- Yuan, P., Condello, C., Keene, C. D., Wang, Y., Bird, T. D., Paul, S. M., ... Grutzendler, J. (2016). TREM2 Haplodeficiency in Mice and Humans Impairs the Microglia Barrier Function Leading to Decreased Amyloid Compaction and Severe Axonal Dystrophy. *Neuron*. <http://doi.org/10.1016/j.neuron.2016.05.003>
- Zhang, H., Vutskits, L., Calaora, V., Durbec, P., & Kiss, J. Z. (2004). A role for the polysialic acid - neural cell adhesion molecule in PDGF-induced chemotaxis of oligodendrocyte precursor cells. *Journal of Cell Science*, 117(1), 93–103. <http://doi.org/10.1242/jcs.00827>
- Zhang, L., He, X., Liu, L., Jiang, M., Zhao, C., Wang, H., ... Lu, Q. R. (2016). Hdac3 Interaction with p300 Histone Acetyltransferase Regulates the Oligodendrocyte and Astrocyte Lineage Fate Switch. *Developmental Cell*. <http://doi.org/10.1016/j.devcel.2016.01.002>
- Zhao, Y. Y., Shi, X. Y., Qiu, X., Lu, W., Yang, S., Li, C., ... Tang, Y. (2012). Enriched Environment Increases the Myelinated Nerve Fibers of Aged Rat Corpus Callosum. *Anatomical Record*, 295(6), 999–1005. <http://doi.org/10.1002/ar.22446>
- Ziskin, J. L., Nishiyama, A., Rubio, M., Fukaya, M., & Bergles, D. E. (2007). Vesicular release of glutamate from unmyelinated axons in white matter. *Nature Neuroscience*. <http://doi.org/10.1038/nn1854>
- Zonta, M., Angulo, M. C., Gobbo, S., Rosengarten, B., Hossmann, K. A., Pozzan, T., & Carmignoto, G. (2003). Neuron-to-astrocyte signaling is central to the dynamic control of brain microcirculation. *Nature Neuroscience*. <http://doi.org/10.1038/nn980>

8 CV

PERSONAL DETAILS

Name **WEIKERT, ULRICH MAXIMILIAN**

Residential Address Krokusweg 4, 67346 Speyer, Germany

Mobil: +49 (172)-7015046

E-Mail ulrich.m.weikert@googlemail.com

Family status Single

Citizenship German

Date of birth 04.11.1988

Place of birth Reutlingen



EDUCATION HISTORY

11/2014 - today PhD student at the Max-Planck Institute of Experimental Medicine, Göttingen, Germany

- Project: "Myelin pruning by microglia during development"
- Taking care of laboratory equipment
- Supervision of students
- Taking part in soft skill and method courses

10/2012-08/2014 **Master of Science in Molecular Cell Biology** at the University of Applied Sciences, Bielefeld, Germany

- **Master thesis** at the **Department of Cell Biology** in the Department of Cell Biology, Faculty of Biology, University of Bielefeld, Germany

03/2011-09/2011 Project: „Altered Neuregulin1 expression and disturbed Axon-Schwann cell interaction in PLEKHG5 knockout mice“

4/2009-03/2012 **Bachelor of Science in Biotechnology** at the University of Applied Sciences in Berlin, Germany

- **Bachelor thesis** at the University Malaya, **Kuala Lumpur**, Malaysia

1999-2009 Project: "Enzyme profile of Panus sp. during Solid Substrate and Submerged Fermentation of sawdust and oil palm trunk tissue"

1999-2009 Secondary School (Gymnasium in Metzingen, Germany), University entrance qualification including an **exchange year at Palmdale High School**, California, USA

INTERNSHIPS

04-06/2010

2 months-internship at the Helmholtz-Center Berlin for Materials and Energy in Berlin, Germany

SPECIAL SKILLS

Languages

German (Mother tongue), fluent English, good French

Soft skills

- Attendance in SCIENCE-PLUS workshop "*Project management for young scientists: Taking off as a project pilot*" (Goblin Wissenschaftsmanagement, Anna Royon-Weigelt)
- Completing the Good Manufacturing Practice (GMP) Course 2017 (Thomas Beer and Tobias Halfpap GbR)

Teaching and Supervision

- Supervision of student during masters (Bachelor course), during PhD (one ERASMUS Bachelor student from Spain for Bachelor Thesis (4 months))
- Participating as a tutor for electron microscopy (2-day) course for Master students of the Neuroscience IMPRS program

Technical Skills

Good computer knowledge in: Windows, Excel, Word, Powerpoint, GraphPad Prism, Adobe Photoshop and Illustrator, ImageJ, Microscopic Image Browser (MIB), Imaris, Mendeley

Scholarship / Awards

GIZ-scholarship for travel expenses

POSTERS

2017

Ulrich Weikert, Marie-Theres Weil, Torben Ruhwedel, Wiebke Möbius, Christoph Wrede, Jan Hegemann, Mikael Simons "*Myelin remodeling during development*", 4th biennial CMPB symposium: Encephalon, Göttingen, Germany

2016

Ulrich Weikert, Mišo Mitkovski, Mikael Simons „*Following Myelination: one patch at a time*“, Current Topics in Myelin Research, Kassel, Germany

2016

Ulrich Weikert, Mišo Mitkovski, Mikael Simons „*Myelin patterning during development*“, PhD retreat, Braunlage, Germany

2015

Ulrich M. Weikert, Mikael Simons „*Molecular Mechanisms of Motor Skill Learning on White Matter Plasticity*“, 3rd biennial CMPB symposium: Encephalon, Göttingen, Germany

2015

Ulrich M. Weikert, Mikael Simons "*Molecular Mechanisms of Motor Skill Learning on White Matter Plasticity in the Mouse Model*", PhD retreat, Berlin, Germany